1976-06

An experimental investigation of microstrip transmission line and coplanar waveguide on ferrite substrate.

Aminelahi, Hooshang

Monterey, California. Naval Postgraduate School

AN EXPERIMENTAL INVESTIGATION OF MICROSTRIP TRANSMISSION LINE AND COPLANAR WAVEGUIDE ON FERRITE SUBSTRATE

Hooshang Aminelahi

NAVAL POSTGRADUATE SCHOOL

Monterey, California

THESIS

AN EXPERIMENTAL INVESTIGATION OF MICROSTRIP TRANSMISSION LINE AND COPLANAR WAVEGUIDE ON FERRITE SUBSTRATE

by

Hooshang Aminelahi

June 1976

Thesis Advisor: Jeffery B. Knorr

UNCLASSIFIED

SECURITY CLASSIFICATION OF THIS PAGE (When Data Entered)

REPORT DOCUMENTATION PAGE		READ INSTRUCTIONS BEFORE COMPLETING FORM
1. REPORT NUMBER	2. GOVT ACCESSION NO.	3. RECIPIENT'S CATALOG NUMBER
4. TITLE (and Subtitle) An Experimental Investigation of Microstrip Transmission Line and Coplanar Waveguide on Ferrite Substrate		5. TYPE OF REPORT & PERIOD COVERED Electrical Engineer; June 1976
		6. PERFORMING ORG. REPORT NUMBER
7. AUTHOR(s) Hooshang Aminelahi		8. CONTRACT OR GRANT NUMBER(s)
9. PERFORMING ORGANIZATION NAME AND ADDRESS Naval Postgraduate School Monterey, CA 93940		10. PROGRAM ELEMENT, PROJECT, TASK AREA & WORK UNIT NUMBERS
11. CONTROLLING OFFICE NAME AND ADDRESS Naval Postgraduate School Monterey, CA 93940		12. REPORT DATE June 1976
		13. NUMBER OF PAGES
14. MONITORING AGENCY NAME & ADDRESS(if different from Controlling Office) Naval Postgraduate School Monterey, CA 93940		15. SECURITY CLASS. (of this report) Unclassified
		15a. DECLASSIFICATION/DOWNGRADING SCHEDULE

16. DISTRIBUTION STATEMENT (of this Report)

Approved for public release; distribution unlimited.

17. DISTRIBUTION STATEMENT (of the abstract entered in Block 20, if different from Report)

18. SUPPLEMENTARY NOTES

19. KEY WORDS (Continue on reverse side if necessary and identify by block number)

20. ABSTRACT (Continue on reverse side if necessary and identify by block number)

In this thesis both a microstrip transmission line and a coplanar waveguide on ferrite substrate were designed, constructed and tested. The behavior of microstrip and coplanar waveguide was experimentally evaluated, using different biasing magnetic fields and directions. The experimental dispersion ($\omega-\beta$) and attenuation diagrams for both structures were compared with theoretical work based on perturbation theory. Also, the

DD FORM 1473 1 JAN 73 EDITION OF 1 NOV 65 IS OBSOLETE
(Page 1) S/N 0102-014-6601 |

Unclassified

SECURITY CLASSIFICATION OF THIS PAGE (When Data Entered)

experimental results were compared with the existing work conducted by different authors.

An Experimental Investigation of Microstrip Transmission Line and Coplanar Waveguide on Ferrite Substrate

by

Hooshang Aminelahi
Commander, Iranian Navy
Diploma in Electrical Engineering, Faraday House Engineering College, London, 1962
B.S.E.E., Naval Postgraduate School, 1975
M.S.E.E., Naval Postgraduate School, 1975

Submitted in partial fulfillment of the requirements for the degree of

ELECTRICAL ENGINEER

from the

NAVAL POSTGRADUATE SCHOOL
June 1976

ABSTRACT

In this thesis both a microstrip transmission line and a coplanar waveguide on ferrite substrate were designed, constructed and tested. The behavior of microstrip and coplanar waveguide was experimentally evaluated, using different biasing magnetic fields and directions. The experimental dispersion ($\omega-\beta$) and attenuation diagrams for both structures were compared with theoretical work based on perturbation theory. Also, the experimental results were compared with the existing work conducted by different authors.

ACKNOWLEDGMENT

The author gratefully expresses his gratitude to Professor Jeffrey B. Knorr for his considerable help and guidance during this study, and his patience for editing this thesis. I am also very obliged to the Imperial IRANIAN NAVY for giving me this opportunity.

TABLE OF CONTENTS

LIST OF TABLES

LIST OF FIGURES

I. INTRODUCTION

The analysis of microstrip is of great importance, as this type of transmission line has found wide use due to its compatibility with microwave integrated circuitry. The open microstrip transmission line has been predominant because it can be etched or deposited easily on substrate. For the above reasons in recent years, a great deal of attention has been paid to the microstrip transmission lines and in particular to microstrip transmission and coplanar waveguide on ferrites. Since ferrite and garnets are magnetic insulators, the electromagnetic field can penetrate these materials and most of the energy is confined in these materials with very little attenuation.

The interaction between the electromagnetic field and the ferrite will render some interesting results, and can be described in terms of an effective permeability. The permeability is a tensor quantity. The presence of off-diagonal imaginary parts in this tensor and the fact that its elements exhibit a resonance when the applied frequency equals the precession frequency of the magnetization vector results in a number of important nonreciprocal effects which are studied in this thesis.

In this thesis two types of transmission lines are studied. First, a microstrip transmission line on ferrite substrate was designed (See Fig. 1-1 and 1-3), constructed and tested. Secondly, a coplanar waveguide on ferrite substrate was designed (See Figs. 1-2 and 1-3) and constructed and tested. There are

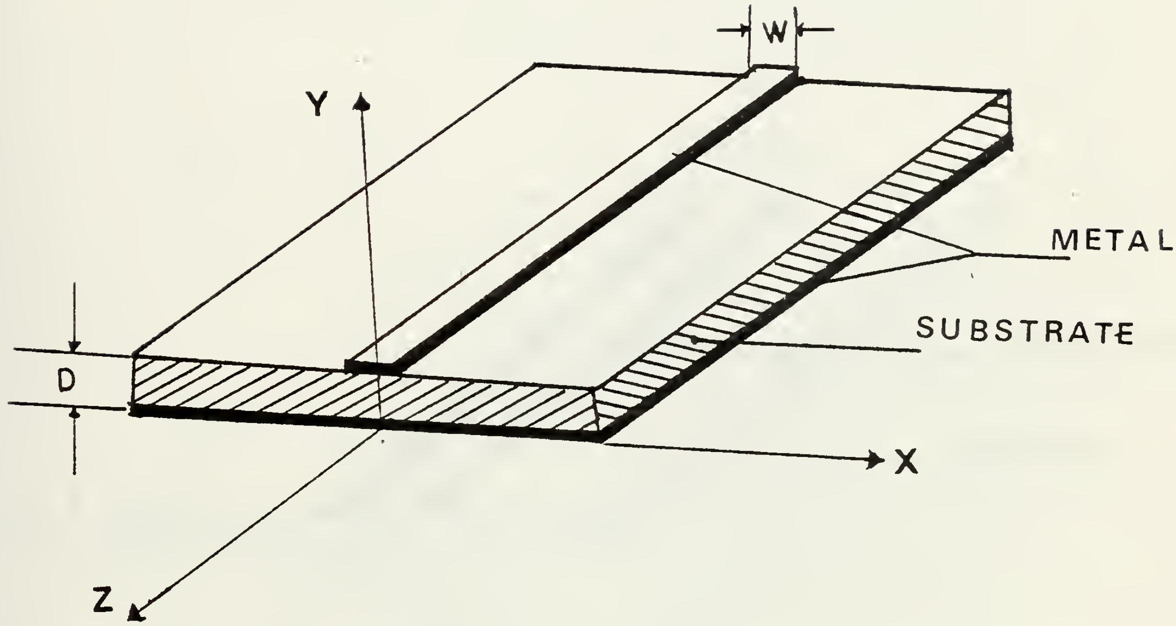

FIGURE 1·1 MICROSTRIP TRANSMISSION LINE

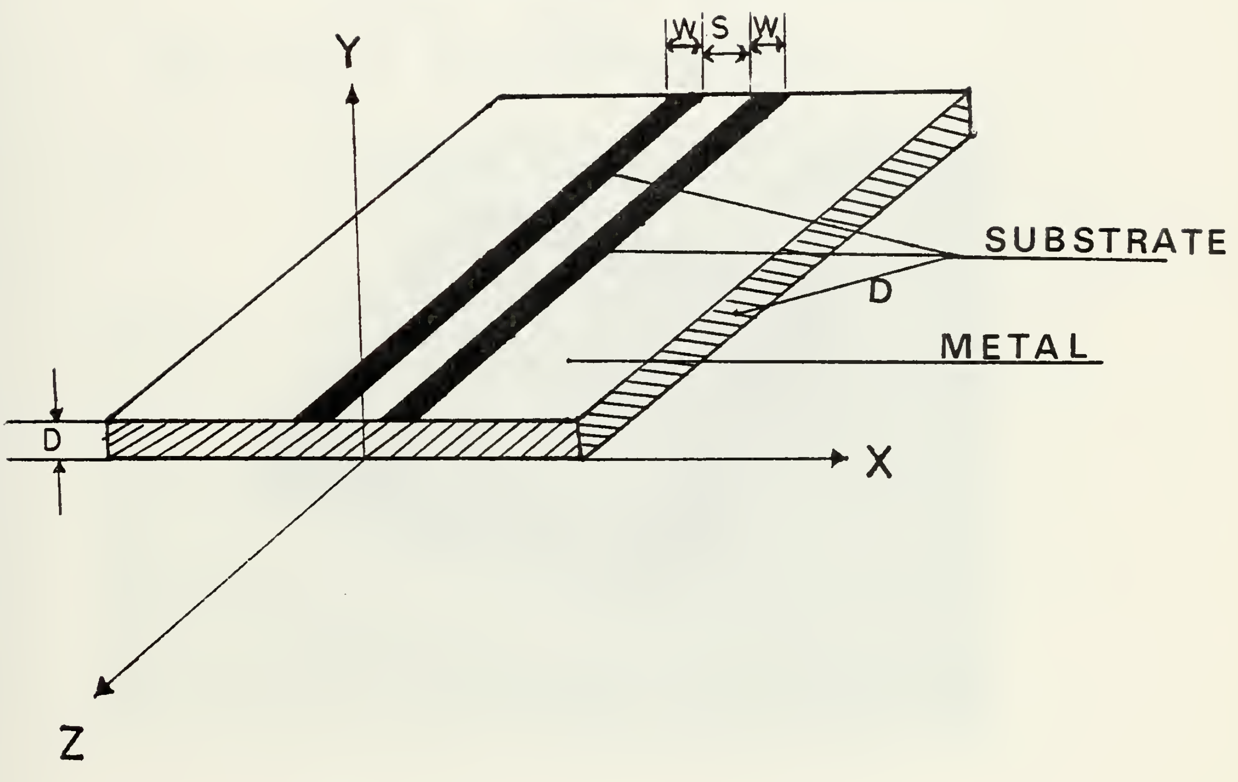

FIGURE 1·2 PARALLEL COUPLED SLOT TRANSMISSION LINE

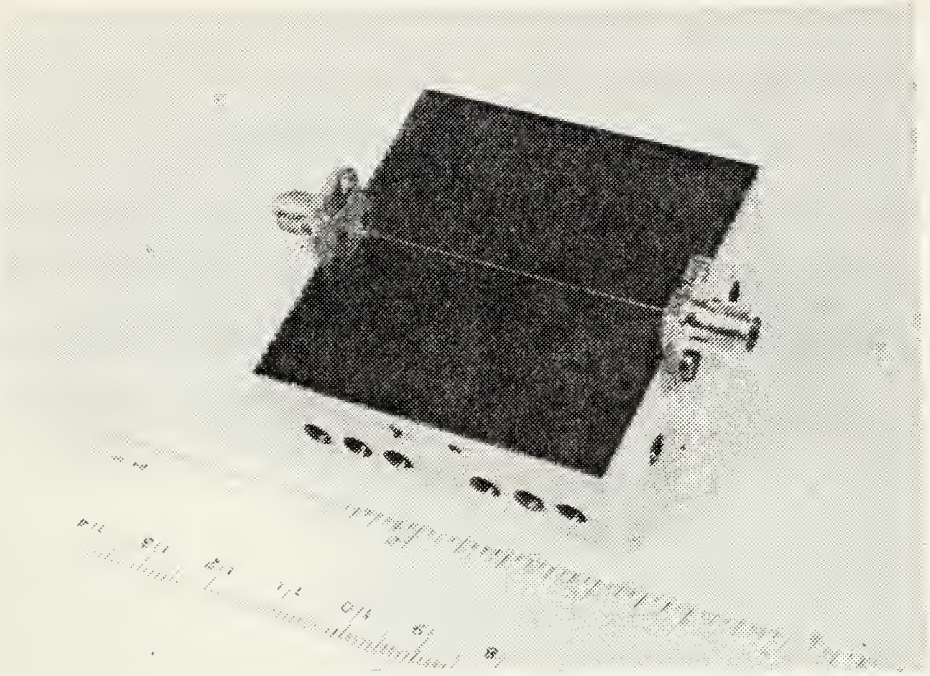

Figure 3.1a
Microstrip Transmission Line

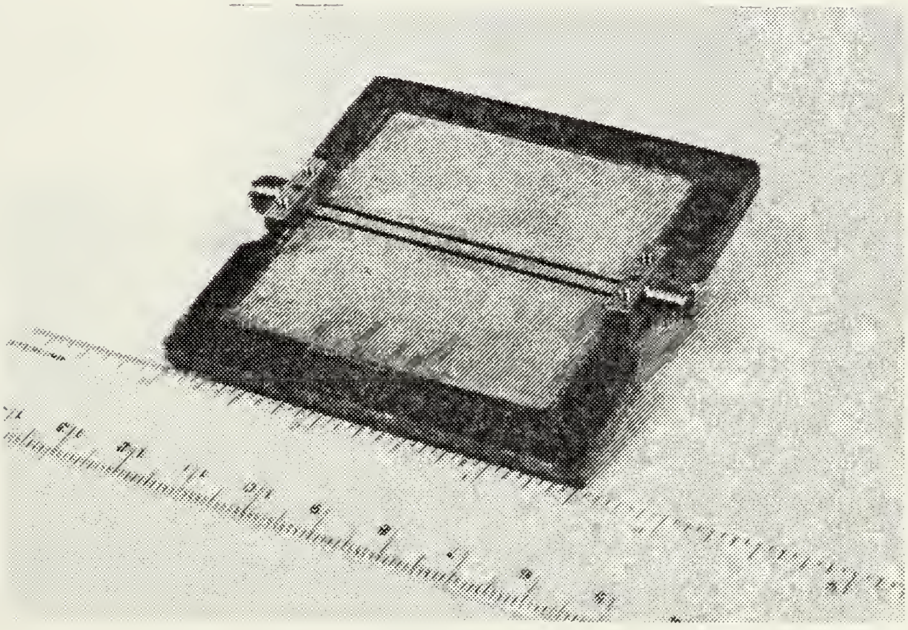

Figure 3.1b

Coplanar Transmission Line

not yet any exact mathematical solutions to describe the behavior of these two structures. Although perturbation theory was used by A. M. Tufekcioglu [Ref. 1] and K. D. Kuchler [Ref. 2] to indicate the attenuation and phase shift for these structures and their results were used to make comparison with the experimental results obtained in this thesis, the comparison is far from satisfactory.

II. MICROSTRIP EXPERIMENTAL RESULTS

A. RESONANT FREQUENCY DIAGRAM

Experiments using microstrip on ferrite substrate were carried out to obtain the resonant frequency of microstrip as a function of the applied biasing magnetic field. The resonant frequency diagram of a transversely magnetized Trans Tech G1001 garnet material ($4\pi M_s$ = 1200 gauss, ε_f = 15.2) was measured using a microstrip of an overall dimension of 1" x 1", having a width of strip W = 0.508, and thickness of substrate D = 0.635 mm. The microstrip was designed to give a nominal 50Ω characteristic impedance for dielectric substrate taking into account Wheeler permittivity [Ref. 6]. It was coupled to the 50Ω input, and output lines of a Hewlett-Packard HP 8410S network analyzer using SMA launchers and 0.085 coax (solid gasket) and the transmission resonance frequencies were measured as a function of the applied biasing magnetic field, directed normal to the substrate (Y direction; see Fig. 1-1). The applied biasing magnetic field was measured by a guass-meter. The results are tabulated in Table 2. Figure 2-1 shows the experimental resonance frequency of the microstrip as a function of the applied magnetizing field. Also shown is the ferromagnetic resonance frequency

$$f_r = \gamma \ (H_a - N_z \ 4\pi M_s) \qquad (1)$$

where

f_r = resonance frequency in MHz.

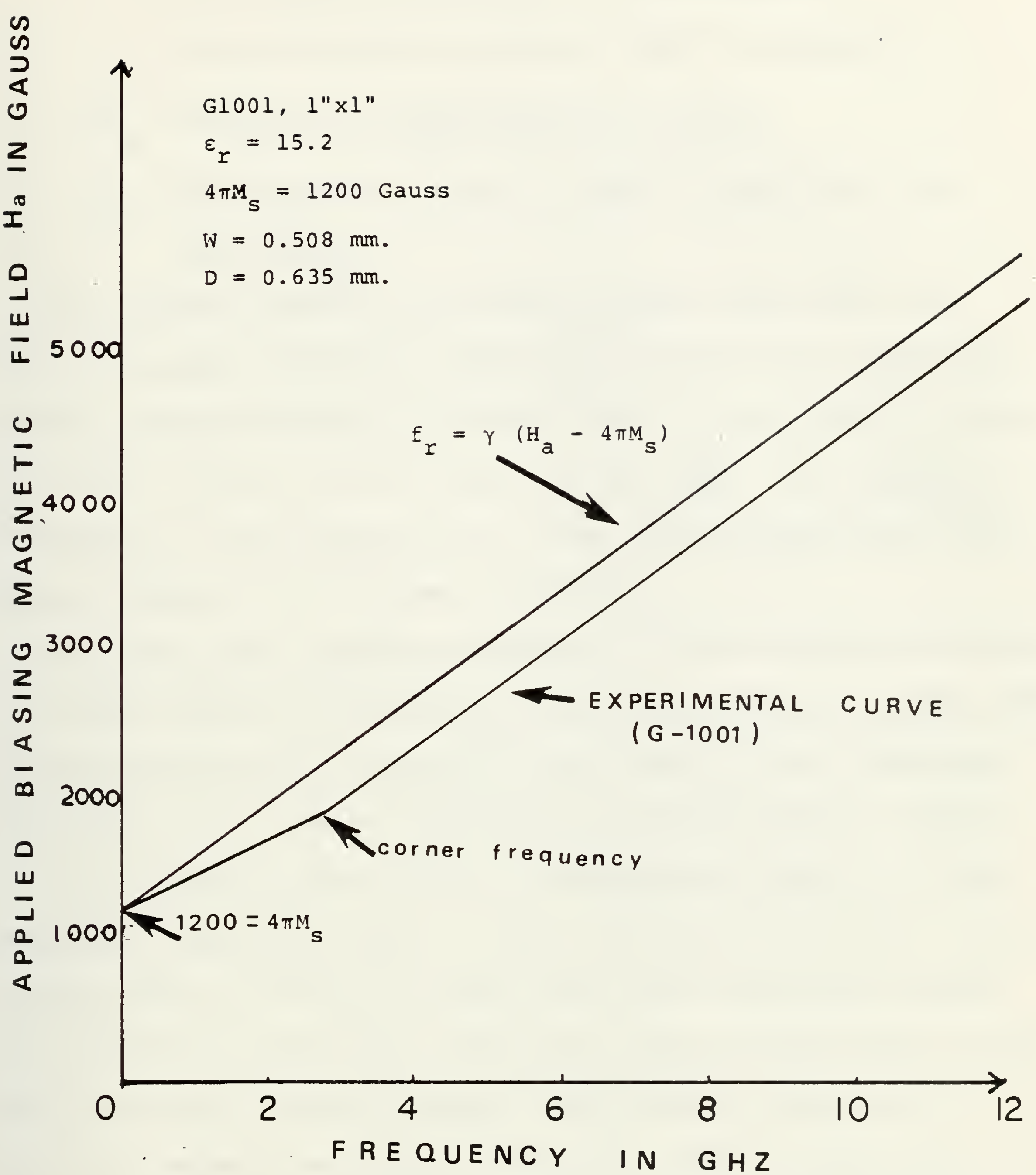

Figure 2-1. Resonance Frequency vs. Transverse Applied Biasing Magnetic Field of Microstrip Transmission Line

γ = gyromagnetic rotation in MHz/oersted.

H_a = applied biasing magnetic field in oersted.

$4\pi M_s$ = saturation magnetization in gauss.

N_a = demagnetizing factor, which is equal to 1 in this case.

The applied magnetic field was raised from 1400.0 to 4860.0 oersteds, while the frequency of the sweep oscillator of the network analyzer was swept from 1 to 12.4 GHz in steps of 1 to 2, 2 to 4, 4 to 8 and 8 to 12.4 GHz. The resonant frequency of the microstrip was read from the amplitude frequency display of the network analyzer.

The amplitude frequency response of the microstrip was that of a band rejection filter and the corresponding frequency for maximum transmission attenuation was taken as the resonance frequency, as a function of applied biasing magnetic field.

With regard to Fig. 2-1, an interesting feature of the resonance frequency curve is that it has two gradients, namely from 1200 to 1700.0 oersteds and 1700.0 oersteds onward. The reason for having two gradients could be attributed to the fact that below 1700.0 oersted, the ferrite substrate is partially magnetized whereas above the 1700.0 oersted the ferrite substrate is fully magnetized.

The experimental curve above 1700.0 oersted runs parallel to the curve plotted from Equation 1.

It is also of interest to notice that the experimental curve eventually intersects the vertical axis at 1200 oersteds which is the saturation magnetization of G1001 and satisfies Equation 1 at this point.

B. DISPERSION DIAGRAM (ZERO APPLIED MAGNETIZATION FIELD)

Experiments using microstrip on ferrite substrate were conducted in order to obtain the phase shift as a function of frequency in the case of zero applied magnetization field. The ferrite was G1001 and the microstrip was of the same dimension and design as the line described in the previous section.

Figures 2-2 to 2-5 show the photographs of the phase-frequency display on the network analyzer. The data obtained from these photographs were tabulated in Table III, Appendix A. The above-mentioned data were plotted in Figure 2-6. Also shown is the result of the computer analysis for dielectric substrate [See Ref. 1].

D. H. Harris, F. J. Rosenbaum and C. G. Aumiller [Ref. 8] have developed a formula for parallel plane waveguide filled with ferrite material. Assuming T.E.M.-limit mode approximation, at zero applied field the formula for propagation constant is

$$\beta_T = \frac{\omega}{C} \sqrt{\mu_e \varepsilon_f} \tag{1}$$

where [Ref. 9]

$$\mu_e = \frac{1}{3} + \frac{2}{3}\left[1 - \left(\frac{\omega_m}{\omega}\right)^2\right]$$

$$\omega_m = 2\pi\gamma(4\pi M_s)$$

The theoretical curve in Figure 2-6 is the plot of equation (1). It is the infinite parallel plane waveguide filled with ferrite substrate (G1001).

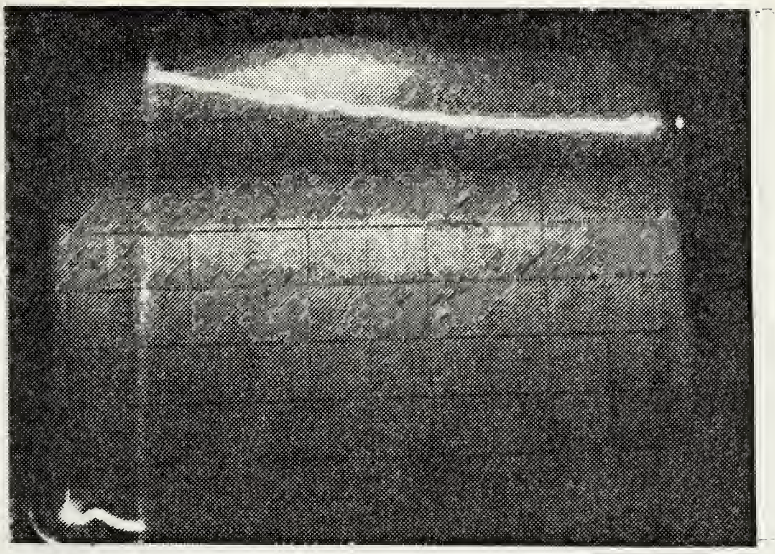

Figure 2-2.
Vertical Axis:
Phase Shift,
Scale 45 deg/DIV

Microstrip phase shift vs. frequency in the absence of external magnetic field, 1" substrate (G1001). Horizontal axis: frequency sweep from 1 to 2 GHz.

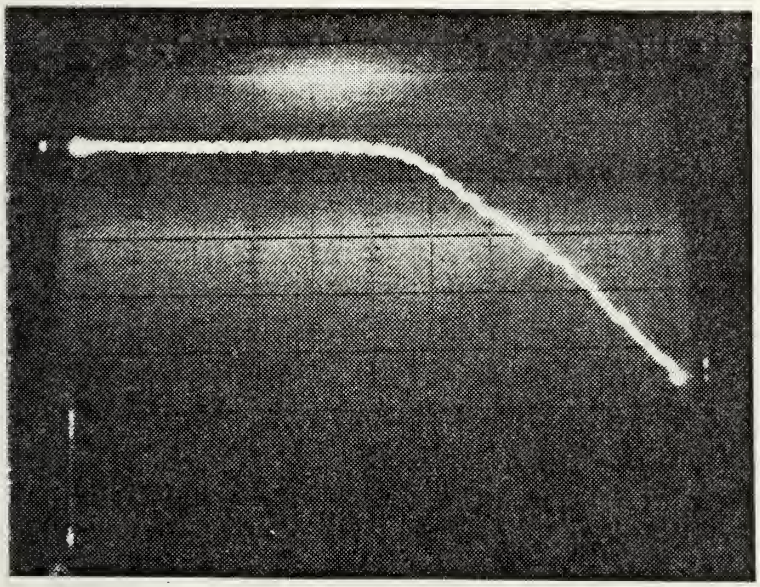

Figure 2-3.
Vertical Axis:
Phase Shift,
Scale 45 deg/DIV

Microstrip phase shift vs. frequency in the absence of external magnetic field, 1" substrate (G1001). Horizontal axis: frequency sweep from 2 to 4 GHz.

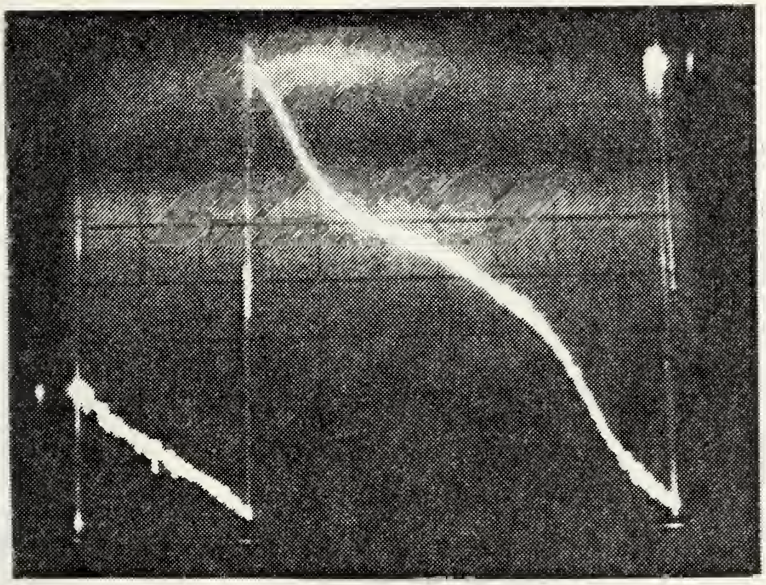

Figure 2-4.
Vertical Axis
Phase Shift,
Scale 45 deg/DIV.

Microstrip phase shift vs. frequency in the absence of external magnetic field, 1" substrate (G1001). Horizontal axis: frequency sweep from 4 to 8 GHz.

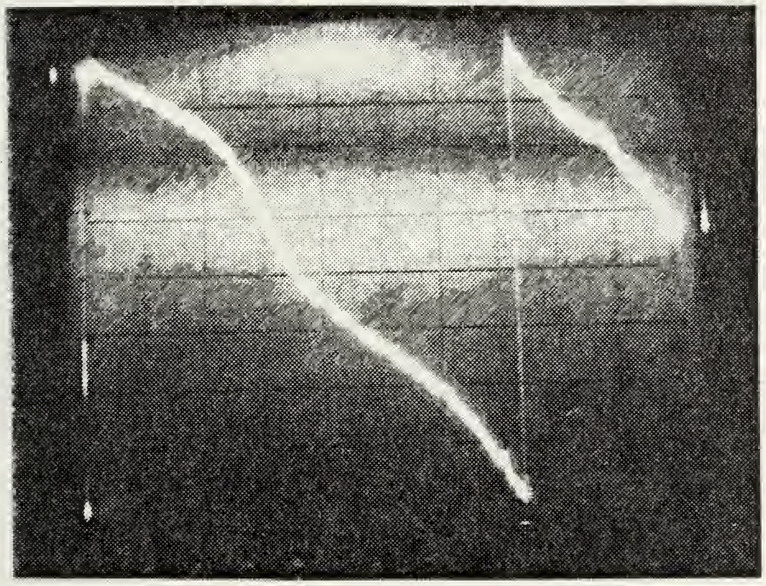

Figure 2-5.
Vertical Axis
Phase Shift
Scale 45 deg/DIV.

Microstrip phase shift vs. frequency in the absence of external magnetic field, 1" substrate (G1001). Horizontal axis: frequency sweep from 8 to 12.4 GHz.

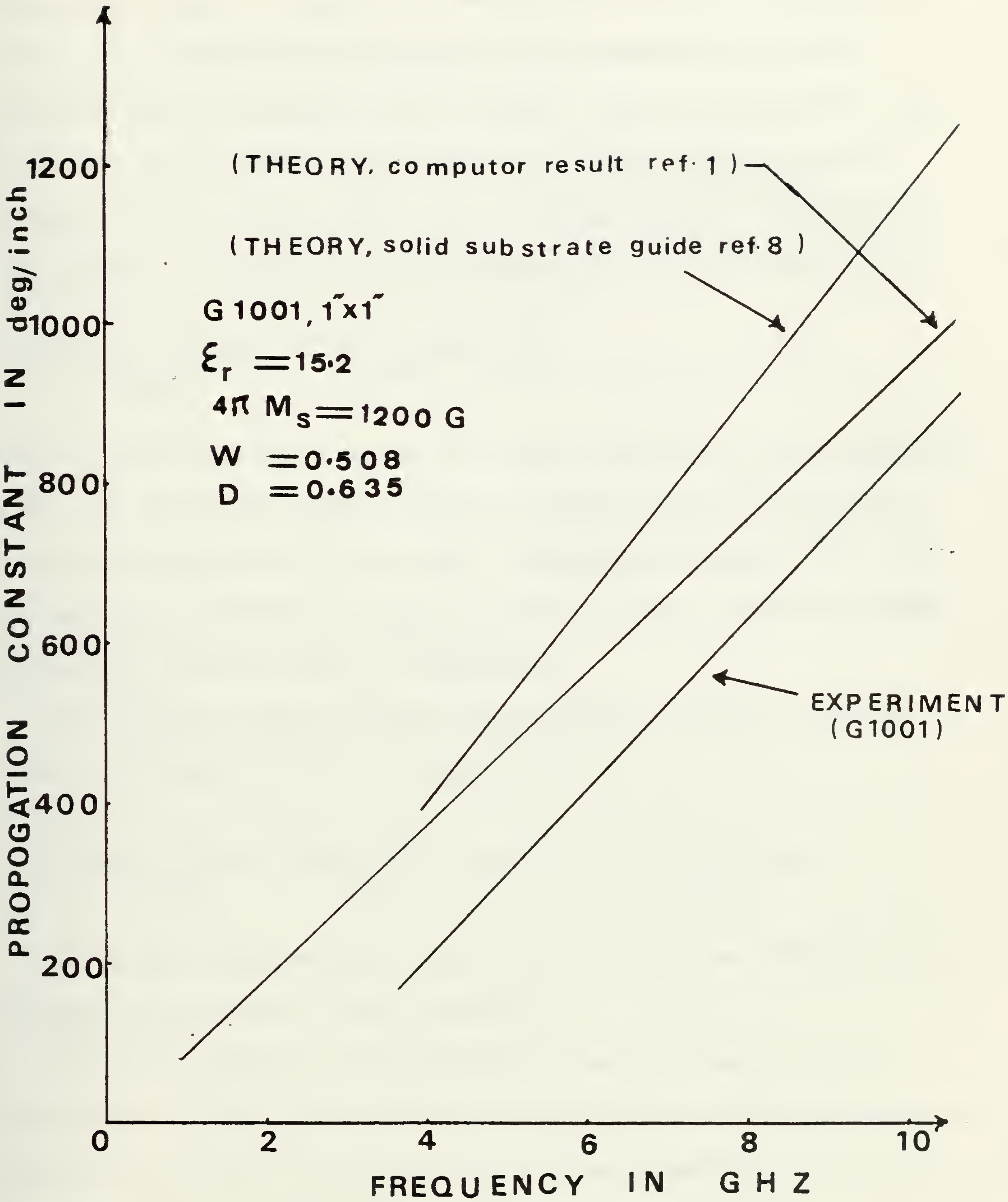

Figure 2-6. Comparison of Experimental and Theoretical Results for Microstrip Transmission Line.

Also plotted is the computer analysis result for dielectric substrate based on the theory developed by A. M. Tufecioglu [Ref. 1]. The experimental curve as measured by network analyzer has a somewhat higher sloper than the computer analysis curve, but smaller than the theoretical slope based on formula (1). One can define an "average error" between the experimental results and the approximate theory (equation 1)

$$\frac{\beta_{theory} - \beta_{exp}}{\beta_{exp}} = \frac{1040 - 740}{740} \times 100 = 40.5\% \text{ at } 9 \text{ GHz.}$$

This is a considerable error at 9 GHz, showing at zero applied field the parallel plane theory is within 40% of microstrip experimental results. At higher frequencies than 9 GHz, the average error decreases from the above figure, where at lower frequencies than 9 GHz, it increases.

The average error between experimental results and the computer analysis [Ref. 1] result is

$$\frac{\beta_{comp} - \beta_{exp}}{\beta_{exp}} = \frac{860 - 740}{740} \times 100 = 16.2\% \text{ at } 9 \text{ GHz.}$$

At higher frequencies than 9 GHz, the above average error decreases and below 9 GHz increases.

This in itself is a significant result showing that at zero applied field, the theory for microstrip on a dielectric substrate is within about 16% of the experimental result for microstrip on a ferrite (G1001) substrate.

From Figure 2-3, it is evident that the phase shift is constant in the frequency range of approximately 2 to 3 GHz, indicating low field losses. In this region the microstrip

is behaving as a band rejection filter because of low field losses [Ref. 3]. The effect of low field loss is better seen in the Insertion Loss Photograph, Fig. 2-8.

C. INSERTION LOSS

Experiments were carried out using the same microstrip as in the previous sections, in order to establish the insertion loss at various frequencies in the absence of any external magnetization field.

The effect of low field losses is very clearly evident in Fig. 2-8 where 20 db loss is indicated from 1.98 to 2.8 GHz. Figure 2-9 indicates the insertion losses from 4 to 8 GHz, with a maximum insertion loss of approximately 10 db at frequencies of 4.5 and 6.4 GHz.

D. REFLECTION

Experiments were carried out on the same microstrip as described in order to establish the reflection at the Input Port. Figures 2-10 and 2-11 are the photographs from 1.98 to 4, 4 GHz to 8 GHz frequency band. On the average, the return loss is approximately 17 db from 2 to 4 GHz and 14 db from 4 to 8 GHz. Figure 2-9 and 2-11 show clearly that an impedance mismatch is present at the input and output connectors and that when the reflections cancel, transmission loss decreases to -2 db, indicating low attenuation due to magnetic loss.

E. DISPERSION AND ATTENUATION WITH A BIASING FIELD

1. Transverse Magnetic Field of 1730 Oersteds

a. Dispersion Diagram

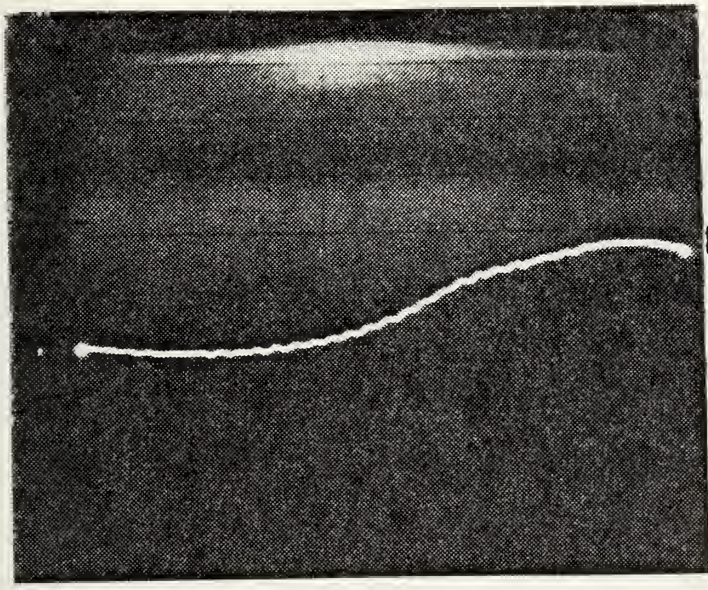

Figure 2-7.
Vertical axis:
Attenuation Scale
10 db/DIV.
Zero db Reference.

Microstrip insertion loss in the absence of external magnetic field, 1" substrate (G1001). Horizontal axis: frequency sweep from 1.981 to 4.09 GHz.

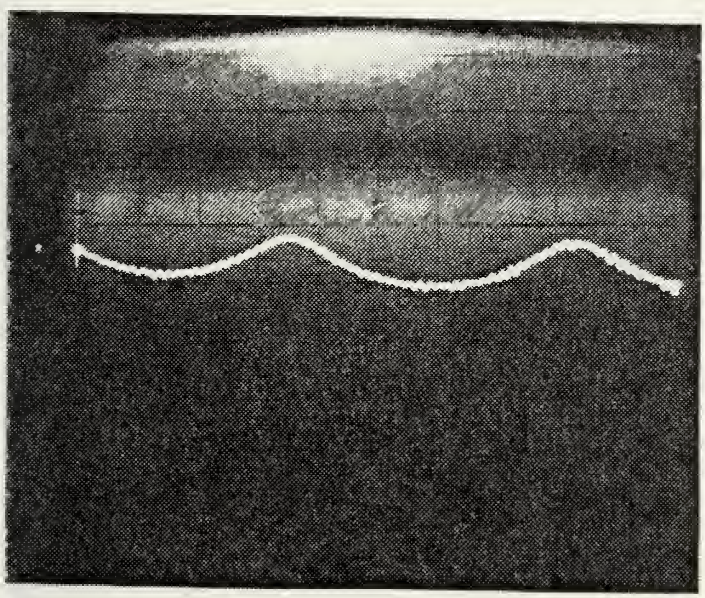

Figure 2-8.
Vertical axis:
Attenuation 10 db/DIV.
Zero db Reference.

Microstrip insertion loss in the absence of external magnetic field, 1" substrate (G1001). Horizontal axis: frequency sweep from 4 to 8 GHz.

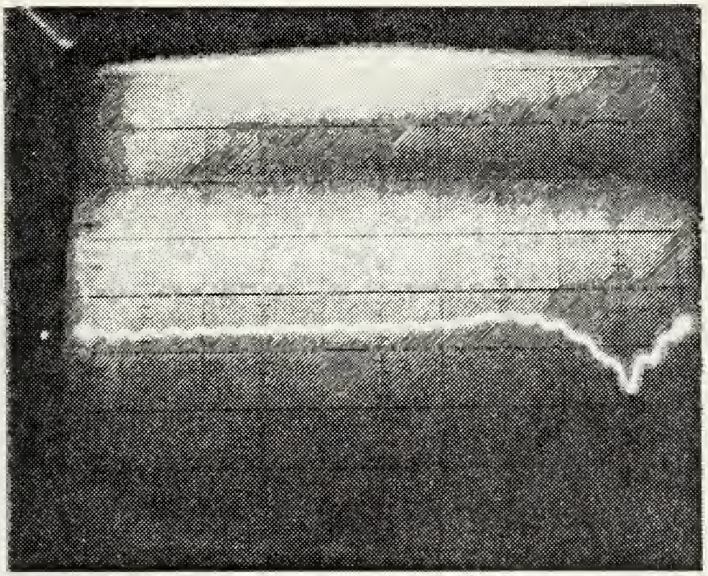

Figure 2-9.
Vertical axis:
Return Loss Scale
10 db/DIV.
Zero db Reference.

Microstrip Return loss vs. frequency in the absence of external biasing magnetic field, 1" substrate (G1001). Horizontal axis: frequency sweep from 1.98 to 4.09 GHz.

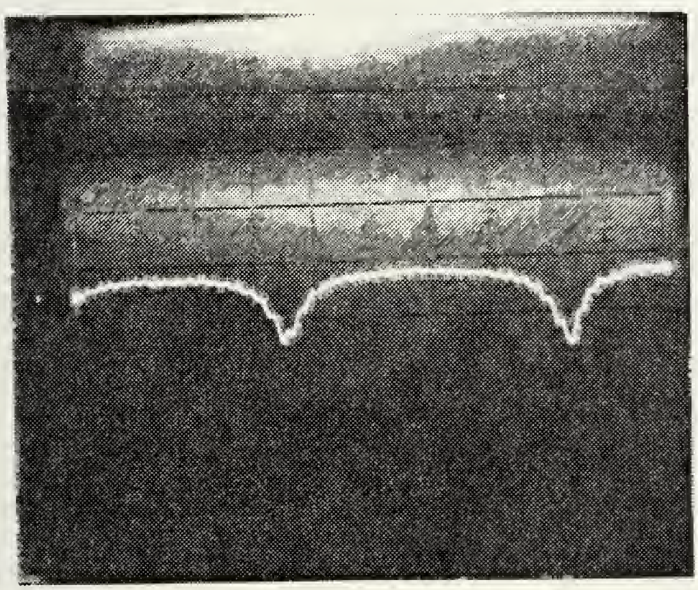

Figure 2-10.
Vertical axis:
Return Loss Scale
10 db/DIV.
Zero db Reference.

Microstrip return loss vs. frequency in the absence of external biasing magnetic field, 1" substrate (G1001). Horizontal axis: frequency sweep from 3.998 to 8.031 GHz.

Experiments were conducted using G1001, 1" substrate with dimensions of $W = .508$ mm, $D = .635$ mm, to obtain the dispersion diagram of the microstrip. The ω-β diagram of a transversely magnetized G1001 garnet material was obtained using a microstrip with an external magnetization field of 1730 oersted in the y direction (See Fig. 1-1). The microstrip was designed to give a nominal 50Ω characteristic impedance taking into account the Wheeler permittivity [Ref. 6].

It was coupled to 50Ω input and output lines to the network analyzer. The phase shift as a function of frequency was photographed on the phase-frequency display of the network analyzer. The external biasing magnetic field was kept constant at 1730 oersted while the frequency was swept from 1.0 to 2.0, 2.0 to 4.0 and 4.0 to 8.0 GHz. Figures 2-11 and 2-12 indicate the phase-frequency display for both directions of propagation. The resonance frequency occurred at approximately 2.8 GHz. The results from pictures 2-11 and 2-12 are plotted in Fig. 2-13 for both directions of propagation. It is evident from Fig. 2-13 that any difference in phase shift for the two directions of propagation is indistinguishable from experimental error. The data is tabulated in Tables 5 and 6.

From Fig. 2-13 it is evident that there are two regions of propagation, a lower branch extending to zero and an upper branch. These are separated by a cutoff region where

$$\mu_{eff} = \frac{\mu^2 - \kappa^2}{\mu} < 0.$$

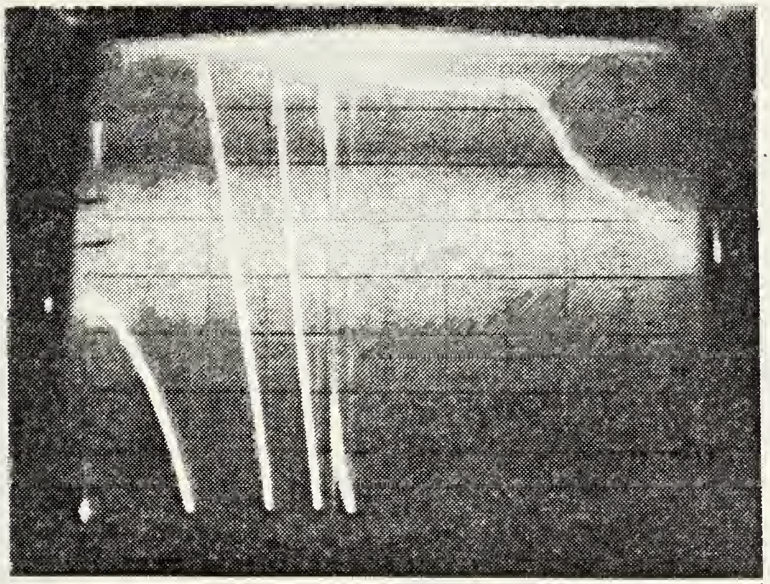

Figure 2-11.
Z^+ Direction of Propagation

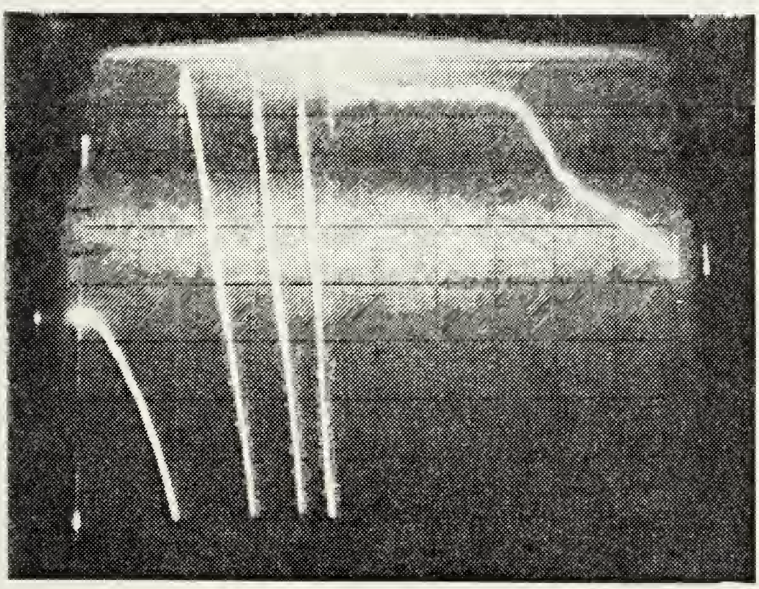

Figure 2-12.
Z^- Direction of Propagation.

Microstrip Phase Shift vs. frequency. External tranverse biasing magnetic field = 1730 oersteds. 1" substrate (G1001). Horizontal axis: frequency sweep from 2 to 4 GHz. Vertical axis: 45 Deg./DIV.

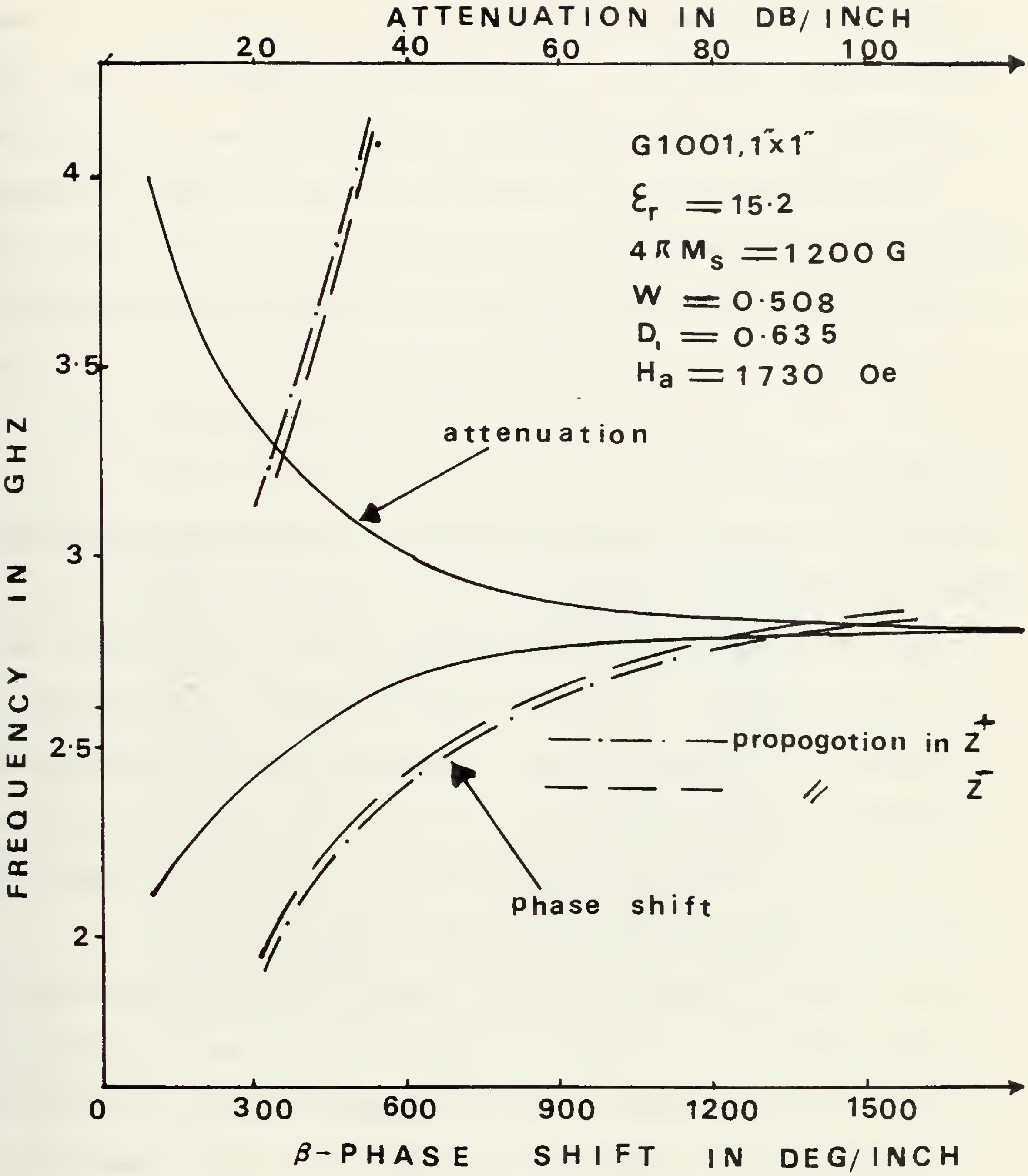

Figure 2-13. Propagation Constant of Transverse Magnetized Microstrip Transmission Line for both Directions of Propagation, Z^-, Z^+

The stop band is centered around the resonance frequency where there is no propagation. The stop band here is approximately from 2.80 to 3.15 GHz, a bandwidth of 0.35 GHz. As the resonance frequency is approached, the slope of the ω-β diagram decreases and beyond the cutoff region it starts increasing again. The cutoff region can be tuned in frequency by changing the applied biasing magnetic field H_a throughout the frequency band.

b. Attenuation

The insertion loss of a 1" length of 50Ω (nominal) characteristic impedance microstrip on G1001 material is shown in Fig. 2-14 for a 1730 oersted of biasing field applied transverse to the direction of propagation. The line width was $W = .508$ mm and substrate height was $D = .635$ mm. The attenuation photograph indicates that the maximum insertion loss occurs at the notch which is at the resonance frequency where more than 120 db of attenuation occurred.

Above and below the resonance, the loss decreases and approaches about the same value of insertion loss as in the absence of an applied magnetic field. The notch depth is a function of applied magnetic field. Throughout the 2 to 4 GHz frequency range, the depth of the notch varied approximately from 60 db to 120 db. Also of interest is the fact that the losses in both directions of propagation were the same which indicates the microstrip is reciprocal in this mode of propagation, although the field configurations for the two directions are probably different. This behavior is a result

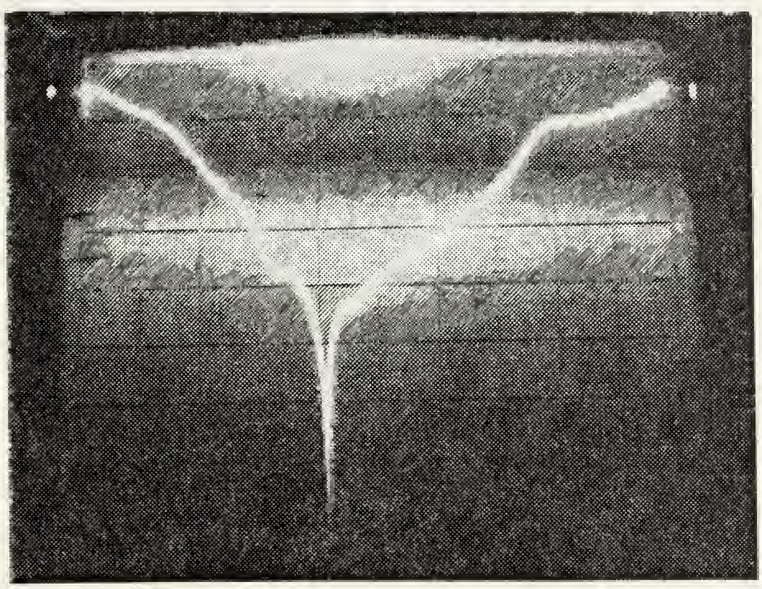

Figure 2-14. Microstrip attenuation vs. frequency. External transverse biasing magnetic field = 1730 oersteds, 1" substrate (G1001). Horizontal axis: frequency sweep from 2 to 4 GHz. Vertical axis: 10 db/DIV. Z^+ Direction of Propagation.

of the absence of a significant longitudinal magnetic field component for <u>this</u> line geometry in this frequency range.

Figure 2-15 indicates the return loss which is almost constant through the frequency band of 2 to 4 GHz and is about -18 db indicating a reasonably good impedance match to the 50Ω coaxial lines.

2. <u>Transverse Magnetic Field of 2670 Oersteds</u>

a. Dispersion Diagram

Experiments were conducted using the same microstrip with an applied magnetization field of 2670 oersted to determine the ω-β diagram of the microstrip. The field was applied in the transverse direction (y direction, see Figure 1-1). Figures 2-16 and 2-17 indicate the phase shift as a function of frequency from 3.998 to 8.031 GHz for both directions of propagation. Figure 2-18 was constructed using the data from Fig. 2-16. The resonance frequency is approximately 5.192 GHz.

The stop band is approximately from 5.1 to 5.7 GHz, a bandwidth of 0.6 GHz.

From Figures 2-16 and 2-17, it is evident that the phase shift is the same in both directions of propagation and the microstrip is acting as a reciprocal tunable band rejection filter. The data are tabulated in Table 6, Appendix A.

b. Attenuation

Experiments were conducted using the same microstrip with an applied magnetization field of 2670 oersted to determine the insertion loss. Figures 2-19 and 2-20 indicate the attenuation in both directions of propagation as a

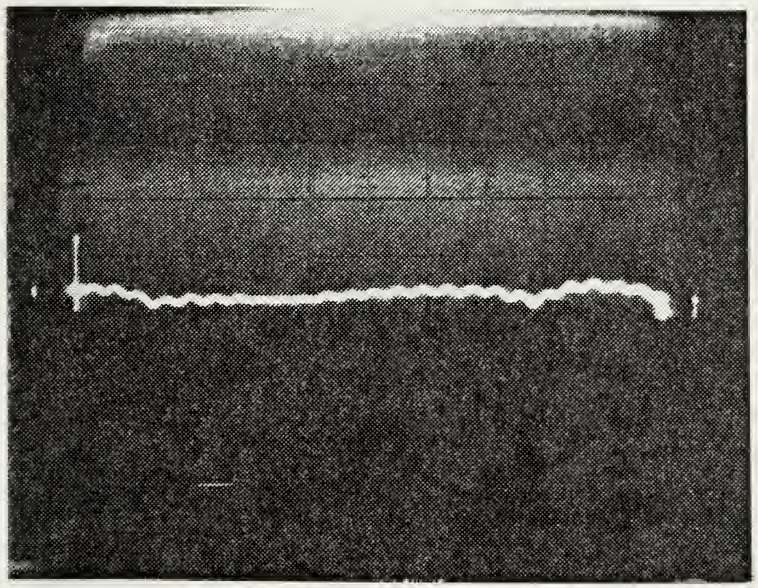

Figure 2-15. Microstrip return loss vs. frequency. External transverse biasing magnetic field = 1730 oersteds, 1" substrate (G1001). Horizontal axis: frequency sweep from 2 to 4 GHz. Vertical axis: 10db/DIV. Z^+ Direction of Propagation.

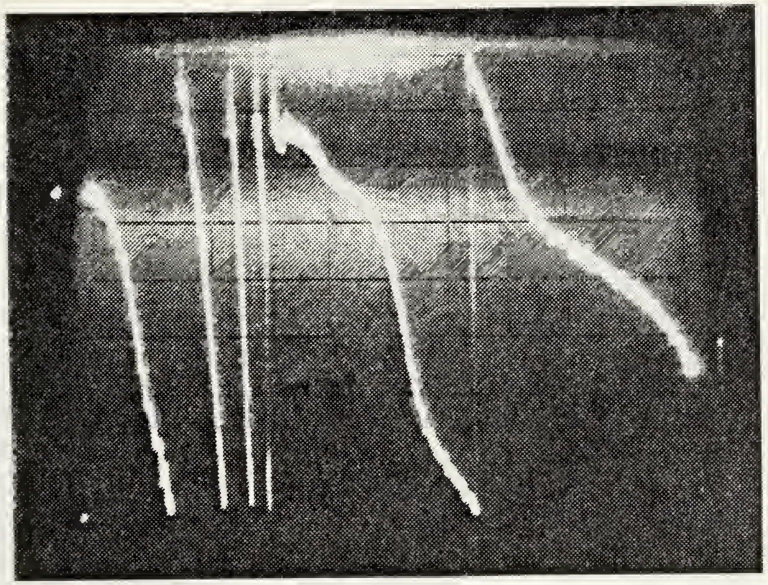

Figure 2-16

Z^{+} Direction of Propagation

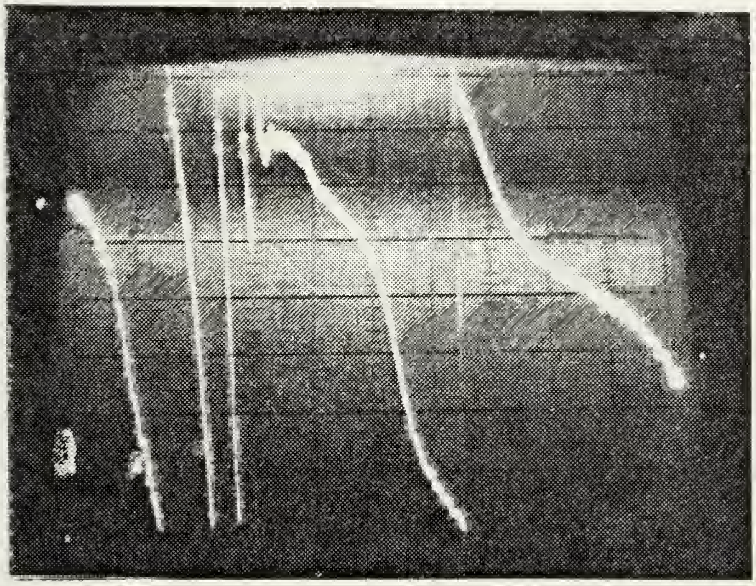

Figure 2-17

Z^{-} Direction of Propagation

Microstrip phase shift vs. frequency. External transverse biasing magnetic field = 2670 oersteds, 1" substrate (G1001). Horizontal axis: frequency sweep from 3.998 to 8.031 GHz. Vertical axis: 45 deg/DIV.

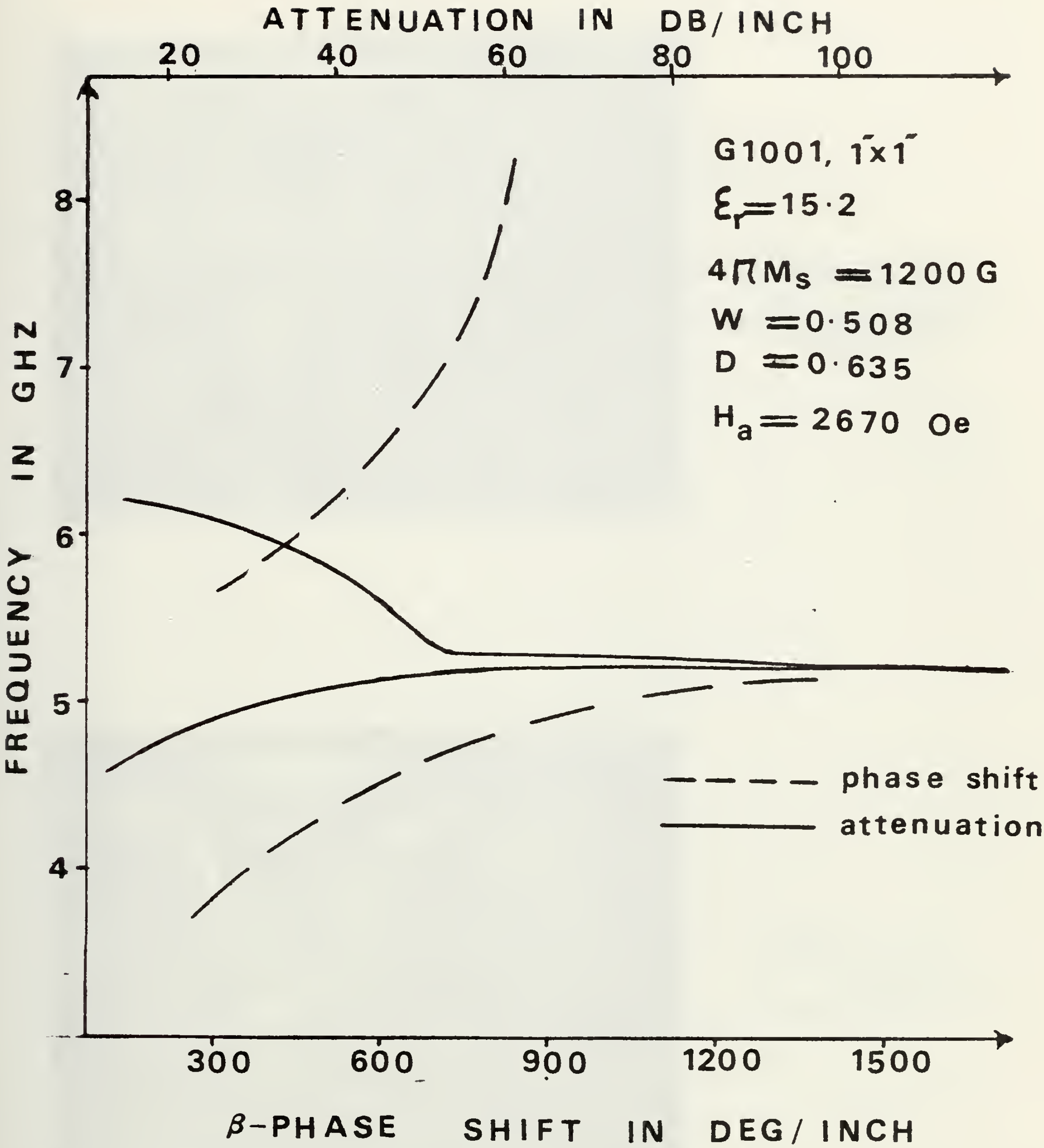

Figure 2-18. Propagation Constant of Transverse Magnetized Microstrip Transmission Line

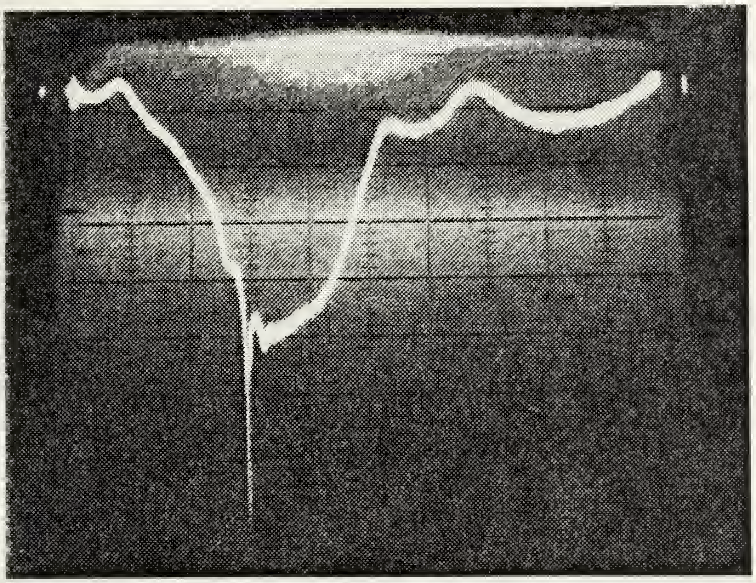

Figure 2-19
Z^+ Direction of
Propagation

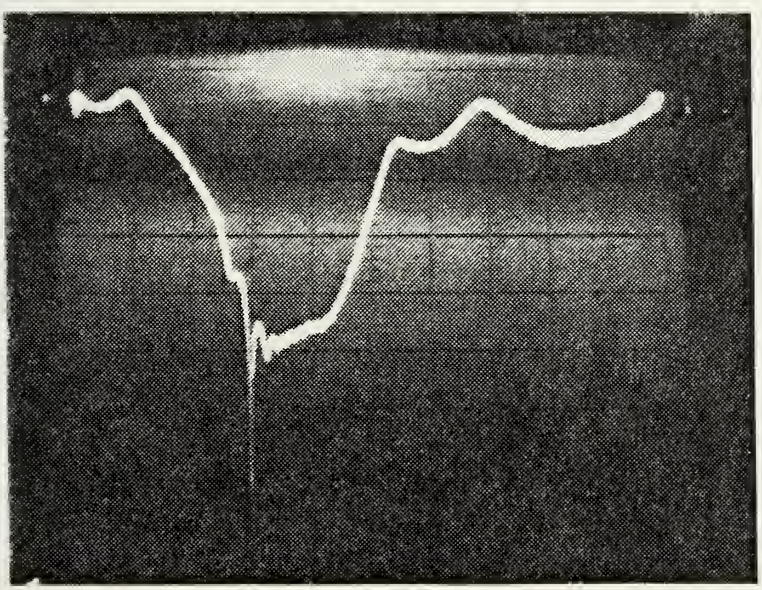

Figure 2-20
Z^- Direction of
Propagation

Microstrip attenuation vs. frequency. External transverse biasing magnetic field = 2670 oersteds, 1" substrate (G1001). Horizontal axis: frequency sweep from 3.998 to 8.031 GHz. Vertical axis: 10 db/DIV.

function of frequency from 3.99 to 8.031 GHz. From the figures it is evident that attenuation is maximum at the notch which is more than 120 db and occurs at the resonance frequency of approximately 5.192 GHz.

The overall loss across the stop band from 5.1 to 5.7 GHz is approximately 46 db.

Figure 2-21 indicates the return loss as a function of frequency from 3.998 to 8.031 GHz.

The value of return loss averages approximately -17 db through the band. Some deterioration of the impedance notch may be may be noted toward the upper end of the band, however.

3. <u>Transverse Magnetic Field of 3100 Oersteds</u>

a. Dispersion Diagram

In this experiment the magnetization was H_a = 3100.0 oersted applied in the transverse direction (y direction, see Fig. 1-1) and the substrate was the same as before. The measured resonance frequency was f_r = 6.364 GHz. Figures 2-22 and 2-23 indicate the phase as a function of frequency from 4 to 8 GHz for both directions of propagation. The dispersion diagram, Figure 2-24, is obtained from Fig. 2-23. The data is tabulated in Table 7 of Appendix A. It is evident from Figure 2-24 that the stop band is from 6.3 to 7.1 GHz, a bandwidth of 0.8 GHz.

D. H. Harris, F. J. Rosenbaum, and C. G. Aumiller [Ref. 7] have developed a formula for propagation constant for infinite ferrite filled parallel plane waveguide. For the ferrite magnetized in the y-direction (Fig. 1-1), the

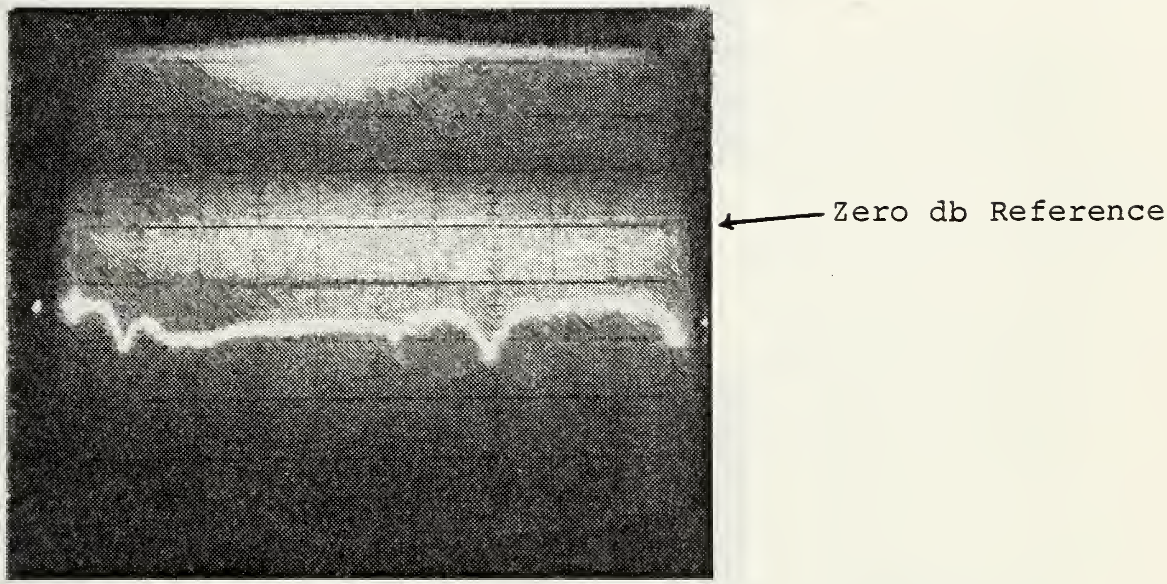

Figure 2-21. Microstrip return loss vs. frequency. External transverse biasing magnetic field = 2680 oersteds, 1" substrate (G1001). Horizontal axis: frequency sweep from 3.998 to 8.031 GHz. Vertical axis: 10 db/DIV. Z^{+} direction of propagation.

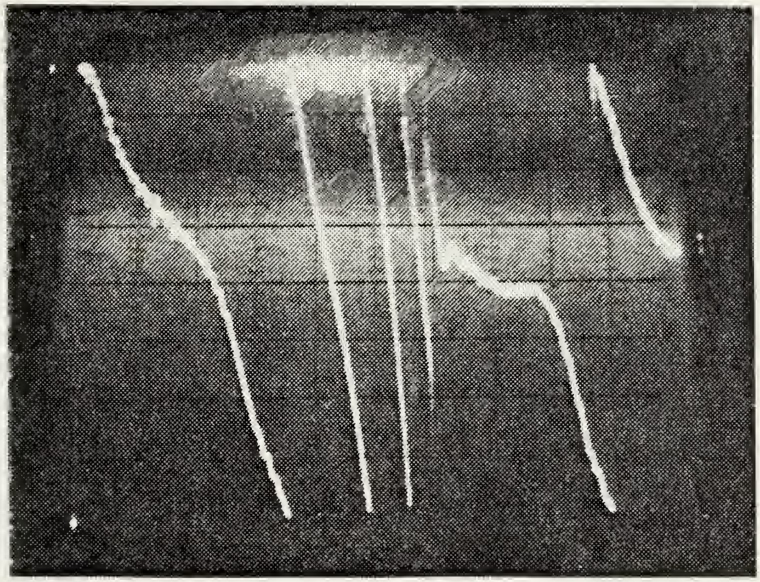

Figure 2-22
Z^- Direction of Propagation

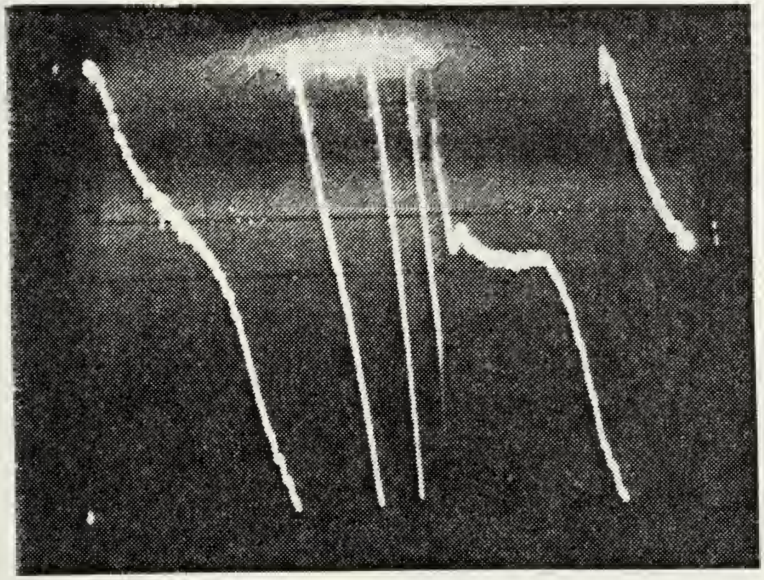

Figure 2-23
Z^+ Direction of Propagation

Microstrip phase shift vs. frequency. External transverse biasing magnetic field = 3100 oersteds, 1" substrate (G1001). Horizontal axis: frequency sweep from 4 to 8 GHz. Vertical axis: 45 deg/DIV.

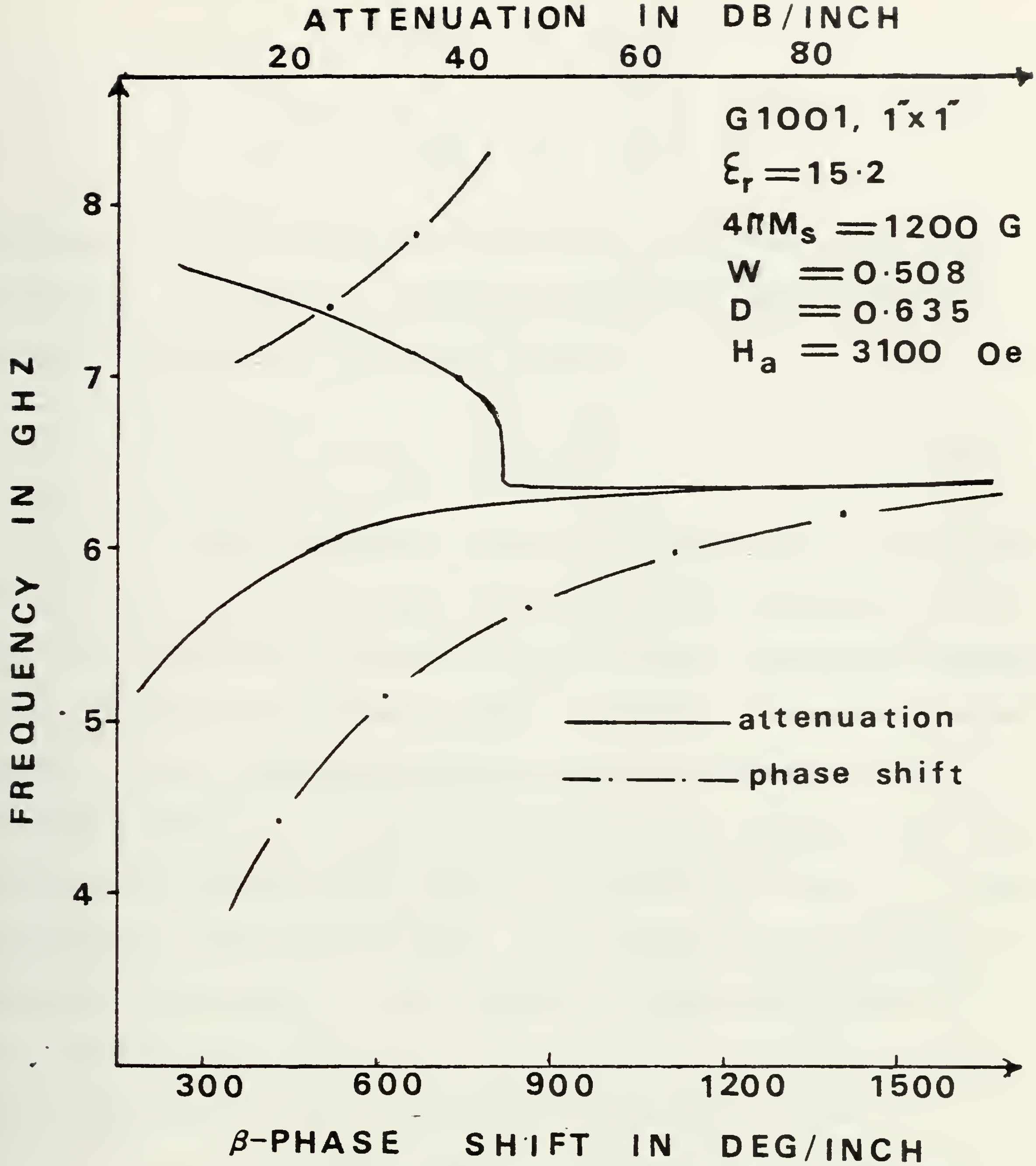

Figure 2-24A. Propagation Constant of Transverse Magnetized Microstrip Transmission Line.

Polder tensor takes the forms where

$$\underline{\mu} = \mu_0 \begin{vmatrix} u & 0 & -JK \\ 0 & 1 & 0 \\ JK & 0 & u \end{vmatrix} . \quad (1)$$

Assuming that the fields in the lowest order mode are independent of x and y, Maxwell's equations yield solutions with the propagation constant given by

$$\beta = \pm K \, (\mu_{eff})^{\frac{1}{2}} \quad (2)$$

The propagation constant in Equation (2) for lossless infinite ferrite filled parallel plane waveguide is the same for longitudinal magnetization and for transverse magnetization normal to the planes [Refs. 7 and 8]. Equation (2) was assumed to be a good approximation for a microstrip ring resonator and was compared with experimental results [Ref. 8]. Figure 2-24B exhibits the plot of Equation (2) for $H_a = 3100$ oersteds for G1001 microstrip. The results are tabulated in Table 8 of Appendix A. Also plotted in the same figure is the experimental result for transverse magnetization normal to the substrate of G1001 microstrip transmission line.

It is evident that the experimental result and the plot of Equation (2) are not in agreement. The theoretical result indicates a much wider stop band than the experimental one.

Another point of interest is that the experimental result as in Fig. 2-36 indicates that the ω-β diagram is different for transverse and longitudinal magnetization whereas

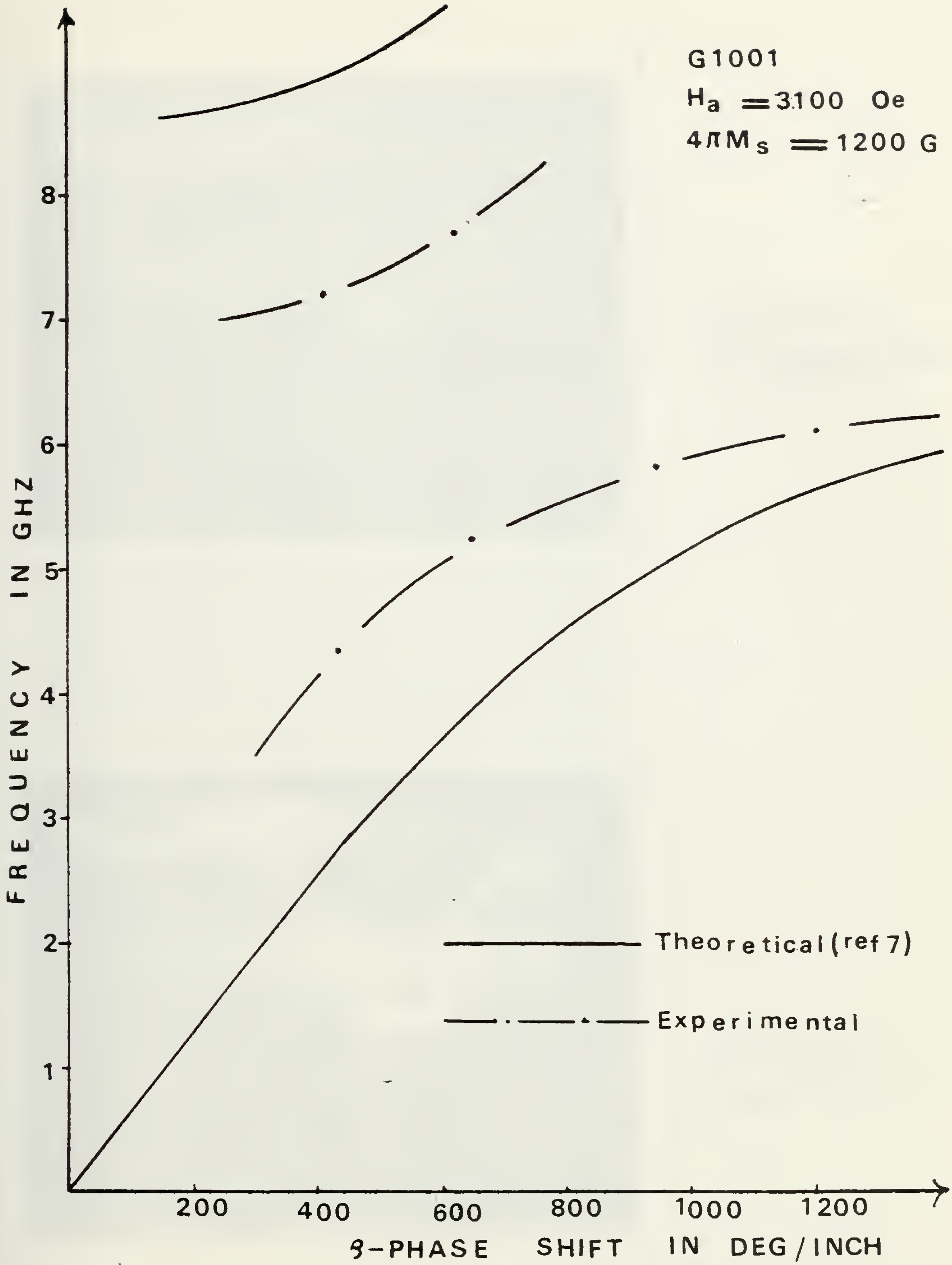

Figure 2-24B. Propagation Constant of Transverse Magnetized Microstrip Transmission Line.

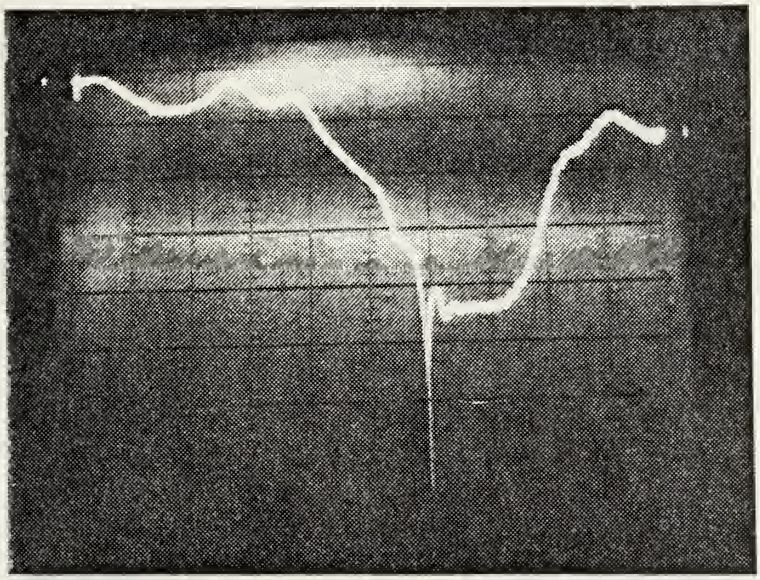

Figure 2-25
Z^- Direction of
Propagation

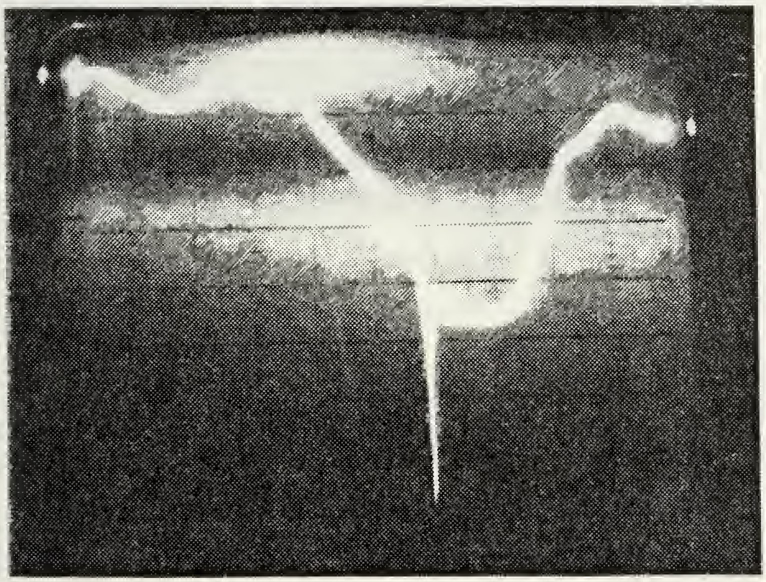

Figure 2-26
Z^+ Direction of
Propagation

Microstrip attenuation vs frequency. External transverse biasing magnetic field = 3100 oersteds, 1" substrate (G1001). Horizontal axis: frequency sweep from 4 to 8 GHz. Vertical axis: 10 db/DIV.

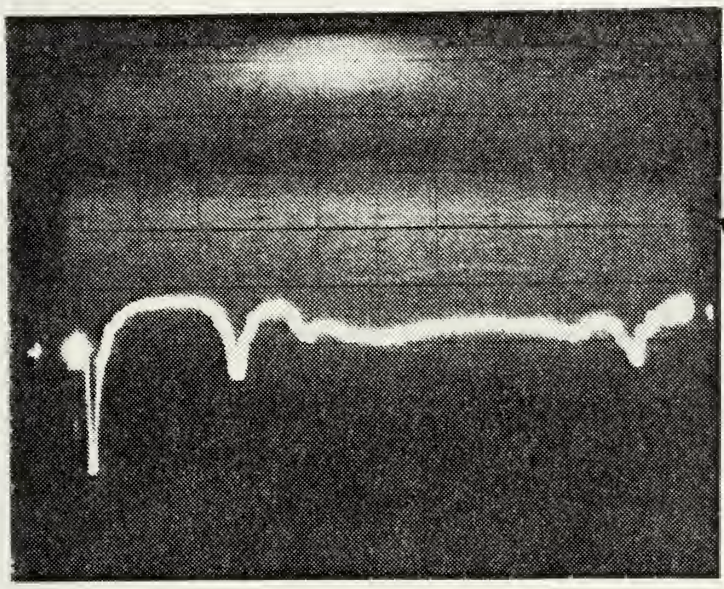

Figure 2-27. Microstrip return loss vs. frequency. External transverse biasing magnetic field = 3100 oersteds, 1" substrate (G1001). Horizontal axis: frequency sweep from 4 to 8 GHz. Vertical axis: 10 db/DIV. Z^+ Direction of Propagation.

Refs. 7 and 8 indicate that Equation (2) approximately holds for both transverse and longitudinal magnetization and they are equal. The above-mentioned fact could not be verified in this work. Equation (2) only roughly indicates the shape of ω-β diagrams for transverse magnetization normal to substrate.

b. Attenuation

Figures 2-25 and 2-26 indicate the loss for both directions of propagation as a function of frequency from 4 to 8 GHz. The applied magnetization was H_a = 3100 oersted and the resonance frequency was f_r = 6.364 GHz. At the resonance frequency a very sharp notch appeared with an attenuation greater than 120 db. The microstrip in general behaves as a band rejection filter. The overall loss across the stop band from 6.3 to 7.2 GHz is approximately 45 db.

Figure 2-27 indicates the return loss from 4 to 8 GHz. The return loss is approximately 17 db except where cancellation of multiple reflections occurs at frequencies of 4.1, 5.05 and 7.7 GHz.

4. <u>Transverse Magnetic Field of 2650 Oersteds</u>

a. Dispersion Diagram

In this case the microstrip designed had a 2" x 2" dimension, line width W = 0.508 mm, and substrate thickness D = 0.635 mm, chosen to give a nominal 50Ω characteristic impedance. The material used was G1001 garnet ($4\pi M_s$ = 1200 G, ϵ_r = 15.2) and it was transversely magnetized (in y direction, see Figure 1-2). The microstrip was connected to 50Ω input and output lines to the network analyzer. The phase shift was

measured as a function of frequency for a fixed applied biasing field H_a directed normal to the substrate.

Figures 2-28 and 2-29 show the photographs of the phase shift as a function of frequency from 4 to 8 GHz for an applied magnetic field of 2650 oersted for both directions of propagation. Figure 2-30 indicates the experimental phase shift as a function of frequency for the fixed applied field of 2650 oersted. The results are tabulated in Tables 10 and 11, Appendix A. The stop band is roughly from 5.3 GHz to 6.4 GHz, or approximately a bandwidth equal to 1.1 GHz. From Figure 2-30 it is evident that the phase shift is again the same for both directions of propagation, and the small discrepancy is due to interpreting the results from photographs of Figs. 2-28 and 2-29.

The stop band is wider in this case in comparison to the 1" x 1" substrate as expected, because the size of the substrate is 2" x 2" which is twice as great as in the previous cases.

b. Attenuation

The attenuation of 2" x 2" of G1001 microstrip were measured as a function of frequency from 4 to 8 GHz for a fixed applied magnetization field H_a = 2650 oersted applied normal to the substrate in the y-direction (Fig. 1-1). Figures 2-31 and 2-32 indicate attenuation for both directions of propagation. It is evident that the microstrip is behaving as a band rejection filter, with the center frequency of its stop band being a function of applied field H_a. The stop band

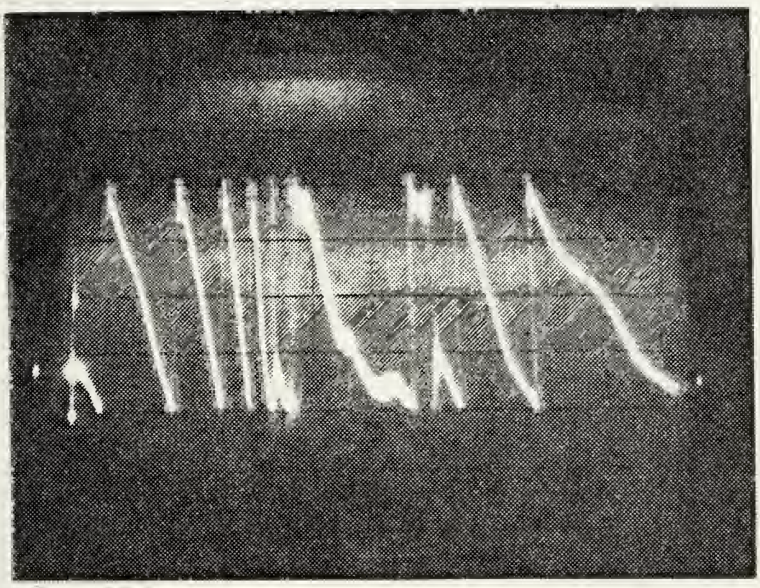

Figure 2-28
Z^{-} Direction of Propagation

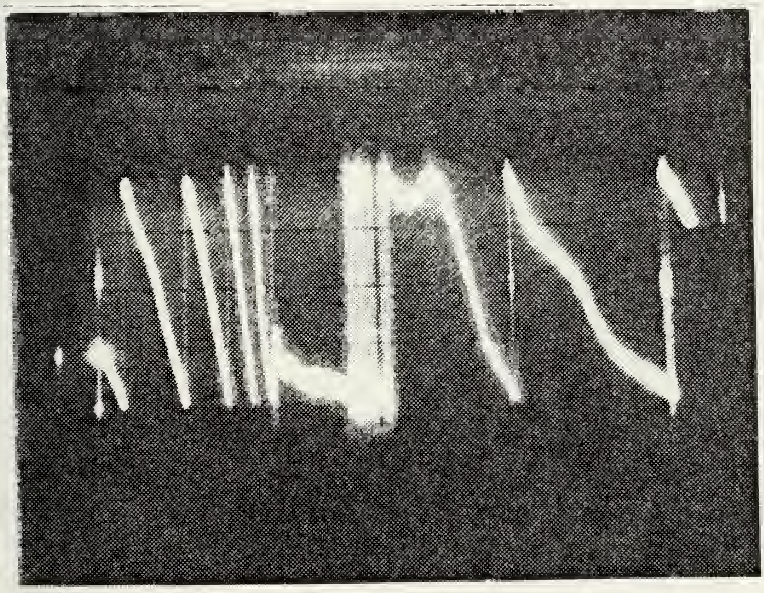

Figure 2-29
Z^{+} Direction of Propagation

Microstrip phase shift vs. frequency, 2" substrate. External transverse biasing magnetic field = 2650 oersteds. Horizontal axis: frequency from 4 to 8 GHz. Vertical axis: 90 deg/DIV.

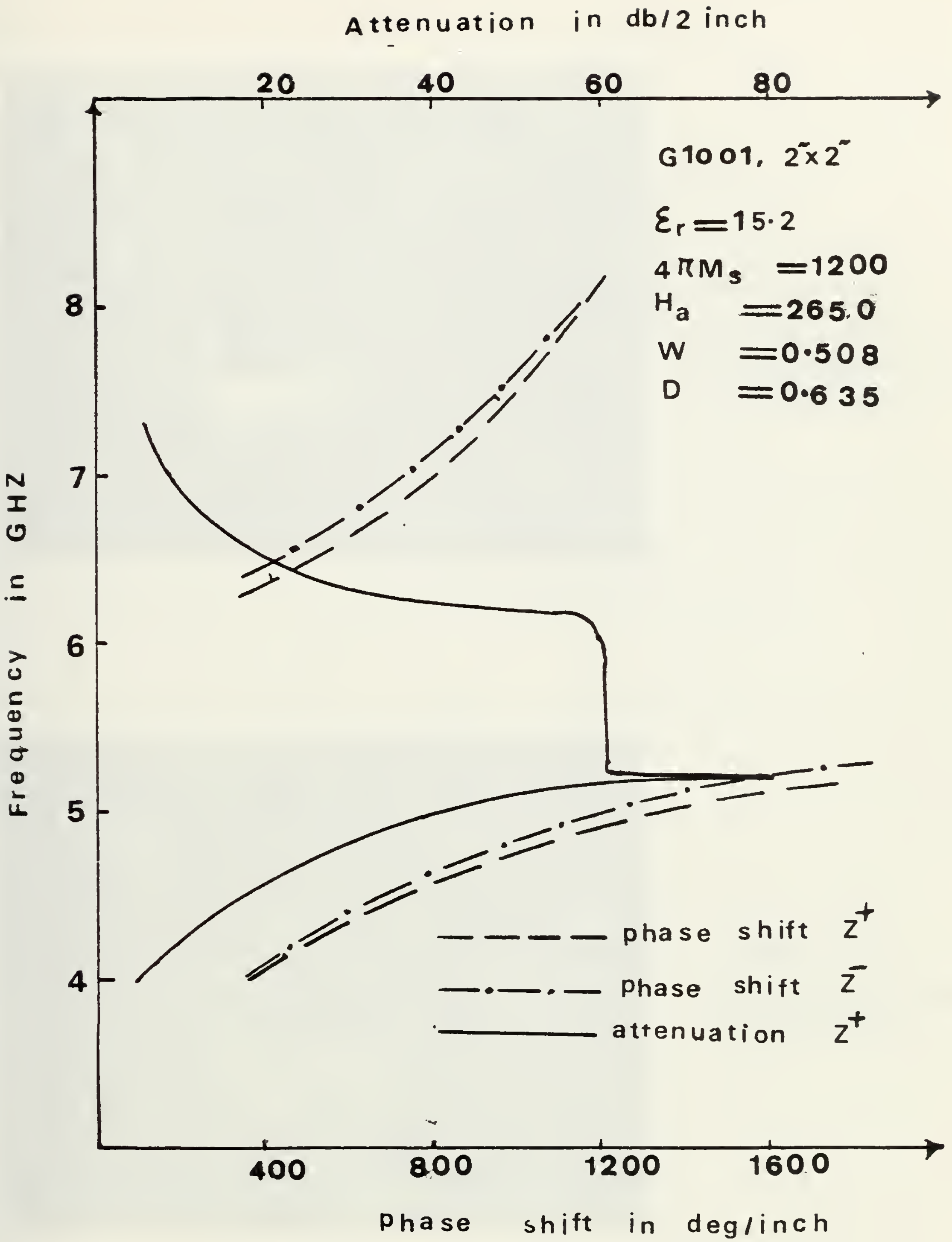

Figure 2-30. Propagation Constant and Attenuation of Transverse (Y-Direction) Magnetized Microstrip Transmission Line.

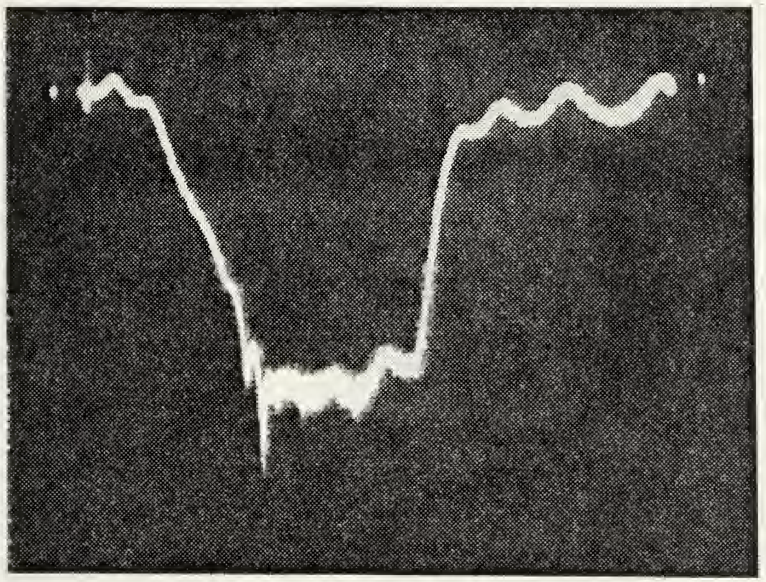

Figure 2-31
Z^+ Direction of Propagation

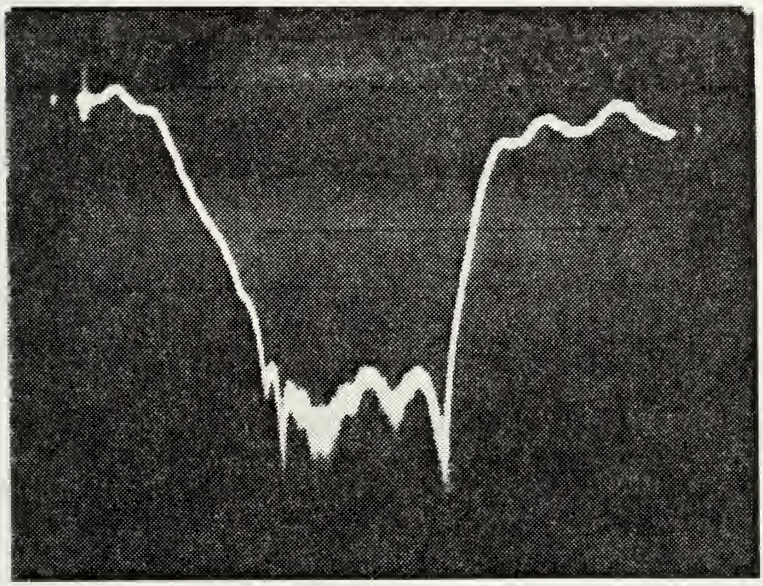

Figure 2-32
Z^- Direction of Propagation

Microstrip attenuation vs frequency, 2" substrate. External transverse biasing magnetic field = 2650 oersteds. Horizontal axis: frequency from 4 to 8 GHz. Vertical axis: 10 db/DIV.

is roughly from 5.3 to 6.4 GHz which gives a bandwidth of approximately 1.1 GHz.

The attenuation in the stop band is approximately 60 db. There are several notches apparent in the stop band which are approximately 20 db greater than the average attenuation in the stop band. Increasing the applied magnetic field will cause the stop band to move to a higher frequency, so the microstrip is acting as a tunable band rejection filter with applied magnetic field as the means of tuning.

It is evident also from Figs. 2-31 and 2-32 that the attenuation is the same for both directions of propagation.

5. Longitudinal Magnetization of 3100 Oersteds

a. Dispersion Diagram

Experiments were conducted using the G1001 1" x 1" substrate with dimensions of $W = 0.508$ mm, $D = 0.635$ mm, to obtain the dispersion diagram of the microstrip. The ω-β diagram of a longitudinally magnetized G1001 garnet substrate material was measured using a microstrip with an external magnetization field of $H_a = 3100$ oersted in the z-direction (See Fig. 1-1). The microstrip was designed to give a nominal 50Ω characteristic impedance taking into account the Wheeler permittivity [Ref. 6].

It was coupled to a 50Ω input and output line to the network analyzer. The phase shift as a function of frequency was photographed on the phase-frequency display of the network analyzer. The external biasing magnetic field was kept constant at $H_a = 3100$ oersted, while the frequency was swept

from 2 to 12.4 GHz. The resonance effect occurred between 8 and 12.4 GHz.

Pictures 2-33 and 2-34 show the ω-β display for both directions of propagation.

The resonance frequency occurred at approximately 9.87 GHz. The results from Figs. 2-33 and 2-34 are plotted in Fig. 2-35 for only one direction of propagation. It is evident from Figs. 2-33 and 2-34 that the phase shift is the same for both directions of propagation. The data is tabulated in Table 9 of Appendix A.

From 2-35 it is evident that there are two regions of propagation, a slow wave (low frequency) branch and a fast wave (high frequency) branch. These are separated by a cutoff region. The stop band here is approximately from 9.63 to 12.16 GHz or of a bandwidth of 2.53 GHz.

The cutoff region can be tuned in frequency by changing the applied biasing magnetic field H_a.

Figure 2-36 shows the ω-β diagram for transverse and longitudinal magnetization (from Fig. 2-35) for the same parameters and conditions. From Fig. 2-36 it is evident that the cutoff region for longitudinal magnetization is much larger than for transverse magnetization; for longitudinal magnetization it is 2.53 GHz bandwidth, whereas for transverse magnetization it is 0.8 GHz bandwidth, or approximately one-third of that for longitudinal magnetization.

It is evident from Fig. 2-36 that for the same conditions and parameters and magnetic biasing field of 3100.0

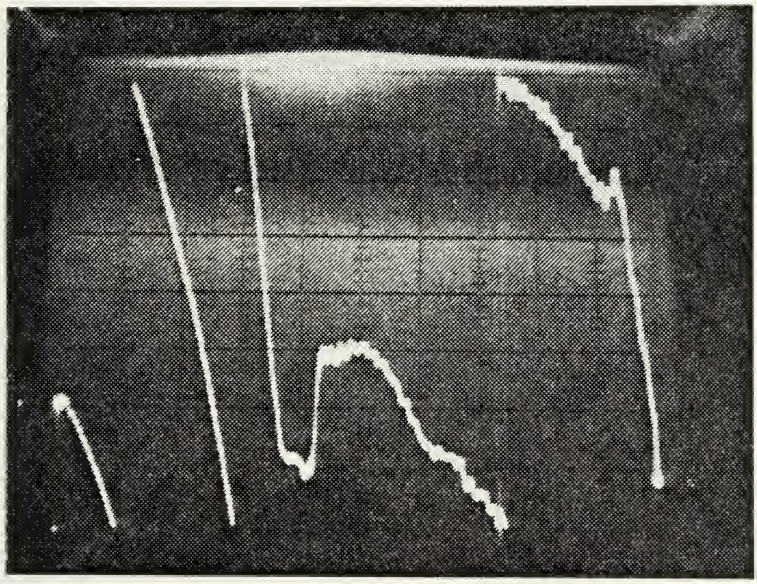

Figure 2-33
Z^+ Direction of Propagation

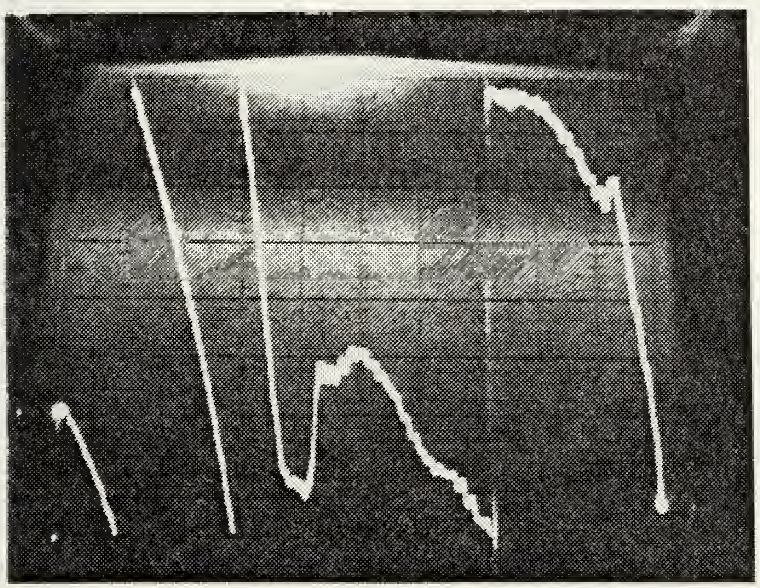

Figure 2-34
Z^- Direction of Propagation

Microstrip phase shift vs. frequency, 1" substrate. External longitudinal biasing magnetic field: 3100 oersteds. Horizontal axis: frequency sweep from 8 to 12.4 GHz. Vertical axis: 45 deg/DIV.

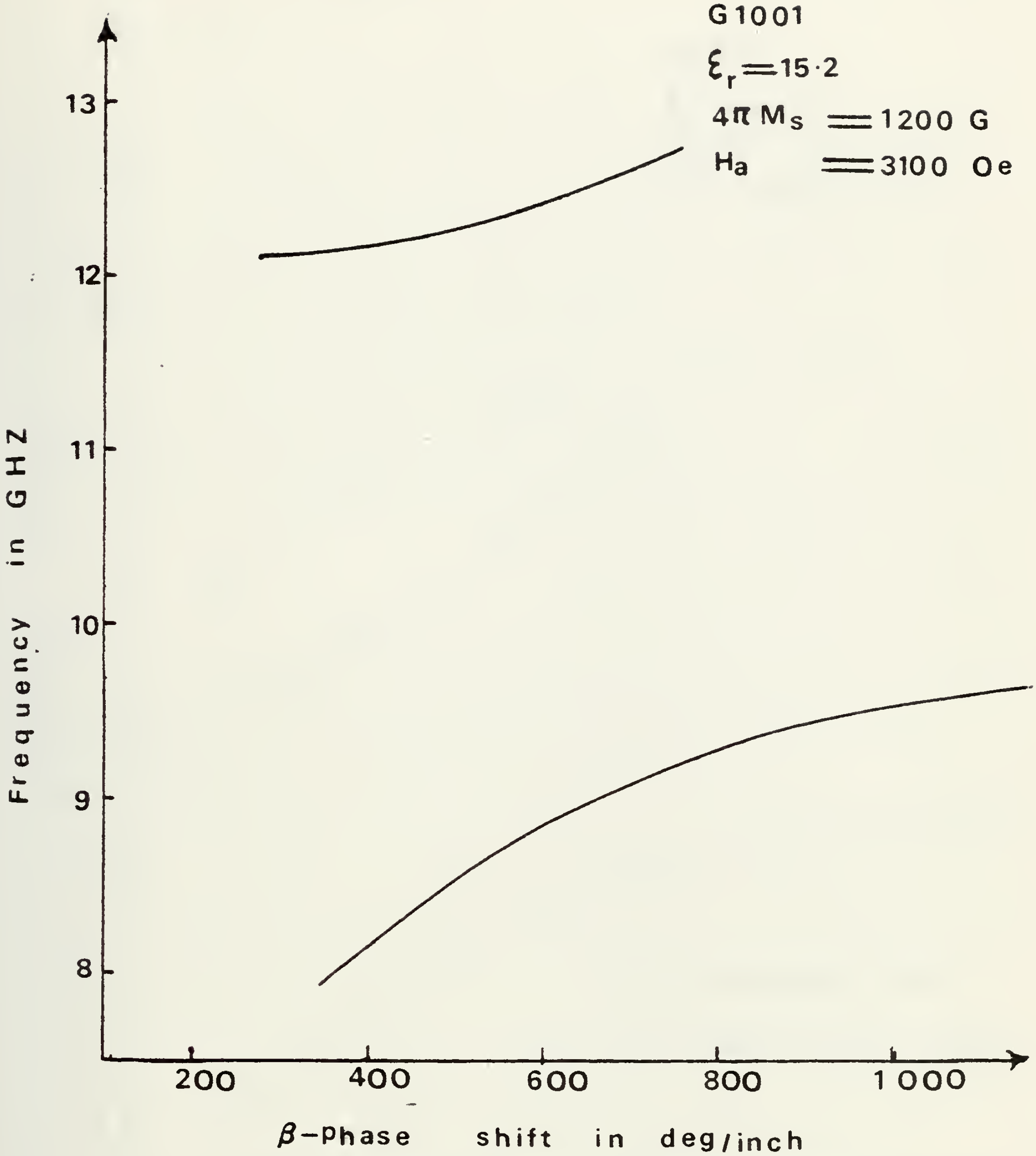

Figure 2-35. Propagation Constant of Longitudinal Magnetized Microstrip Transmission Line.

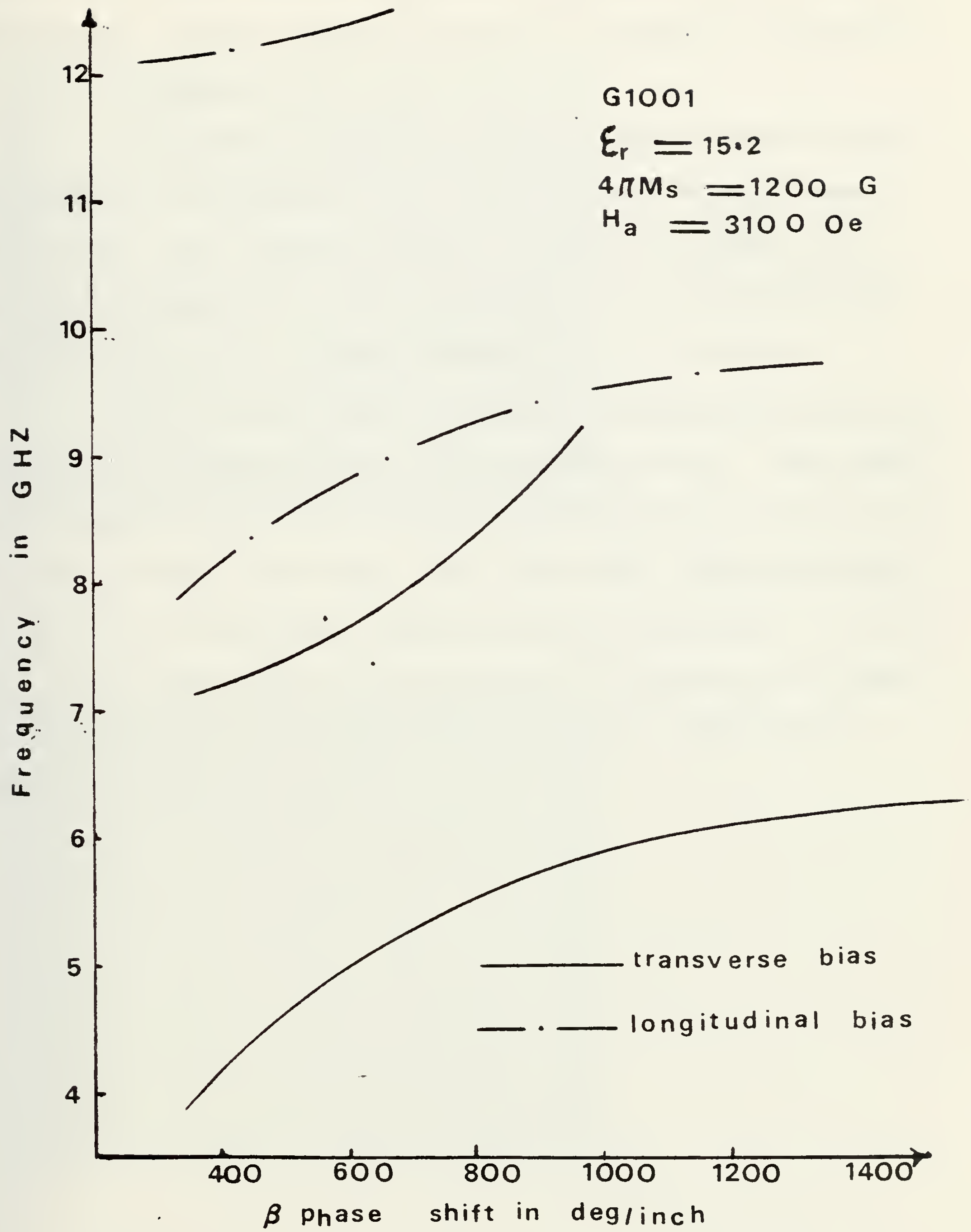

Figure 2-36. Propagation Constant of Longitudinal and Transverse Magnetized Microstrip Transmission Line.

oersted, the stop band and resonant frequency in the case of longitudinal biasing magnetic field has shifted in frequency.

b. Attenuation

Figures 2-37 and 2-38 indicate the loss for both directions of propagation as a function of frequency from 8 to 12.4 GHz. The applied biasing magnetic field was H_a = 3100 oersted applied in the longitudinal direction and the resonance frequency was approximately $f_r = 9.87$ GHz.

At the resonance frequency a very sharp notch appears with an attenuation of approximately 60 db. The amount of attenuation varies through the stop band from 60 db to 30 db as can be seen from Figs. 2-37 and 2-38. Comparing Figs. 2-25 and 2-26 (transverse magnetization) with Figs. 2-37 and 2-38, it is clear that the attenuation in the case of transverse magnetization is much higher than for longitudinal magnetization.

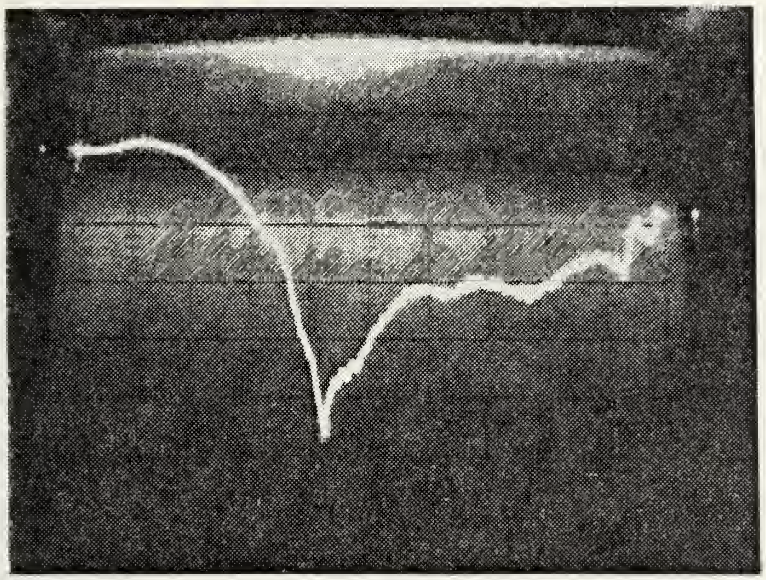

Figure 2-37
Z^+ Direction of Propagation

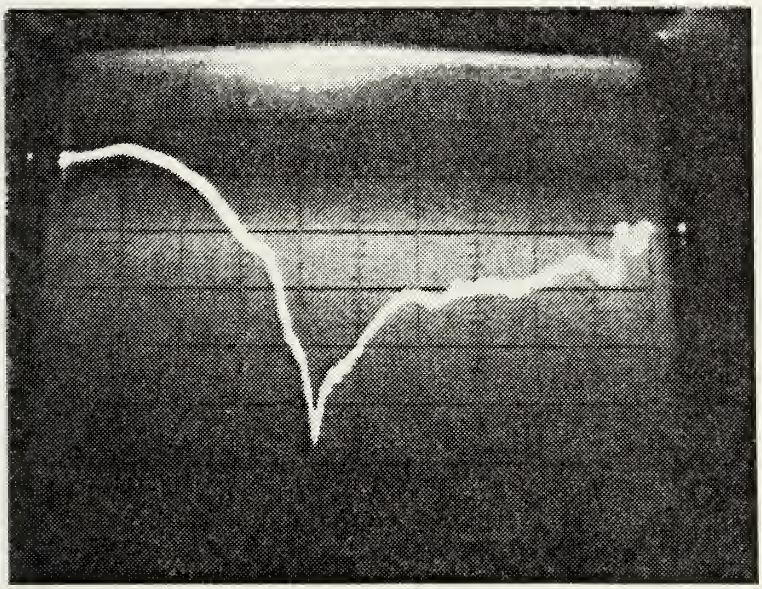

Figure 2-38
Z^- Direction of Propagation

Microstrip attenuation vs. frequency, 1" substrate. External longitudinal biasing magnetic field = 3100 oersteds. Horizontal axis: 8 to 12.4 GHz. Vertical axis: 10 db/DIV.

III. COMPUTER RESULTS FOR MICROSTRIP

A hybrid mode analysis of microstrip by the method of moments applied in the spectral or (Fourier) transform domain has been developed by A. M. Tufekcioglu [Ref. 1]. For ferrite substrate, the method developed by Tufekcioglu calculates the propagation constant and attenuation based on perturbation theory, assuming a transversely magnetized substrate. Numerical evaluation of the resulting expressions has been carried out in the spectral domain and a computer program has been developed for this analysis. Using the above-mentioned computer analysis, the following results were obtained.

A. DISPERSION AND ATTENUATION DIAGRAMS (TRANSVERSE MAGNETIZATION)

1. Dispersion Diagram

A computer analysis for microstrip transmission lines on G1001 garnet material with different applied biasing magnetic fields and resonance frequencies with the following specifications were obtained:

G1001, 1" x 1" dimension

$W = 0.508$ mm $\qquad$ $D = 0.635$ mm.

$4\pi M_s = 1200.0$ Gauss $\qquad$ $\varepsilon_r = 15.2$

Figures 3-1, 3-4 and 3-6 indicate the ω-β diagrams for both directions of propagation for resonance frequencies of 2.8 5.192, and 6.364 GHz and applied magnetic fields of 1730, 2670 and 3100.0 oersteds. The results are tabulated in Tables 12, 13 and 14 of Appendix A.

From all these computer generated dispersion (ω-β) diagrams it is evident that there are two propagation branches, a low frequency (slow wave) branch below the resonance frequency, and a high frequency (fast wave) branch above the resonance frequency.

As frequency is increased from zero, the phase shift decreases, reaches a minimum value, and then at resonance frequency it switches sharply to a maximum value of phase shift and beyond resonance decreases as frequency increases.

The phase ve. frequency diagrams for opposite directions of propagation are of the same shape except that maximum and minimum values of phase shifts are approximately halved. The computer generated dispersion (ω-β) diagrams exhibit no cutoff region as it was evidenced from experiments. Also evident from Figs. 3-1, 3-4 and 3-6 is that as the resonance frequency increases the maximum and minimum values of phase shift increase as well.

2. Attenuation Diagrams

The computer analysis of attenuation of 1" microstrip transmission line on G1001 material with the same condition and specification as in III.A.1 with different applied biasing magnetic fields and resonance frequencies were obtained. Figures 3-2, 3-5 and 3-8 indicate the attenuation diagrams for both directions of propagation for resonance frequencies of 2.8, 5.192, and 6.64 GHz and applied magnetic fields of 1730, 2670 and 3100.0 oersteds.

The results are tabulated in Tables 12, 13 and 14 of Appendix A.

Computer analysis attenuation diagrams exhibit a sharp attenuation at resonance frequency and fall off rapidly to a zero value above and below resonance frequency. Computer analysis also indicates a stop band as it was evidenced from experiment results. Also plotted is characteristic impedance in Fig. 3-3 for microstrip assuming the dielectric substrate.

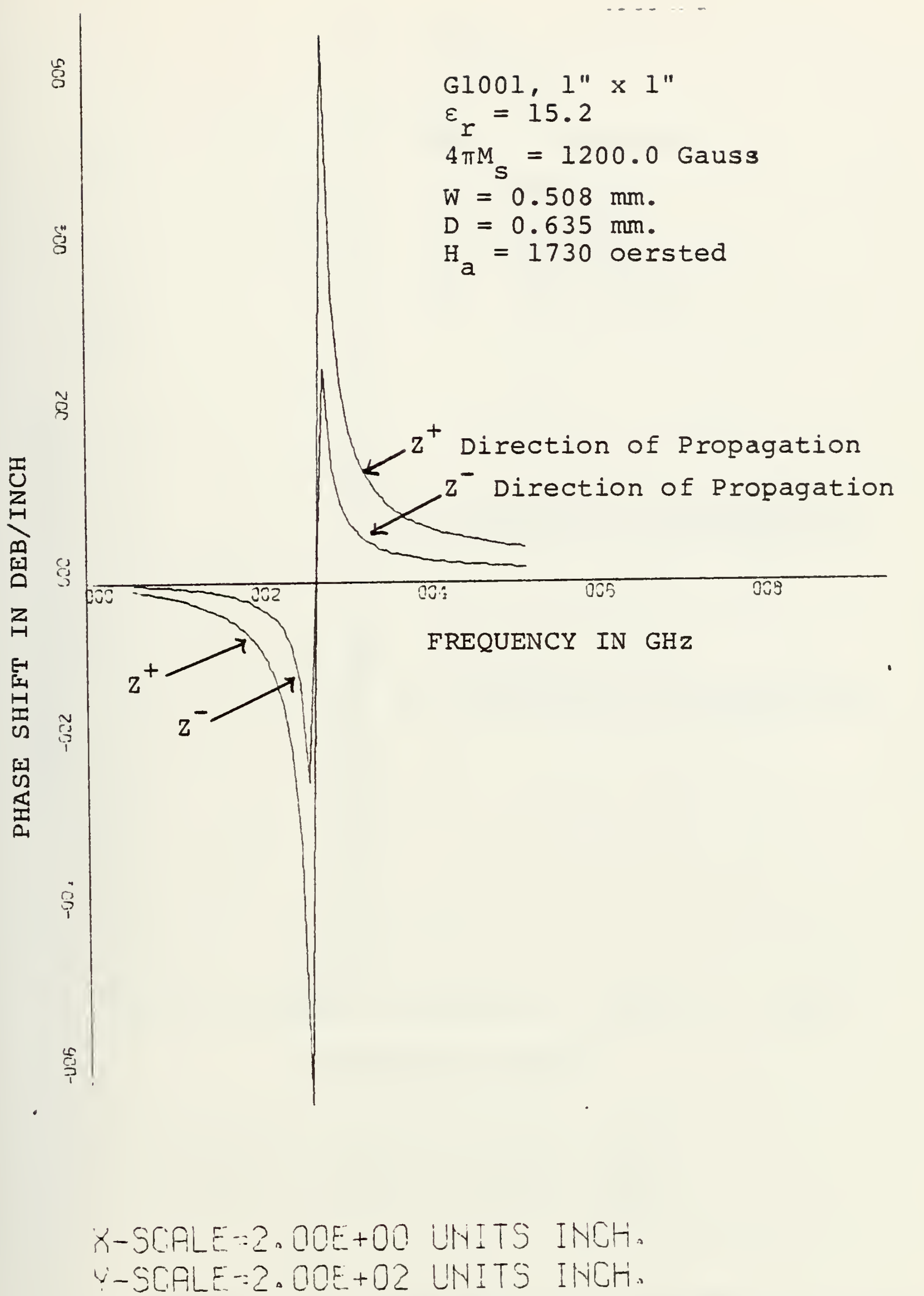

Figure 3-1. Propagation Constant of Transverse Magnetized Microstrip Transmission Line.

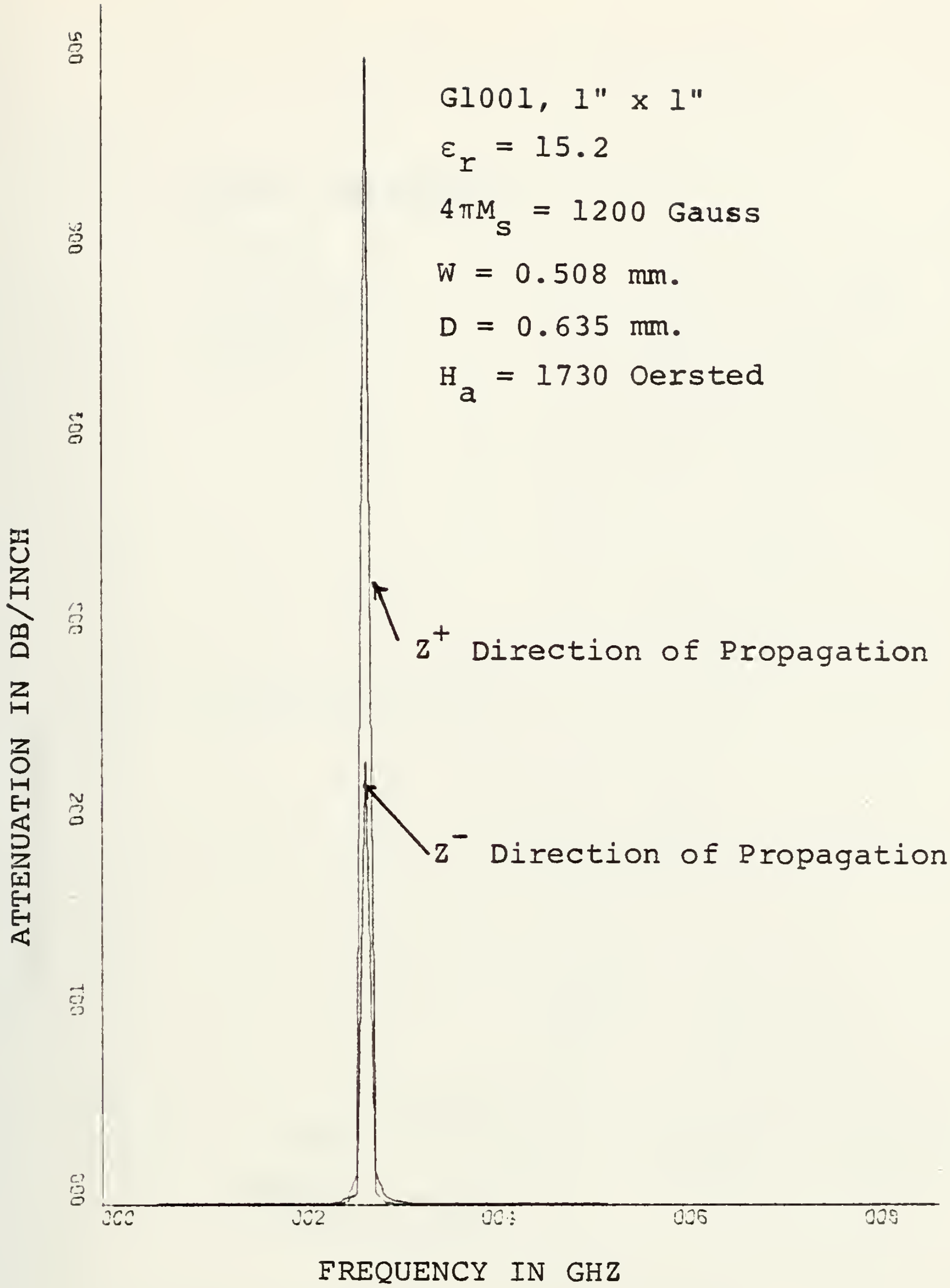

X-SCALE=2.00E+00 UNITS INCH.
Y-SCALE=1.00E+02 UNITS INCH.

Figure 3-2. Attenuation vs. Frequency of Transversely Magnetized Microstrip Transmission Line.

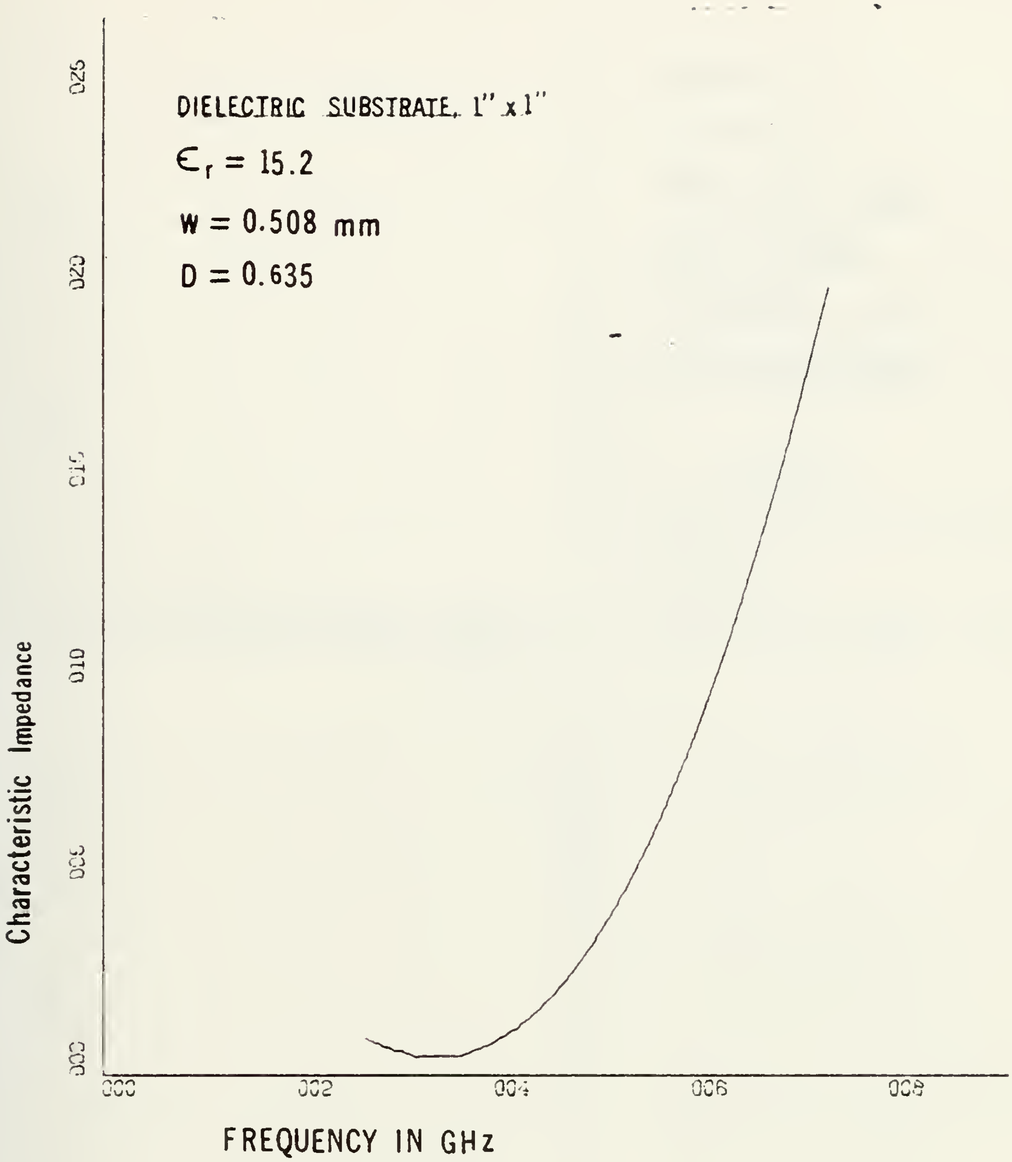

X-SCALE=2.00E+00 UNITS INCH.
Y-SCALE=5.00E-02 UNITS INCH.

ADD +4.62E+01 UNITS TO ALL Y VALUES.

Figure 3-3. Characteristic Impedance of Microstrip Transmission Line on Dielectric Substrate.

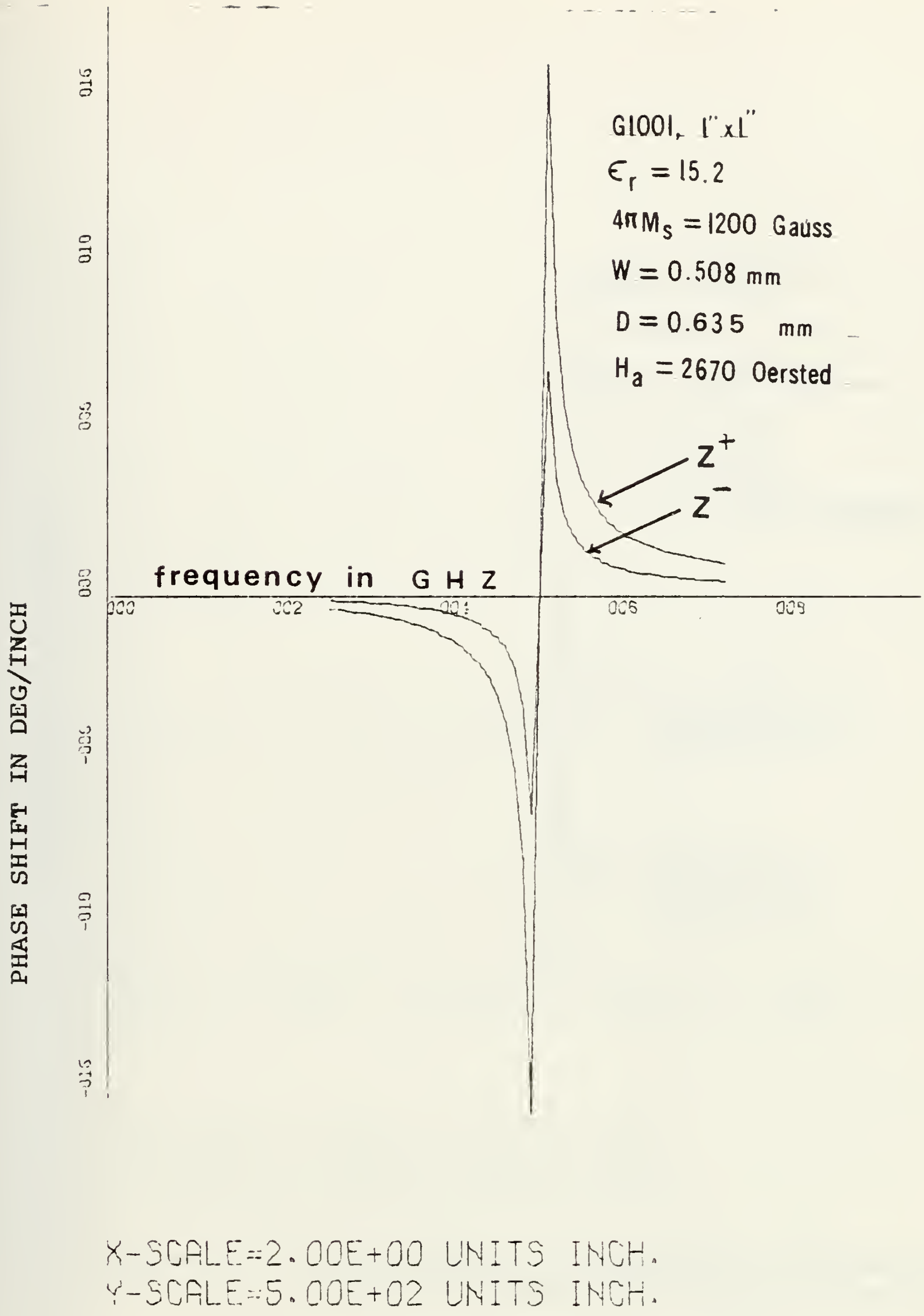

Figure 3-4. Propagation Constant of Transverse Magnetized Microstrip Transmission Line.

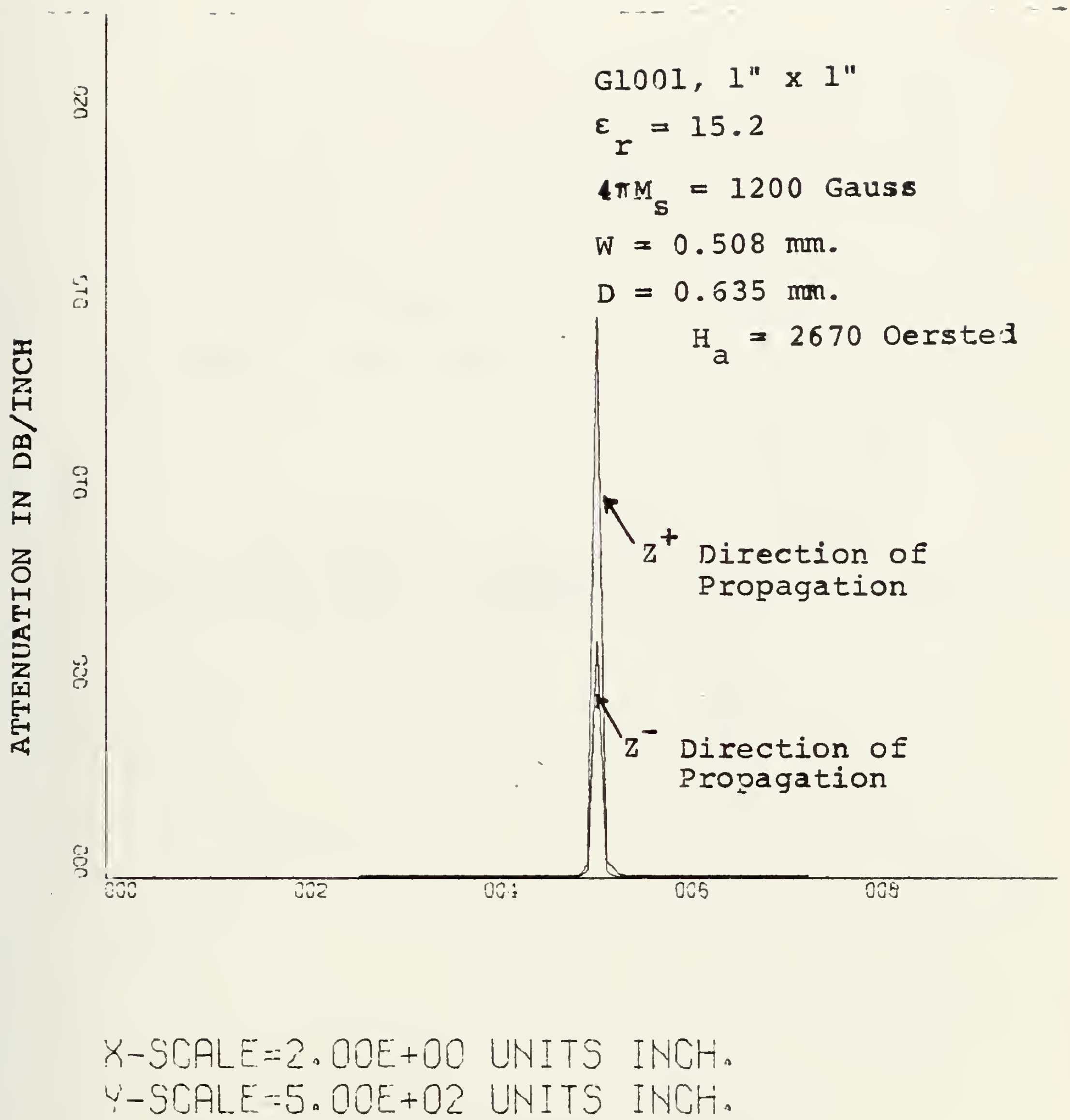

Figure 3-5. Attenuation vs. Frequency of Transversely Magnetized Microstrip Transmission Line.

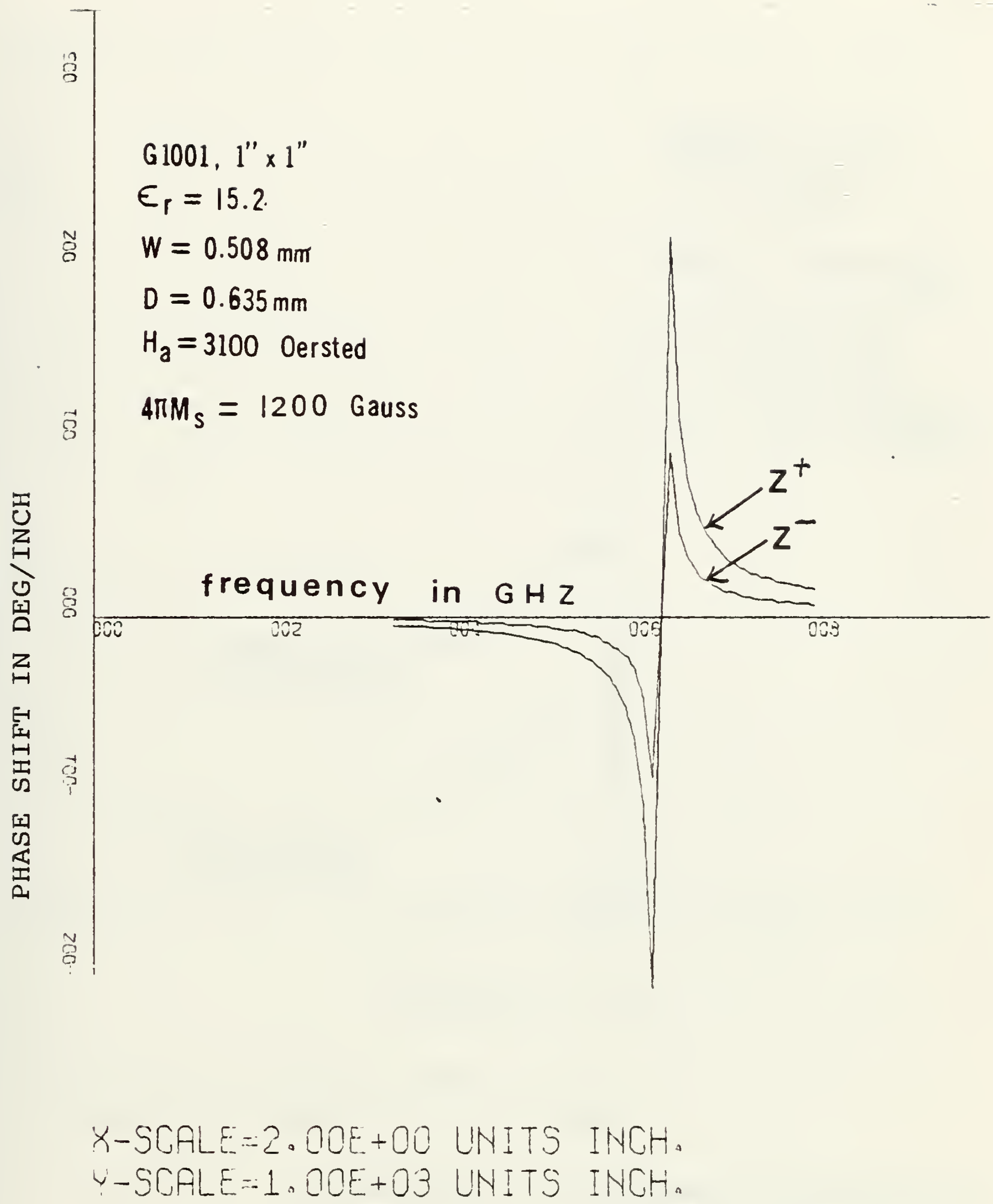

Figure 3-6. Propagation Constant of Transverse Magnetized Microstrip Transmission Line.

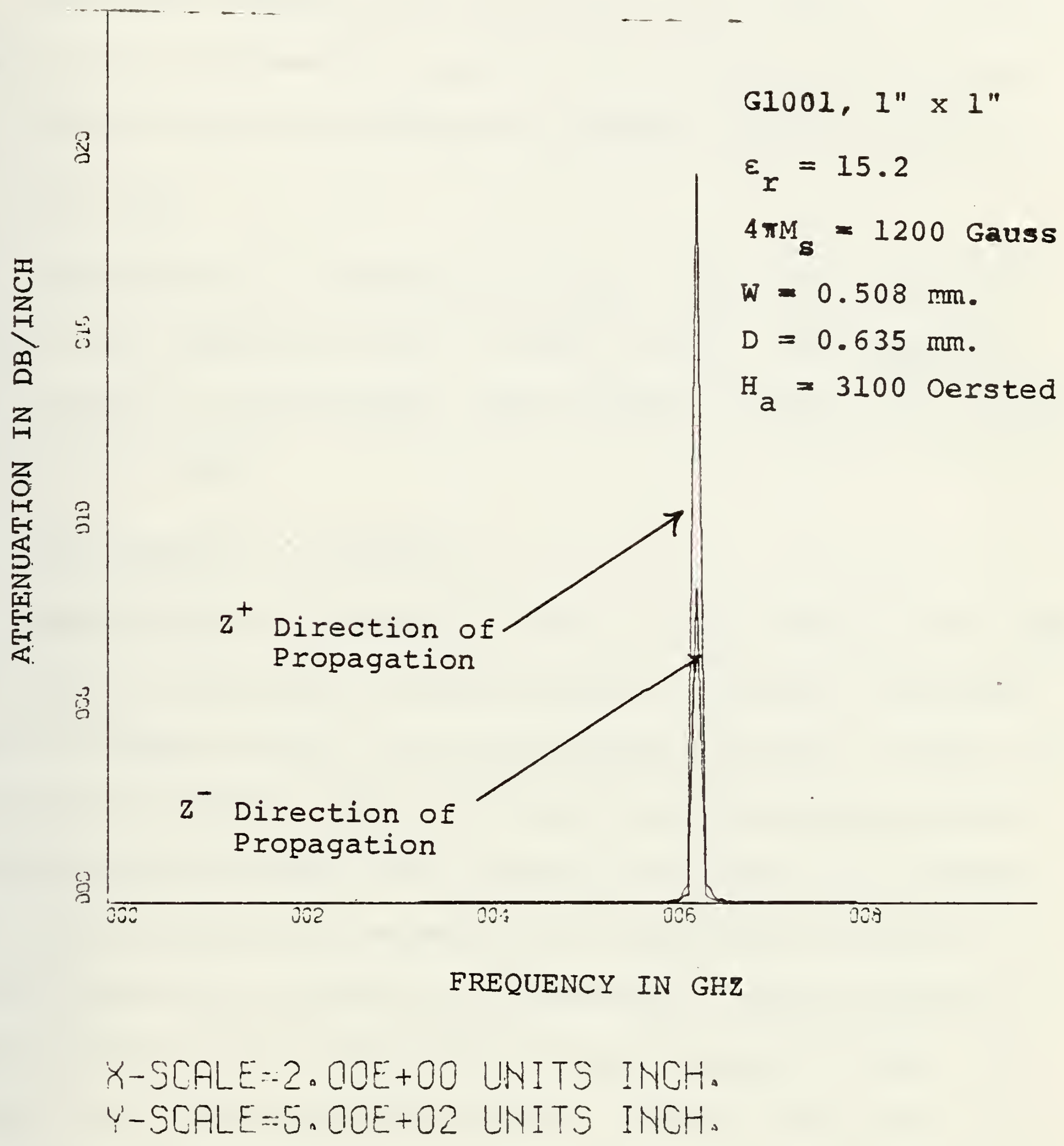

Figure 3-7. Attenuation vs. Frequency of Transversely Magnetized Microstrip Transmission Line.

IV. COMPARISON BETWEEN EXPERIMENTAL AND COMPUTER ANALYSIS FOR MICROSTRIP TRANSMISSION LINE

Comparison between the experimental and computer analysis results of a transversely magnetized microstrip transmission line indicate certain differences between them as follows.

A. STOP BAND

Experimental ω-β diagrams of Figs. 2-13, 2-18 and 2-24 exhibit stop bands of 0.35, 0.6 and 0.8 GHz. The shape of ω-β diagrams of experimental and computer analysis are not in agreement as well.

B. EXPERIMENTAL ω-β DIAGRAM

Experimental ω-β diagram of Figs. 2-13, 2-18 and 2-24 indicate that as frequency increases below resonance, the phase shift increases as well, whereas computer results of Figs. 3-1, 3-4 and 3-6 indicate that the phase shift decreases with increasing frequency till the resonance frequency is reached. Also beyond resonance frequency the experimental curve increases again as a function of frequency, whereas computer results indicate the phase shift having reached a peak, decreases as a function of frequency. The fact that the computer analysis exhibits the change of sign of phase shift above and below resonance frequency indicates the propagation changes direction. This is not in agreement with experimental results.

C. GRADIENTS OF ω-β DIAGRAMS

The gradients of ω-β diagrams of experimental and computer analysis differ at each frequency.

D. PHASE SHIFT

The values of phase shift at each frequency is radically different (far greater) for computer analysis in comparison to the experimental results.

E. ATTENUATION

Experimental attenuation pictures of Figs. 2-14, 2-20 and 2-25 exhibit a stop band and within the stop band a sharp notch which its frequency were taken as resonance frequency. The computer analysis of attenuation figures 3-2, 3-5 and 3-7 (does not indicate any stop band) exhibits a very sharp indication of attenuation. The notch is centered at the resonance frequency.

Also attenuation for both directions of propagation differs approximately by a factor of two, which is contrary to the experimental results of attenuation. This could be due to dynamic range and sensitivity limitations of the analysis.

The computer analysis indicating the sharp notch of attenuation at resonance frequency is in agreement with the notch exhibited in the stop band of experimental results, although the values of attenuation for the former is much higher than the one obtained in the experiment.

F. NON-RECIPROCALITY

The computer analysis indicated that the microstrip transmission line is behaving as a non-reciprocal band rejection filter, a hypothesis which was hard to establish from experimental results obtained.

The reason for contradiction between theory and practice stated above could be attributed to the following.

1. The computer analysis is based on perturbation theory, and perturbation theory is only valid if the changes predicted are very small [Ref. 5].

2. Reference 7 indicates that the characteristic impedance of a microstrip transmission line have generally a shape similar to the experimental ω-β diagram; it has high and low frequency branches, separated by a cutoff region.

Characteristic impedance used in computer analysis [Ref. 1] was for a dielectric substrate and its values changed very little with frequency as indicated in Fig. 3-3. So, this could have led also to a very different result from the actual one.

V. COPLANAR WAVEGUIDE ON FERRITE SUBSTRATE

A. DISPERSION DIAGRAM (ZERO APPLIED MAGNETIZATION FIELD)

Experiments using coplanar waveguide on ferrite substrate were conducted in order to obtain the phase shift as a function of frequency in the case of zero-applied magnetization field.

The ferrite was G1001 and the coplanar waveguide had the following specifications:

Overall dimensions: 2" x 2"

Thickness of dielectric: .635 mm

W/D = 1.260, S/D = 3.15

Permittivity = 15.2

The coplanar waveguide was designed to give a nominal 50Ω characteristic impedance for dielectric substrate. The coplanar [Ref. 2] computer program was run in order to obtain the ratio of S/D, W/D for a nominal characteristic impedance of 50Ω.

The coplanar waveguide was coupled by 50Ω input and output lines to the network analyzer.

Figures 4-1 and 4-2 show the photographs of the phase-frequency display on the network analyzer when the substrate is unbiased. The data obtained from these photographs are tabulated in Table 15 of Appendix A. The above-mentioned data are plotted in Fig. 4-3. Also shown is the result of the computer analysis for dielectric substrate [Ref. 2].

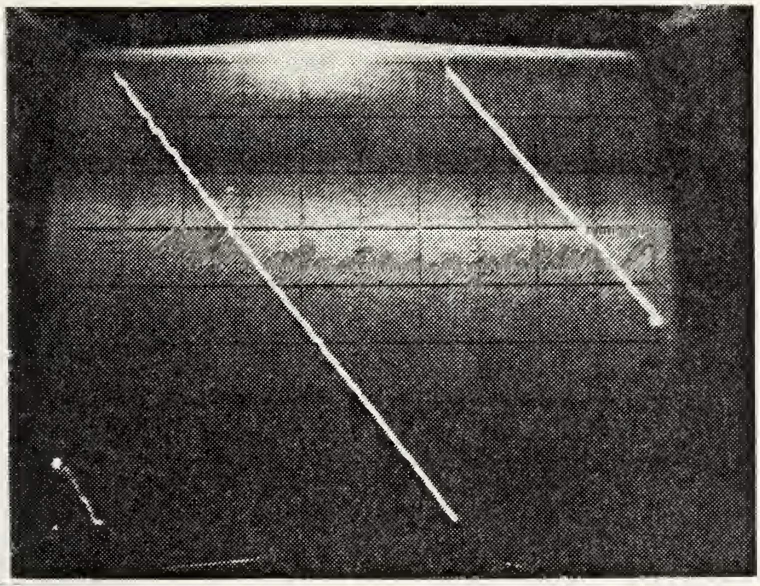

Figure 4-1.
Vertical Axis:
Phase Shift
Scale 45 deg/DIV

Coplanar phase shift vs. frequency in the absence of external magnetic field, 2" substrate. Horizontal axis: frequency sweep from 4 to 8 GHz.

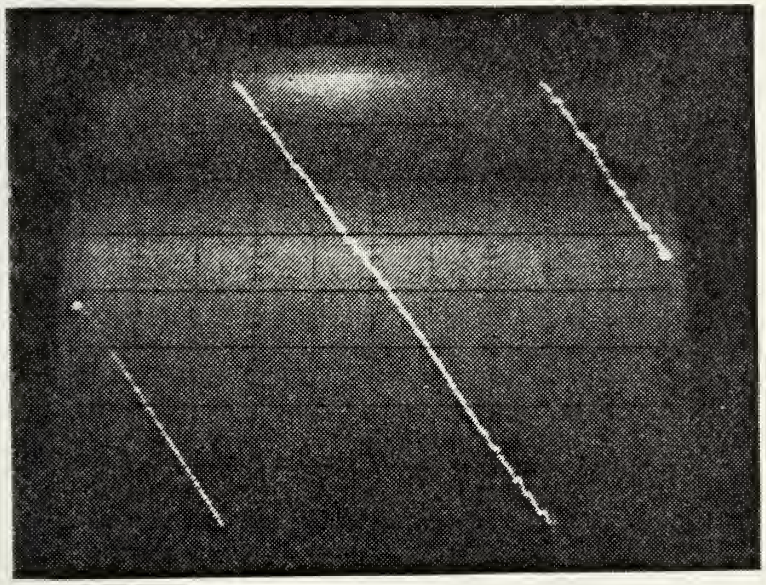

Figure 4-2.
Vertical Axis:
Phase Shift
Scale 45 deg/DIV

Coplanar phase shift vs. frequency in the absence of external magnetic field, 2" substrate. Horizontal axis: frequency sweep from 8 to 12.4 GHz.

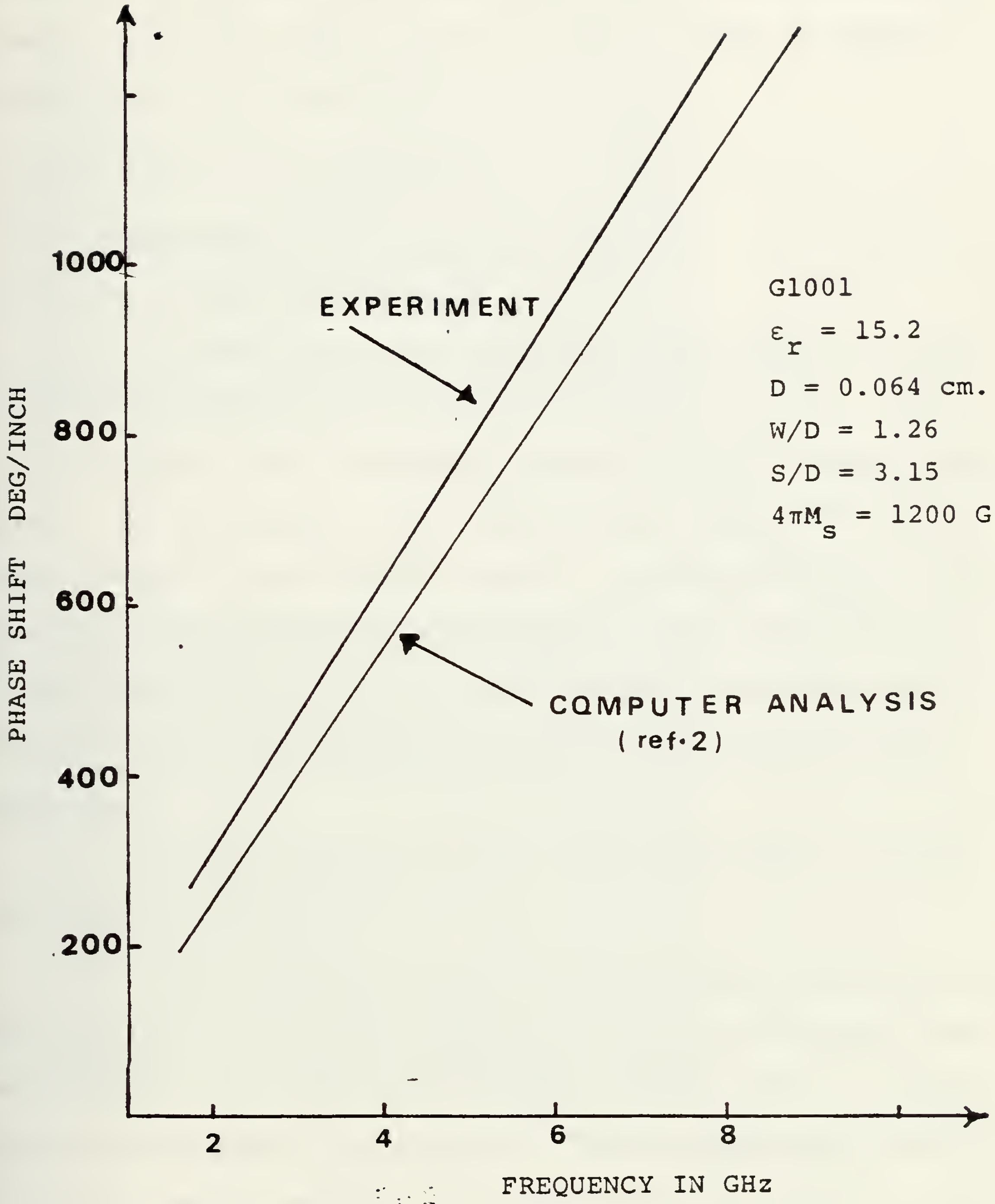

Figure 4-3. Coplanar waveguide ω-β diagram in the absence of external magnetic field.

From Figure 4-3 it is evident that the experimental ω-β diagram has a higher slope than the result obtained from the computer analysis [Ref. 2], which could be due to magnetic properties of the substrate.

B. DISPERSION AND ATTENUATION

1. Transverse Magnetic Field

a. Dispersion Diagram

Experiments were conducted using G1001, 2" substrate with dimensions D = 0.635 mm, W/D = 1.260, S/D = 3.15, to obtain the dispersion diagram of the coplanar waveguide. The ω-β diagram of a transversely magnetized G1001 garnet material was obtained using a coplanar waveguide with external magnetization fields of 2950.0 and 3215 oersteds in x direction (See Fig. 1-2). The coplanar waveguide was designed to give approximately a nominal 50Ω characteristic impedance.

It was coupled by 50Ω input and output lines to the network analyzer.

The external biasing magnetic fields were kept constant at 2950.0 and 3215.0 oersteds while the frequency was swept from 4 to 8, and 8 to 12.4 GHz, respectively. Figures 4-4 and 4-5 indicate the phase vs. frequency display for 2950.0 oersteds external magnetic field for both directions of propagation. The results from Figs. 4-4 and 4-5 are plotted in Fig. 4-6 for both directions of propagation. The data is tabulated in Table 16 of Appendix A. Pictures 4-12 and 4-13 indicate the phase vs. frequency display for 3215.0 oersteds

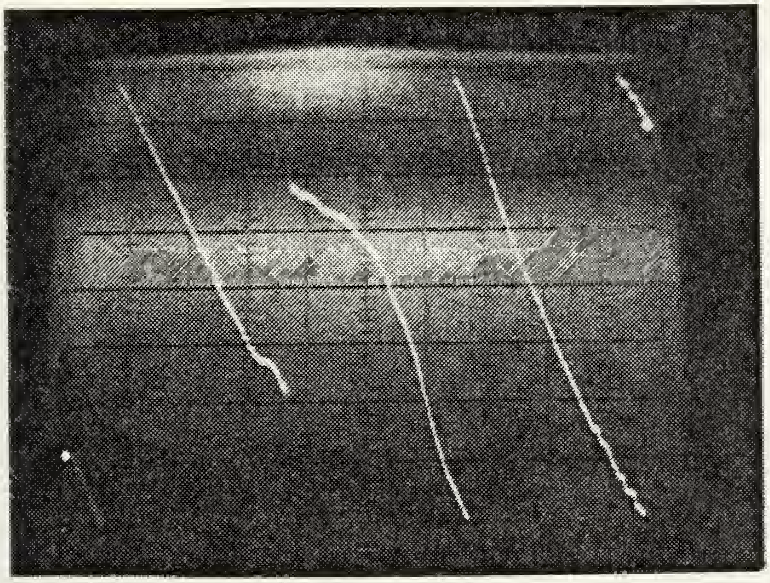

Figure 4-4.
Z^+ Direction of
Propagation.

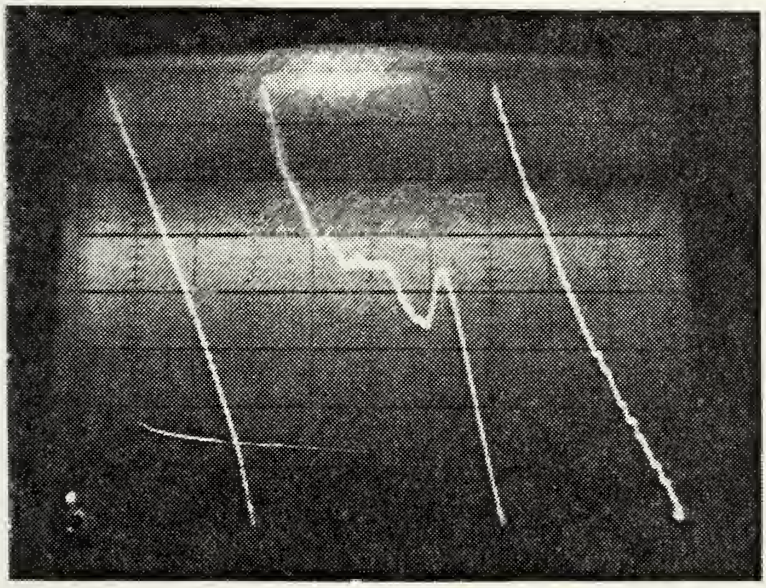

Figure 4-5.
Z^- Direction of
Propagation.

Coplanar phase shift vs. frequency, 2" substrate. External transverse biasing magnetic field = 2950 oersteds. Horizontal axis: frequency sweep from 8 to 12.4 GHz. Vertical axis: 45 deg/DIV.

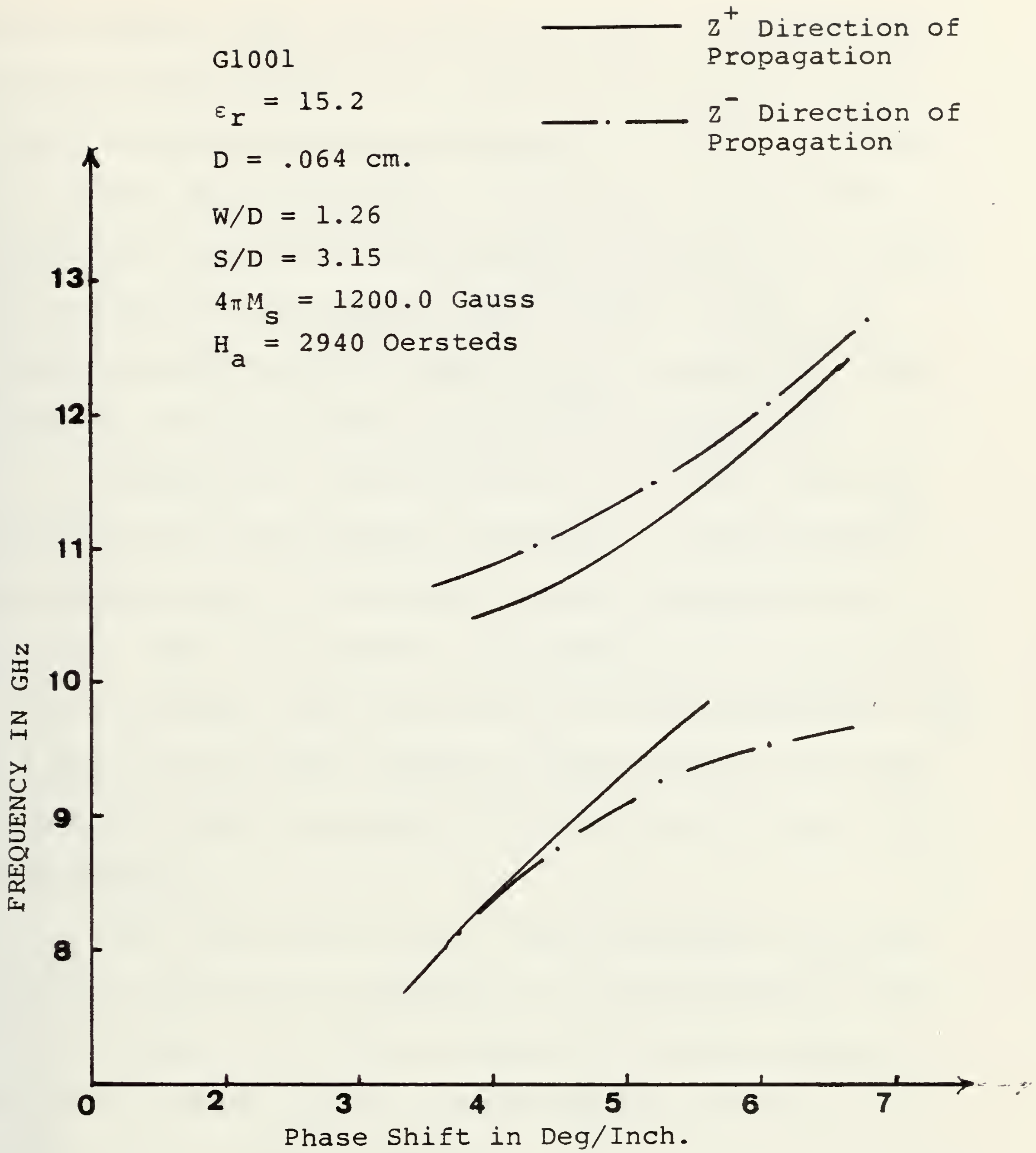

Figure 4-6. Coplanar Phase Shift vs. Frequency for Transverse Magnetization (X-Direction).

external magnetic field for both directions of propagation. The results from pictures 4-12 and 4-13 are plotted in Fig. 4-14 for both directions of propagation. The data are tabulated in Table 17 of Appendix A. From Figs. 4-6 and 4-14 it is evident that there are two regions of propagation, a lower branch extending to zero and an upper branch. These are separated by a cutoff region where μ_{eff} is negative. The stop band is the region where there is no propagation.

From Figs. 4-4, 4-5, 4-6, 4-12, 4-13, and 4-14, it is evident that the coplanar waveguide is nonreciprocal, namely the stop band is different for both directions of propagation. For one direction of propagation in the case of H_a = 2940.0 oersteds, the stop band is from approximately 9.42 to 10.2 GHz, or 0.78 GHz; whereas for the opposite direction of propagation, the stop band is from 9.54 to 10.74 GHz, or 1.2 GHz bandwidth.

For the case of H_a = 3215.0 oersteds, the stop band for one direction of propagation is approximately from 10.2 to 11.08 GHz, or 0.88 GHz bandwidth, and for opposite direction of propagation, it is approximately from 9.98 to 11.33 GHz, or 1.35 GHz bandwidth.

The bandwidth for one direction of propagation designated arbitrarily as Z^- is higher than the stop band for the other direction of propagation which indicates that the coplanar waveguide as a band rejection filter is nonreciprocal.

The frequency of the cutoff region throughout the frequency band can be tuned by changing the applied biasing magnetic field H_a.

b. Attenuation

The insertion loss of a 2" length of 50 (nominal) characteristic impedance coplanar waveguide on G1001 material is shown in Figs. 4-7, 4-8, 4-15, and 4-16 for 2950.0 and 3215.0 oersteds of biasing fields applied transverse to the direction of propagation (x-direction, See Fig. 1-2).

The dimensions of the coplanar waveguide were D = 0.635 mm, W/D = 1.260, S/D = 3.15, and the experiments were conducted with the same conditions as in Part B.1.a. The attenuation photograph in the case of $H_a = 2950.0$ oersteds indicates that the maximum insertion loss occurs at the notch in Fig. 4-7, which is more than 80 db; whereas Fig. 4-8 indicates a constant 40 db attenuation throughout the stop band from approximately 9.4 to 10.74 GHz.

In Fig. 4-7 the attenuation varies throughout the stop band, and it is approximately 30 db from 9.4 to 10.7 GHz, while the notch has more than 80 db of attenuation. Figs. 4-15 and 4-16 indicate attenuation in the case of $H_a = 3215.0$ oersteds. In Fig. 4-15 the attenuation is 30 db throughout the stop band and there is a peak of -48 db at 10 GHz. In Fig. 4-16, the attenuation is from -35 db to -40 db throughout the stop band. From attenuation photographs, it is evident that the shape and the amount of losses are different for both directions of propagation giving support to the theory that the coplanar waveguide is nonreciprocal as was seen in the case of dispersion diagrams. Fig. 4-9 indicates the return loss from 4 to 8 GHz in the absence of any biasing magnetic field. The

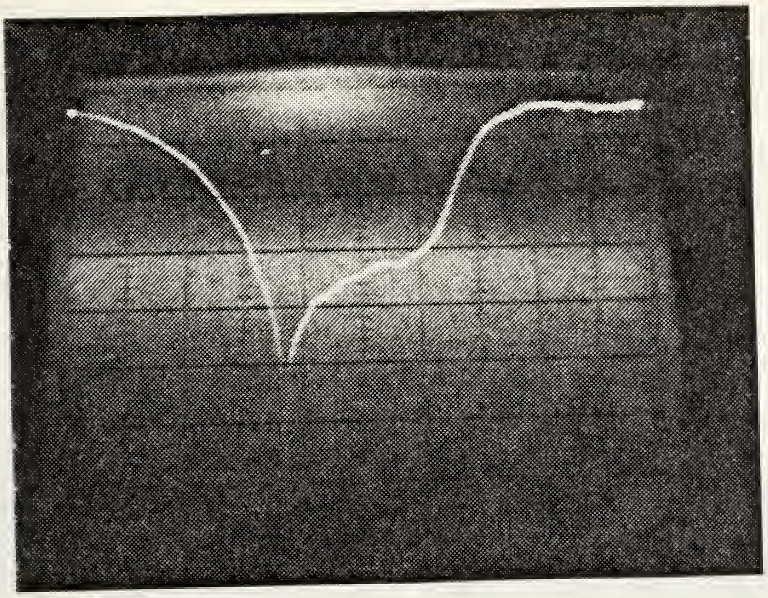

Figure 4-7.
Z^+ Direction of Propagation

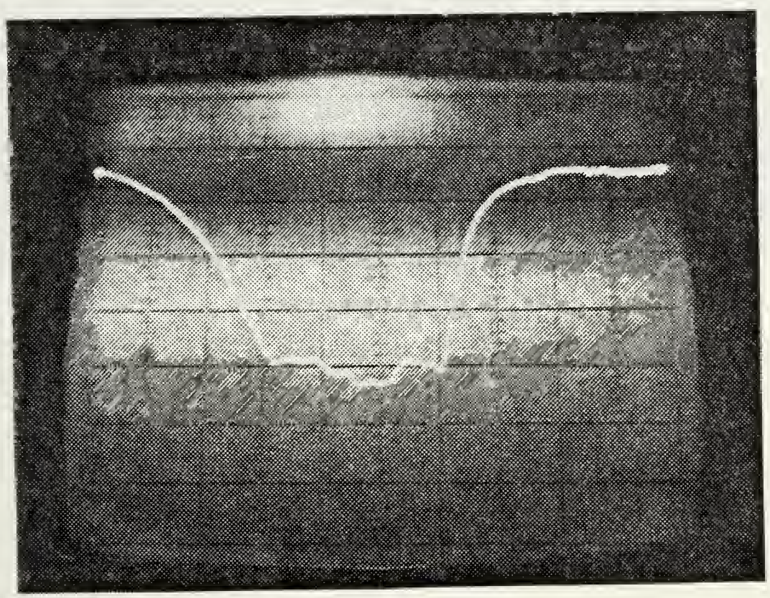

Figure 4-8.
Z^- Direction of Propagation.

Coplanar attenuation vs. frequency, 2" substrate (G1001).
External transverse biasing magnetic field = 2950 oersteds.
Horizontal axis: frequency sweep from 8 to 12.4 GHz.
Vertical axis: 10 db/DIV.

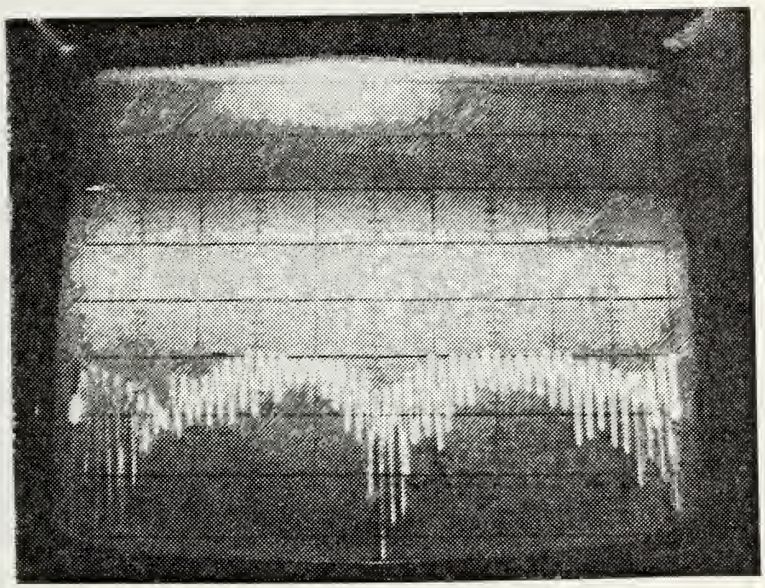

Zero db
Reference.

Figure 4-9. Coplanar return loss vs. frequency in the absence of external biasing magnetic field, 2" substrate (G1001). Horizontal axis = frequency sweep from 4 to 8 GHz. Vertical axis = 10 db/DIV.

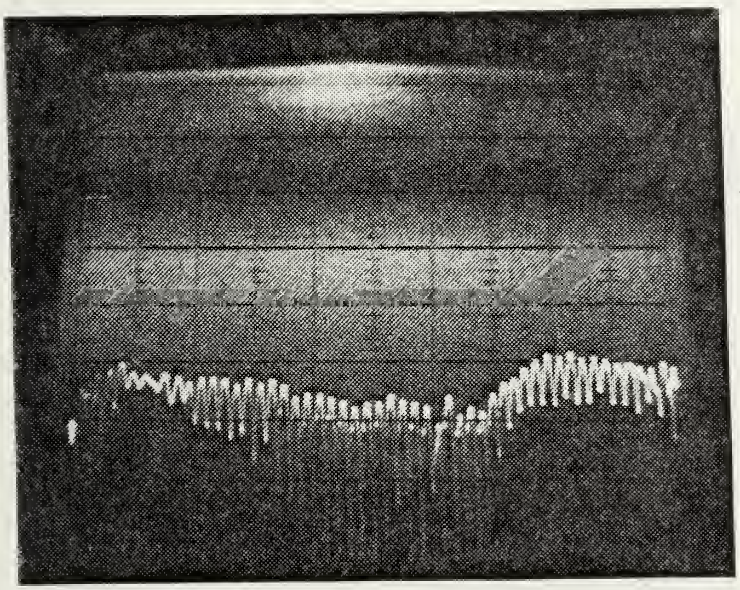

Zero db Reference.

Figure 4-10. Coplanar return loss vs. frequency. External transverse biasing magnetic field = 2950 oersteds. 2" substrate (G1001). Horizontal axis = frequency sweep from 4 to 8 GHz. Vertical axis = 10 db/DIV.

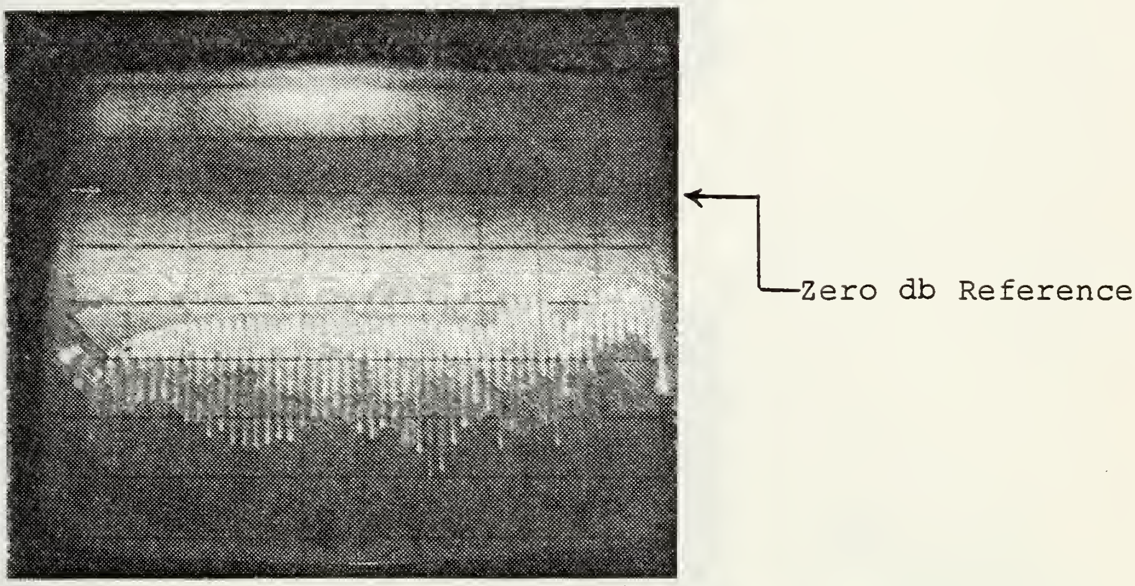

Figure 4-11. Coplanar return loss vs. frequency. External transverse (X direction) biasing magnetic field = 2950 oersteds, 2" substrate (G1001). Horizontal axis: frequency sweep from 8 to 12.4 GHz. Vertical axis: 10 db/DIV.

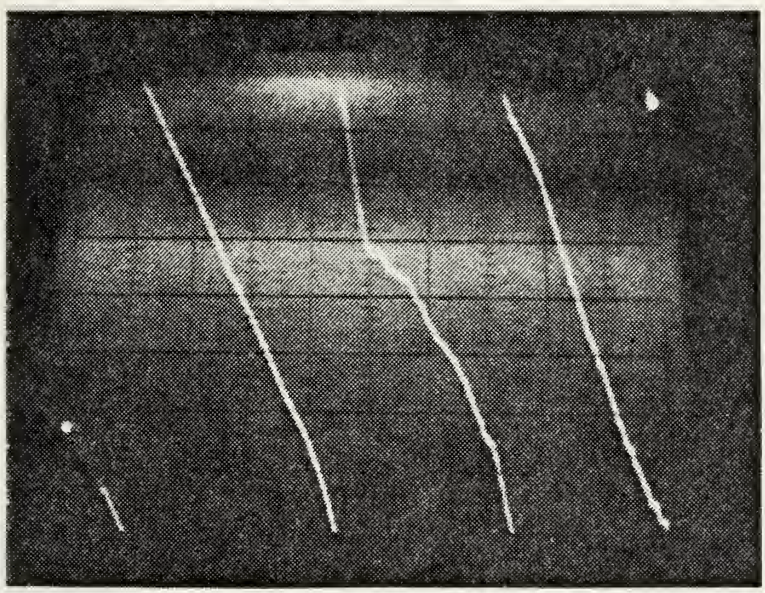

Figure 4-12.
Z^+ Direction of Propagation

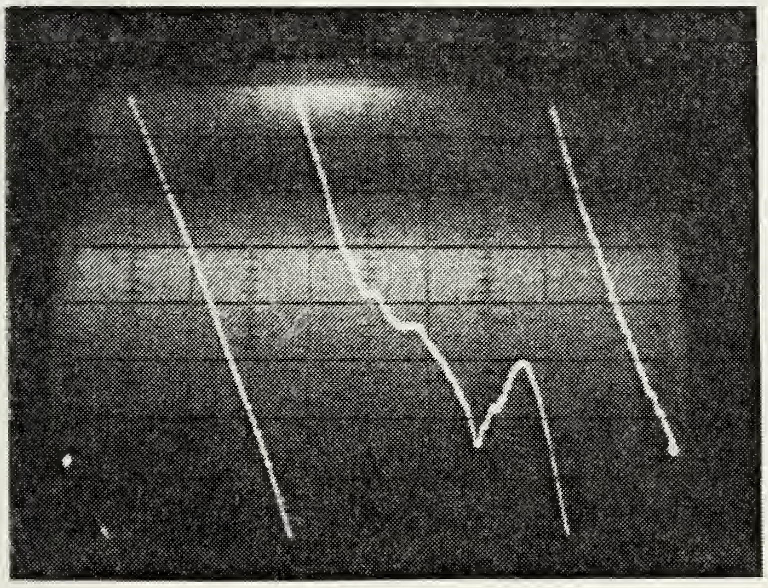

Figure 4-13.
Z^- Direction of Propagation

Coplanar phase shift vs. frequency, 2" substrate (G1001).
External transverse (x direction) biasing magnetic field = 3215 oersteds.
Horizontal axis: frequency sweep from 8 to 12.4 GHz.
Vertical axis: 45 deg/DIV.

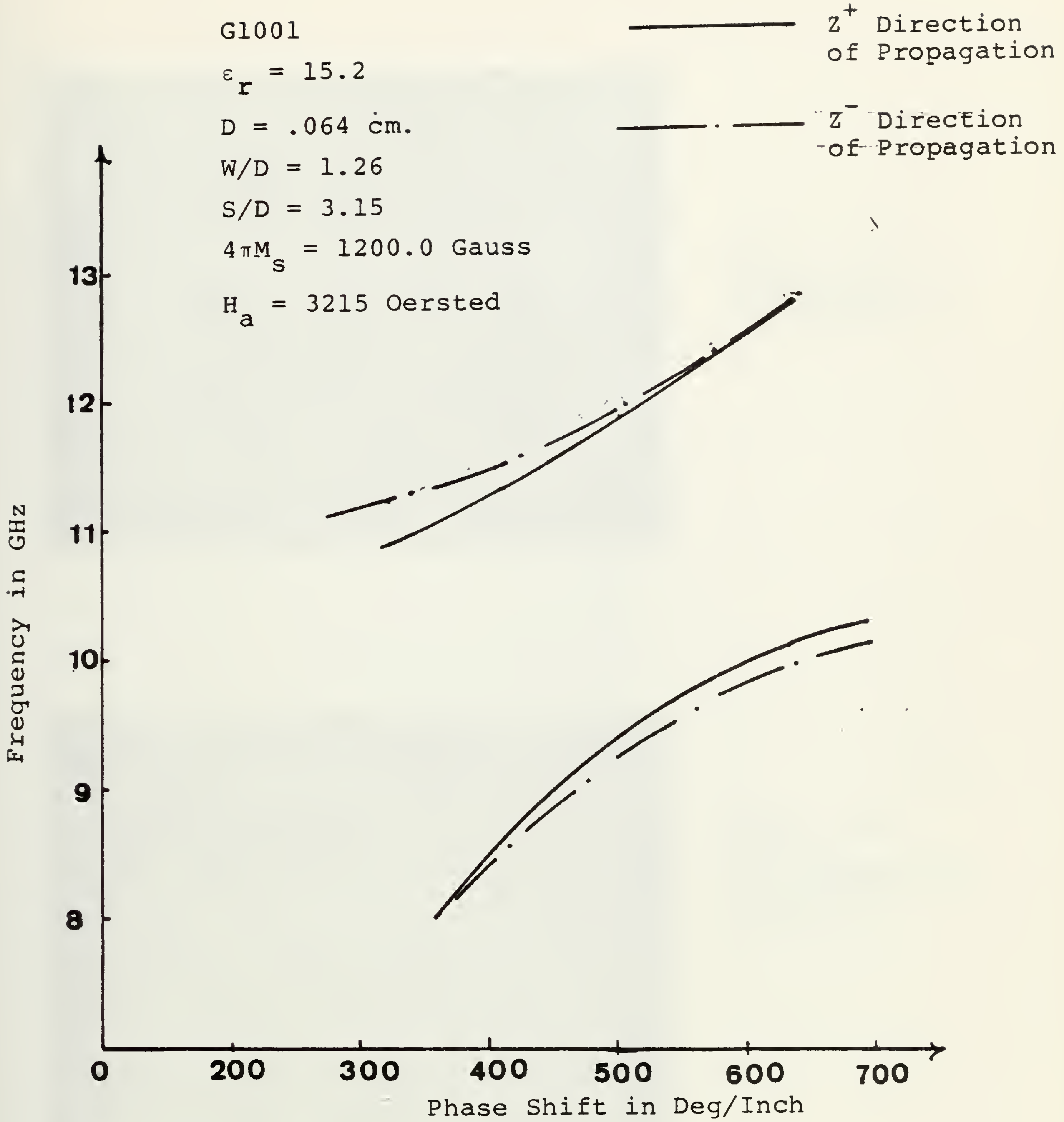

Figure 4-14. Coplanar Phase Shift vs. Frequency for Transverse Magnetization (X-Direction).

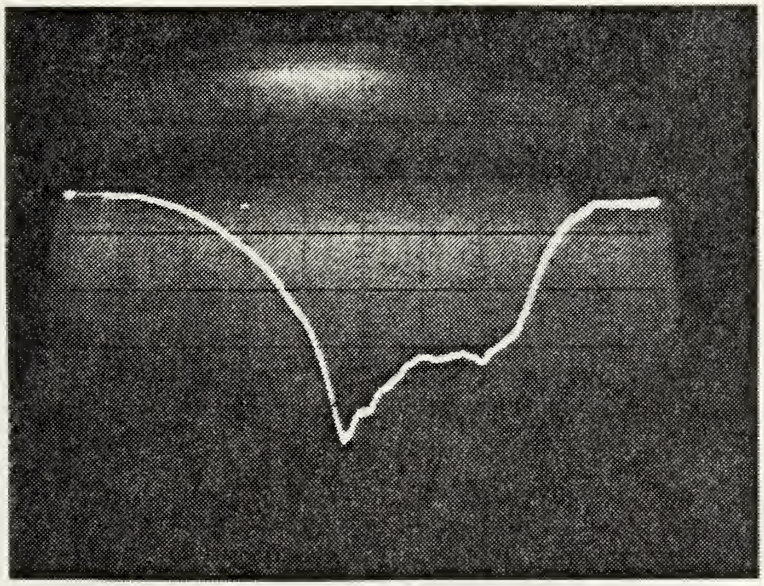

Figure 4-15.
Z^+ Direction of
Propagation

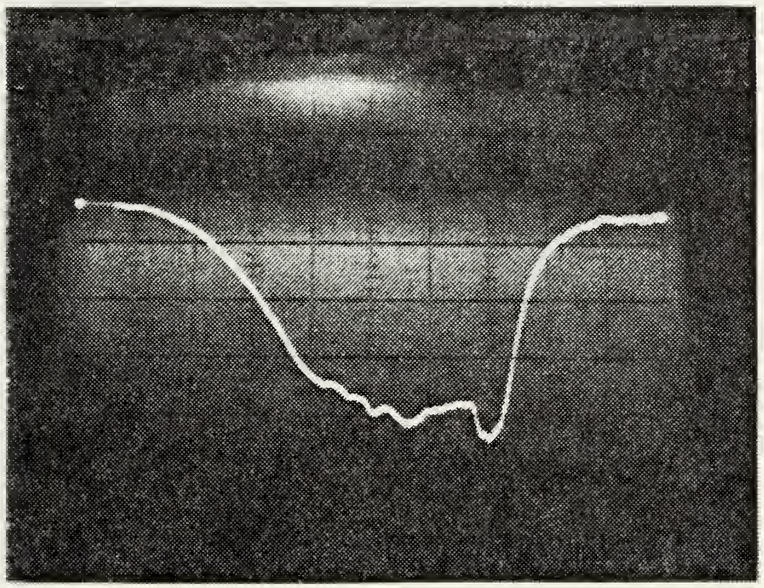

Figure 4-16
Z^- Direction of
Propagation

Coplanar attenuation vs. frequency, 2" substrate (G1001).
External transverse (x direction) biasing magnetic field =
3215 oersteds.
Horizontal axis: frequency sweep from 8 to 12.4 GHz.
Vertical axis: 10 db/DIV.

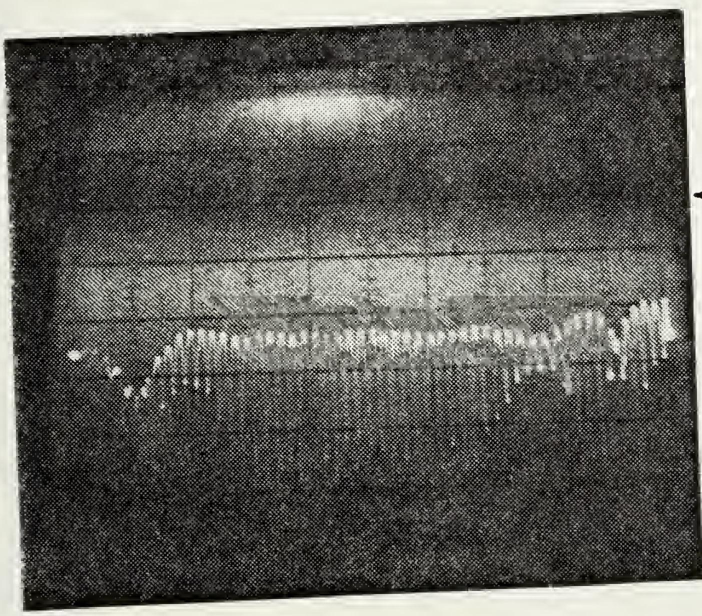

Figure 4-17. Coplanar return loss vs frequency. External transverse (x direction) biasing magnetic field = 3215 oersteds, 2" substrate (G1001). Horizontal axis: frequency sweep from 8 to 12.4 GHz. Vertical axis: 10 db/DIV.

return loss is approximately -30 db throughout the band, indicating a very good impedance match.

Figure 4-10 indicates the return loss from 4 to 8 GHz with an applied biasing magnetic field of 2940.0 oersteds. The return loss is somewhat more than -30 db throughout most of the band.

Figure 4-11 indicates the return loss from 8 to 12.4 GHz with an applied transverse biasing magnetic field of 2950 oersteds and it is approximately -24 db from 8 to 11.1 GHz and -20 db from 11.1 to 12.4 GHz bandwidth.

Figure 4-17 indicates the return loss from 8 to 12.4 GHz with an applied biasing magnetic field of 3215.0 oersteds. The return loss on average is -24 db throughout the band. Thus, the impedance match is not as good as from 4 to 8 GHz but is still quite acceptable.

2. Transverse Magnetic Field

Experiments were conducted on coplanar waveguide with the same conditions as in b. except that the bias field was changed to be in the y-direction (See Fig. 1-2). Pictures 4-18 and 4-19 indicate the phase vs. frequency display and pictures 4-20 and 4-21 show the attenuation for both directions of propagation with H_a = 2940.0 oersteds.

Figures 4-22 and 4-23 indicate the attenuation and phase displays for H_a = 3215.0 oersteds for Z^+ direction. These pictures indicate that external magnetization in the x and y-directions does not produce the same effect. There is a certain attenuation bandwidth more than -30 db of

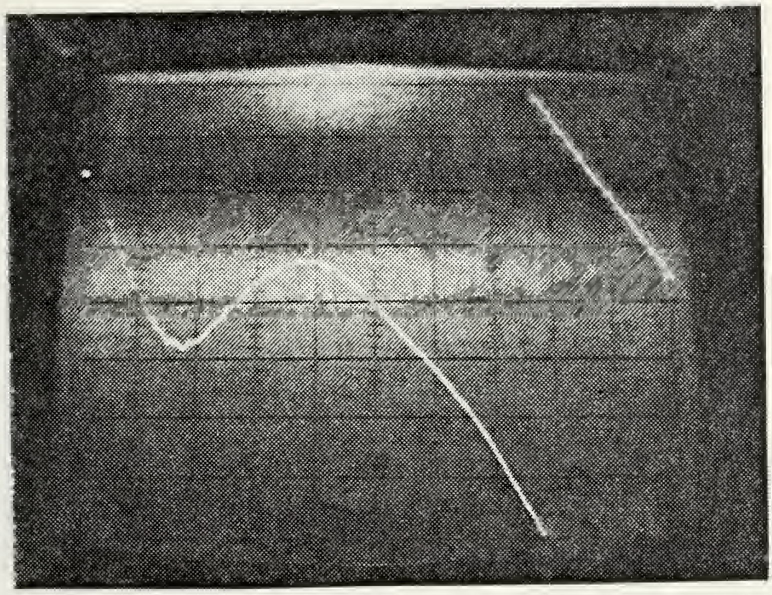

Figure 4-18.
Z^+ Direction of Propagation

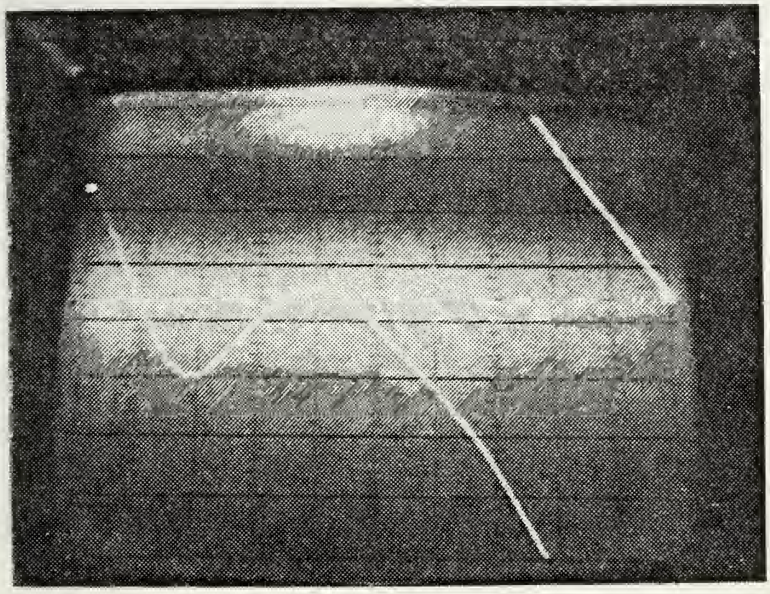

Figure 4-19.
Z^- Direction of Propagation.

Coplanar phase shift vs. frequency, 2" substrate (G1001).
External transverse (y direction) biasing magnetic field = 2950 oersteds.
Horizontal axis: frequency sweep from 4 to 8 GHz.
Vertical axis: 45 deg/DIV.

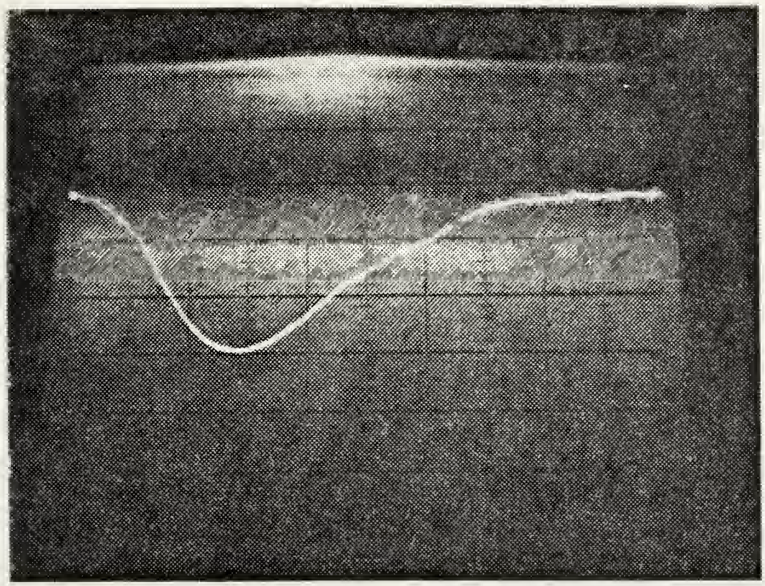

Figure 4-20.
Z^+ Direction of
Propagation

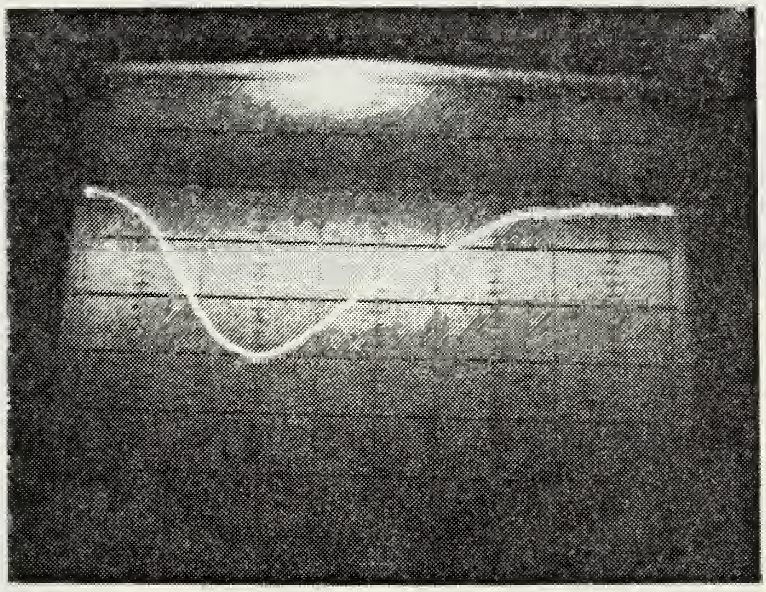

Figure 4-21.
Z^- Direction of
Propagation

Coplanar attenuation vs. frequency, 2" substrate (G1001).
External transverse (y direction) biasing magnetic field =
2950 oersteds.
Horizontal axis: frequency sweep from 4 to 8 GHz.
Vertical axis: 10 db/DIV.

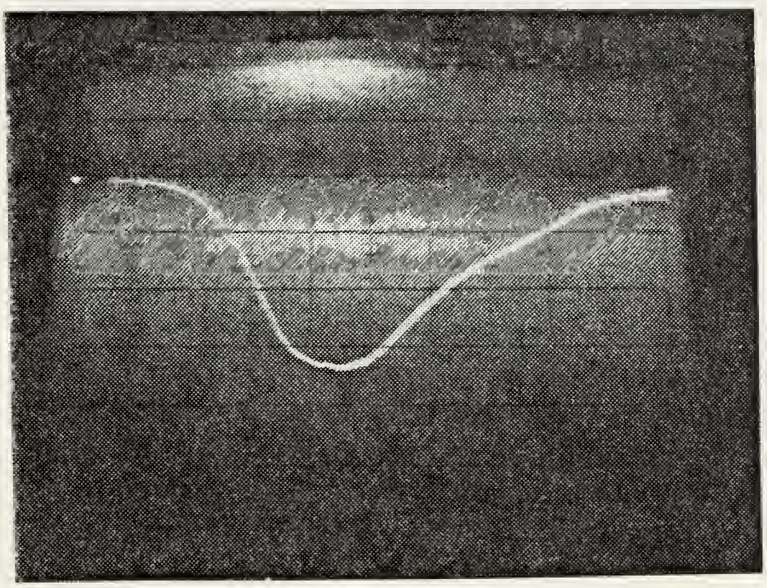

Figure 4-22. Coplanar attenuation vs. frequency, 2" substrate (G1001). External transverse (y direction) biasing magnetic field = 3215 oersteds. Horizontal axis: frequency sweep from 4 to 8 GHz. Vertical axis: 10 db/DIV.

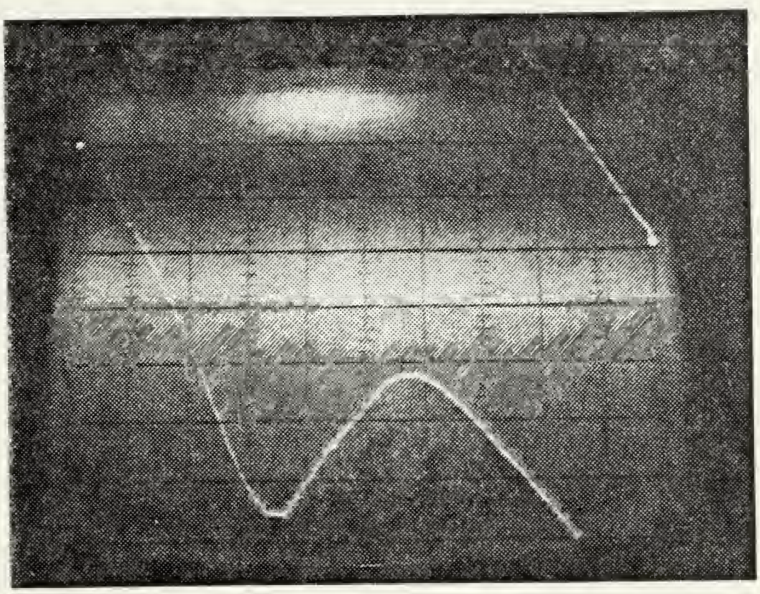

Figure 4-23. Coplanar phase shift vs. frequency, 2" substrate (G1001). External transverse (y direction) biasing magnetic field = 3215 oersteds. Horizontal axis: frequency sweep from 4 to 8 GHz. Vertical axis: 45 deg/DIV.

attenuation, but the coplanar waveguide is also reciprocal for this mode of propagation.

3. Longitudinal Magnetic Field

Experiments were conducted on coplanar waveguide with the same conditions as in b. except that the bias field was changed to be in the longitudinal direction. Pictures 4-24 and 4-25 show the attenuation and phase shift with $H_a = 2940$ oersteds. Pictures 4-26 and 4-27 show the return loss. The attenuation and phase shift was the same for both directions of propagation. In Figure 4-24 the attenuation is 50 db from 10 to 11.3 GHz, and attenuation is greater than the case of transverse magnetic bias.

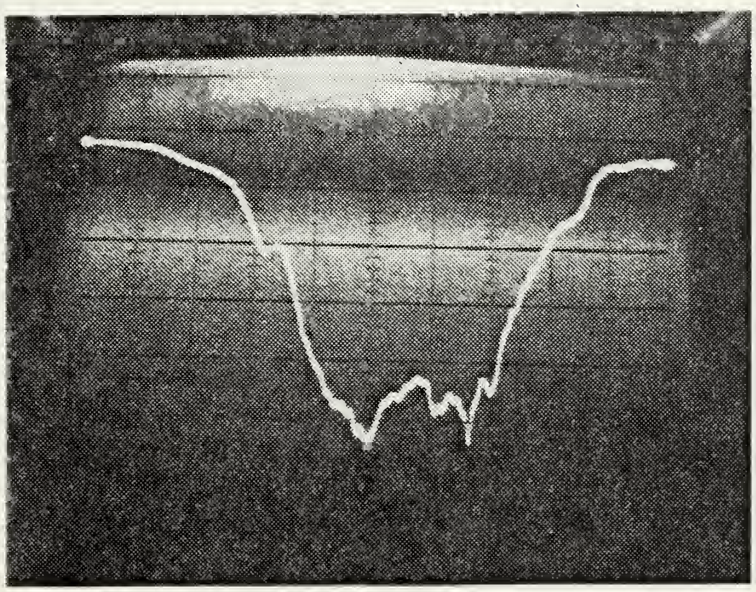

Figure 4-24. Coplanar Attenuation vs. Frequency, 1" substrate (G1001). External longitudinal biasing magnetic field = 2940 oersted. Horizontal axis: frequency sweep from 8 to 12.4 GHz. Vertical axis: 10 db/DIV.

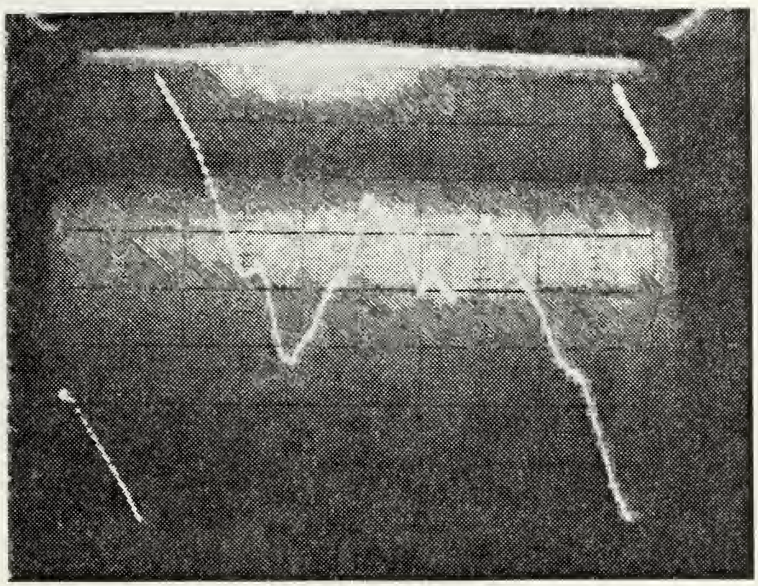

Figure 4-25. Coplanar Phase Shift vs. Frequency, 1" substrate (G1001). External longitudinal biasing magnetic field = 2940 oersteds. Horizontal axis: frequency sweep from 8 to 12.4 GHz. Vertical axis: 45 deg/DIV.

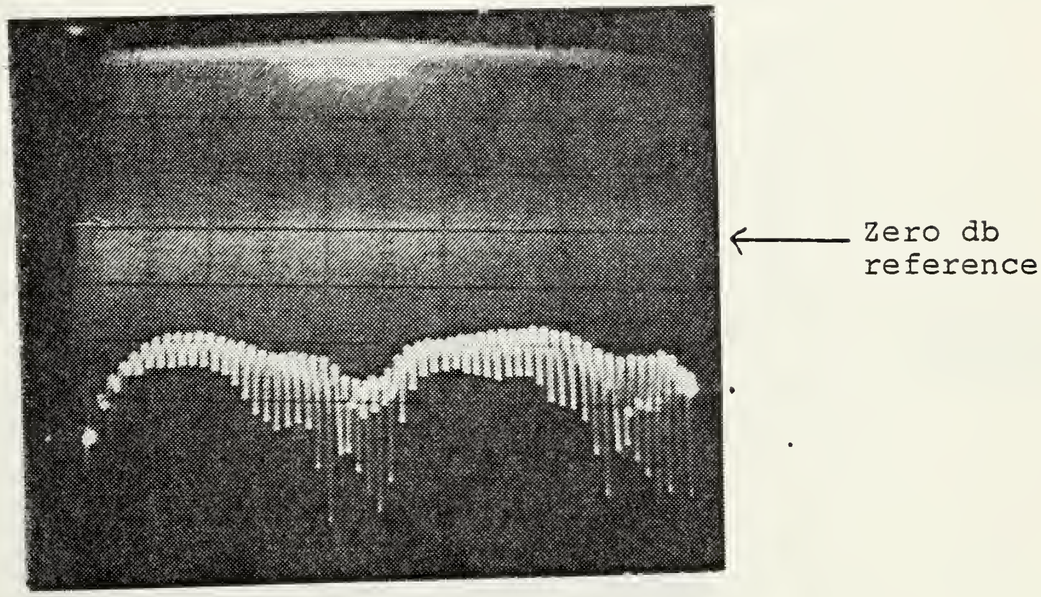

Figure 4-26. Coplanar Return Loss vs. Frequency in the Absence of External Biasing Magnetic Field. 1" substrate (G1001). Horizontal axis: frequency sweep from 8 to 12.4 GHz. Vertical axis: 10 db/div.

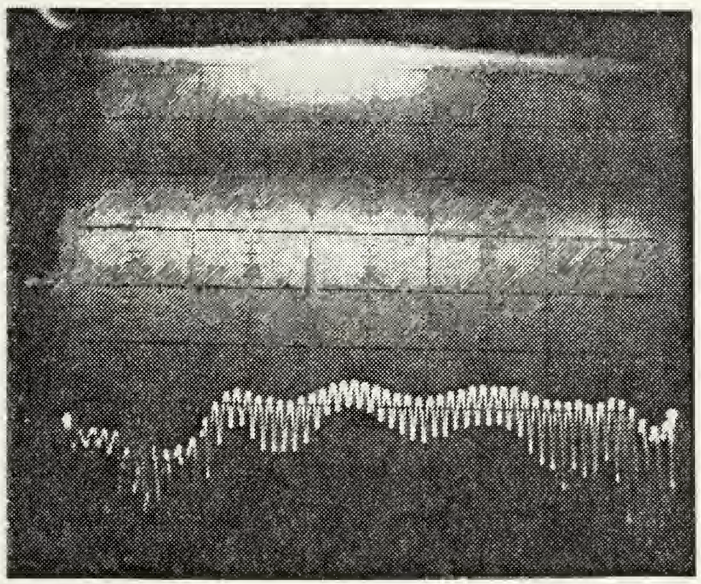

Zero db
reference

Figure 4-27. Coplanar Return Loss vs. Frequency. External Longitudinal Magnetic Field = 2940 oersteds. 1" substrate (G1001). Horizontal axis: frequency sweep from 8 to 12.4 GHz. Vertical axis: 10 db/div.

VI. COMPUTER RESULTS FOR COPLANAR WAVEGUIDE

A frequency dependent hybrid mode analysis of general coplanar transmission lines on ferrite substrate has been developed by K. D. Kuchler [Ref. 2]. A Fourier transform technique was applied and the resulting expressions were evaluated using the method of moments. An extension of this technique was used in a perturbational analysis of coplanar waveguide on ferrite substrate. The computer programs developed by K. D. Kuchler were used to solve the coplanar waveguide and the following results were obtained.

A. DISPERSION AND ATTENUATION DIAGRAMS (TRANVERSE MAGNETIZATION, X-DIRECTION)

1. Dispersion Diagram

A computer analysis for coplanar waveguide on G1001 garnet material with different applied biasing magnetic fields with the following specifications were obtained.

G-1001, 2" x 2" dimension

D = 0.635 mm. S/D = 3.15 W/D = 1.260

$4\pi M_s$ = 1200.0 ε_r = 15.2

Figures 4-28 and 4-29 indicate the ω-β diagrams for both directions of propagation for applied biasing magnetic fields of 2940 and 3215 oersteds. The results are tabulated in Tables 18 and 19 which is both for coplanar waveguide on dielectric material as well as ferrite material.

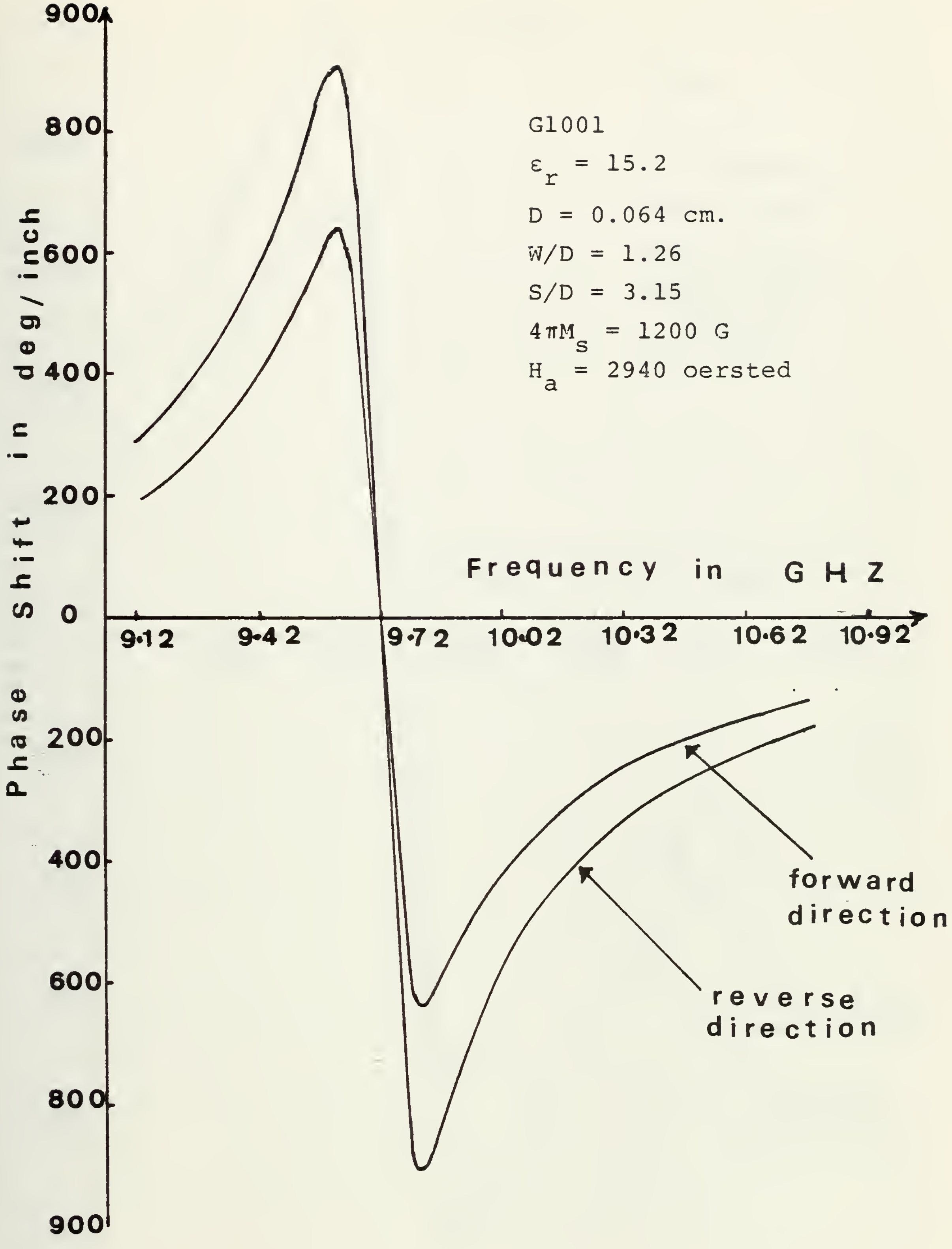

Figure 4-28. Coplanar Waveguide Phase Shift vs. Frequency. Transverse Magnetization (X-Direction), Computer Analysis.

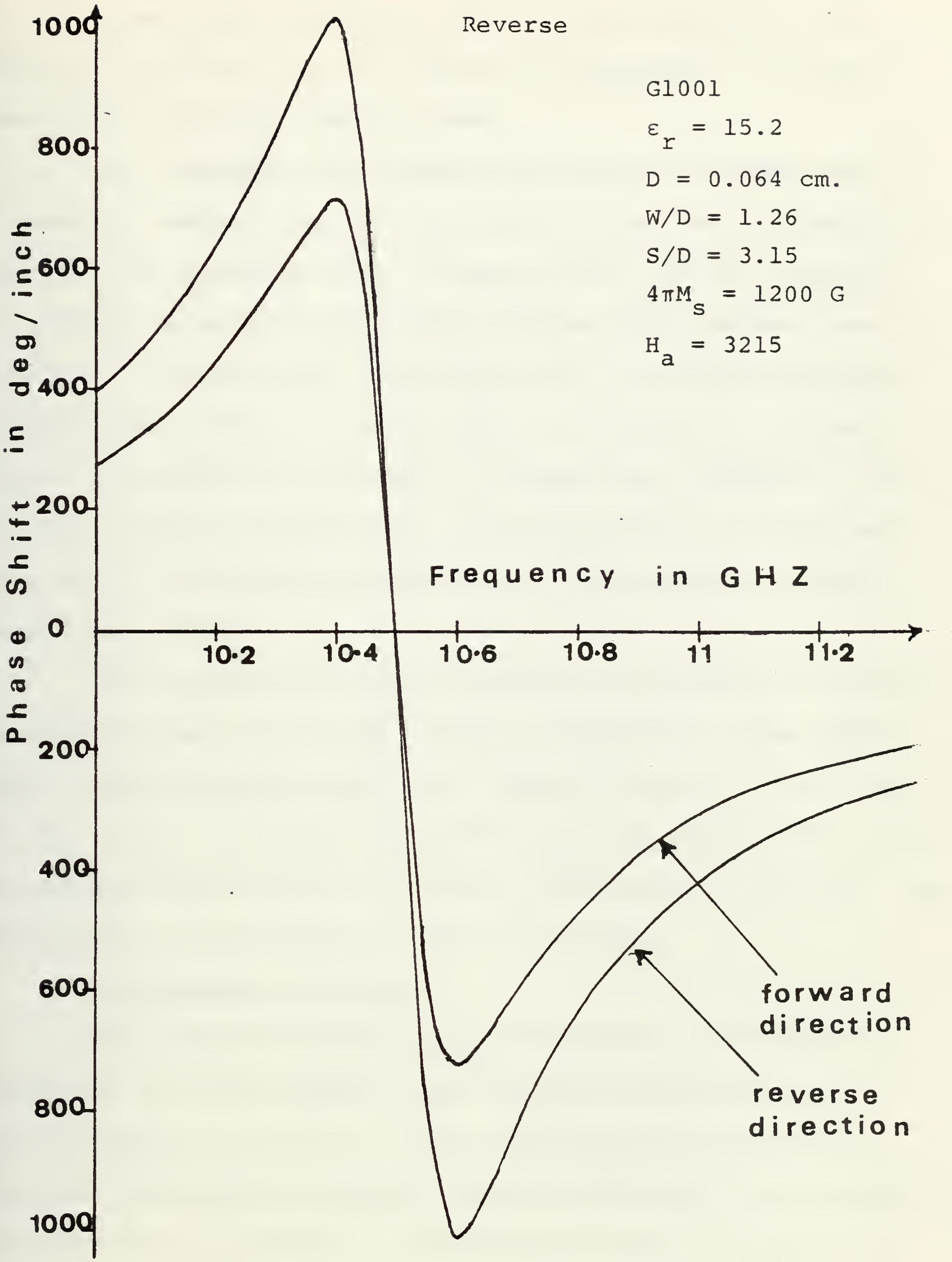

Figure 4-29. Coplanar Waveguide Phase Shift vs. Frequency, Transverse Magnetization (X-Direction), Computer Analysis.

From Figures 4-28 and 4-29, the ω-β diagram, it is evident that there are two propagation branches, a low frequency and a high frequency branch.

As frequency is increased from zero, the phase shift increases, reaches a maximum and then at resonance it switches sharply to a negative value of phase shift; and as frequency is further increased, the value of phase shift becomes less negative. The fact that the phase shift is negative does not indicate that the wave has changed its direction of propagation; it is merely a mathematical convenience inherent in the solution. The ω-β diagram for opposite direction of propagation are of the same shape except that the maximum, minimum values are reduced.

The computer analysis dispersion diagrams (ω-β) exhibit no cutoff region as it was noticed (interpreted) from experiments. Maximum phase shift for forward direction in the case of H_a = 3215.0 oersteds was 1009.2 deg/inch at 10.4 GHz, while the minimum phase shift was -1008.24 deg/inch at 10.6 GHz. The phase shift at 10.5 GHz was -57.87 deg/inch.

2. <u>Attenuation Diagrams</u>

The computer analysis of attenuation of 2" coplanar waveguide on G1001 material with the same conditions and specifications as in VI.A.1 with different applied biasing magnetic fields was obtained. Figures 4-30 and 4-31 indicate the attenuation diagrams for both directions of propagation for applied magnetic fields of 2940.0 and 3215.0 oersteds. The results are tabulated in Tables 18 and 19.

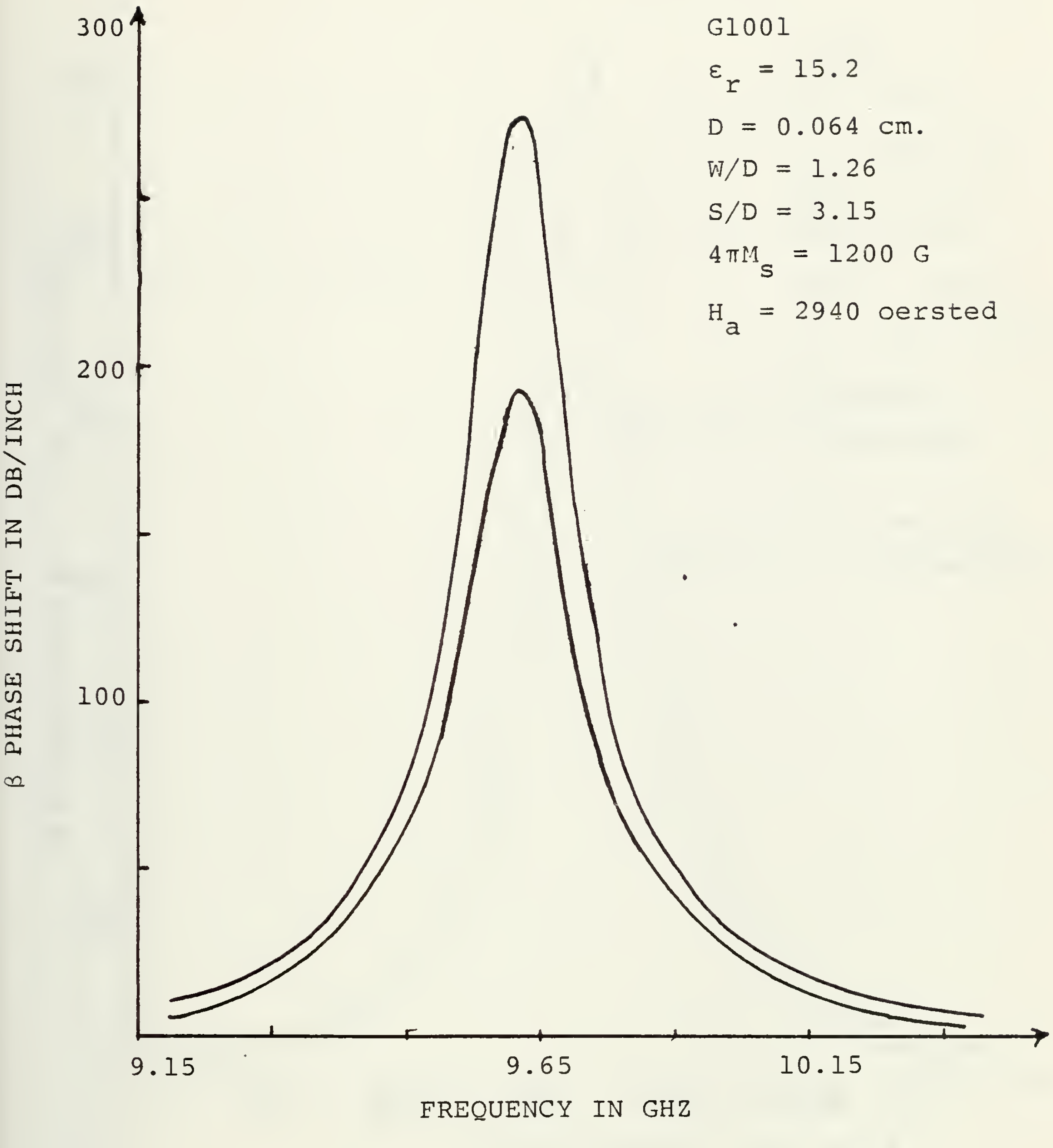

Figure 4-30. Attenuation vs. Frequency of Coplanar Waveguide Transverse Magnetization (X-Direction), Computer Analysis.

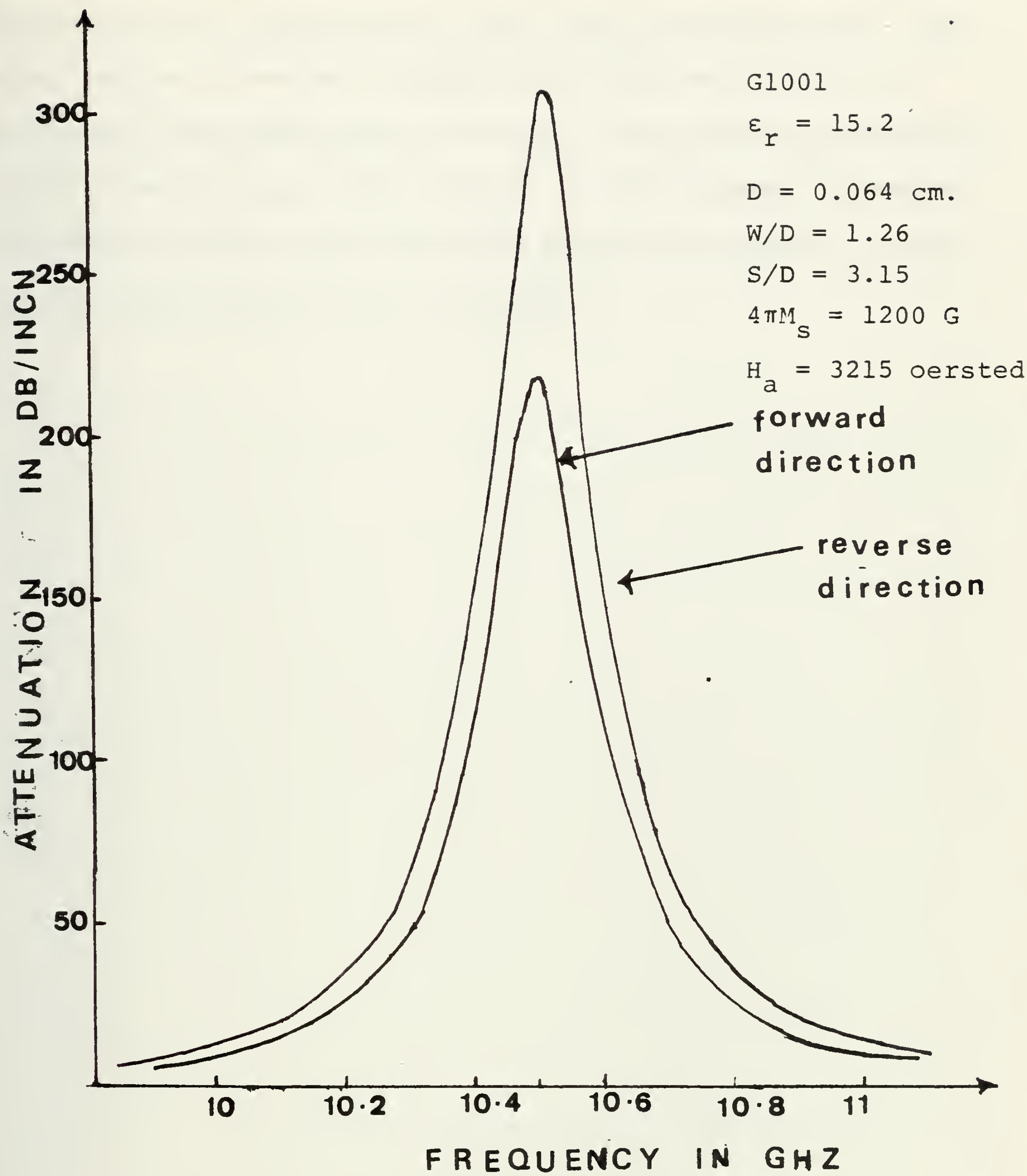

Figure 4-31. Attenuation vs. Frequency of Coplanar Waveguide. Transverse Magnetization (X-Direction) Computer Analysis.

Computer analysis attenuation diagrams exhibit a sharp attenuation at resonance and falls off rapidly to zero. Computer analysis does not indicate any stop band as it was evidenced from experimental results. The maximum attenuation in the case of H_a = 3245 oersteds for the forward direction was 218.42 db/cm; whereas for the reverse direction, it was 306.255 db/cm occurring at 10.5 GHz.

VII. COMPARISON BETWEEN EXPERIMENTAL AND COMPUTER ANALYSIS FOR COPLANAR WAVEGUIDE

Comparisons between the experimental and computer analysis results of a transversely magnetized (x-direction, see figure 1-2) coplanar waveguide indicate certain differences as well as agreement between them as follows.

A. STOP BAND

From experimental results, the phase photographs of Figures 4-5 and 4-13 exhibit a stop band; whereas the plots based on the computer analysis do not indicate a stop band.

B. EXPERIMENTAL ω-β DIAGRAM

Experimental ω-β diagrams of Figs. 4-6 and 4-14 indicate that as frequency increases in lower frequency branch, the phase shift increases as well, which is in agreement with the computer analysis results.

Also experimentally in the upper frequency branch, the phase shift increases with frequency; whereas the computer analysis results indicate that the phase shift from a minimum value which in the case of H_a = 3215.0 oersteds is -1008.24 deg/inch will increase as frequency is increased; again, this is in agreement with the experiment, although the phase shift change from -1008.24 to -254.0 deg/inch was interpreted as an increase in the phase shift.

If the change of sign is interpreted as the change of direction of propagation, then the computer analysis result

is not in agreement with the interpretation of experimental results.

C. GRADIENTS OF ω-β DIAGRAMS

The gradients of ω-β diagrams of experimental and computer analysis differ at each frequency.

D. ATTENUATION

Experimental attenuation pictures of Figs. 4-7, 4-8, 4-15 and 4-16 exhibit a stop band for both directions of propagation. The stop bands for the case of $H_a = 2940.0$ oersteds for both directions of propagation were 1.2 and 0.78 GHz.

For the case of $H_a = 3215.0$ oersteds, the stop bands were 0.88 and 1.35 GHz. The computer analysis results plotted in Figs. 4-9 and 4-10 do not indicate any stop band. The amount of attenuation is far greater from computer results than by the experiment for both directions of propagation.

Computer analysis indicates almost a sharp notch at a frequency which could be taken as the resonance frequency, which is contrary to the experimental results.

E. EXPERIMENTAL RESULTS OF COPLANAR WAVEGUIDE

The experimental results indicate that the coplanar waveguide roughly behaves as a nonreciprocal band rejection filter.

VIII. CONCLUSION

In this thesis both a microstrip transmission line and a coplanar waveguide on G1001 ferrite substrate were designed. The experimental dispersion (ω-β) and attenuation diagrams for different external magnetic fields were obtained. The experimental microstrip transmission line results were compared with theoretical work based on perturbation theory, and they did not agree well. The microstrip experimental results were in agreement with the experimental results of other investigations. It was established that the microstrip on ferrite substrate is a reciprocal band rejection filter, which can be tuned by external applied magnetic field.

The experimental coplanar waveguide results were roughly in agreement with the theory based on perturbation except in few cases. The coplanar waveguide is also a nonreciprocal band rejection filter which can be tuned by external applied magnetic field.

While the agreement between theory and experiment leaves much to be desired, it should be stressed that one should not expect high accuracy from a perturbational analysis of the changes which occur are too great. In the absence of any rigorous theory, however, perturbation theory can be useful as an indicator of interaction between the electromagnetic field and the material and can reveal certain features of the interaction. The need for further theoretical work on these structures is clear, however.

APPENDIX A

TABLE 1

PROPERTIES OF MAGNETIC SUBSTRATE

CHARACTERISTICS	G-1001 GADOLINIUM DOPED IRON GARNET
Saturation Magnetization ($4\pi M_s$) in gauss @ 23°C	1200 $\pm$ 5%
g-effective @ 9.4 GHz	1.99 $\pm$ 1%
Line Width (ΔH) in oersteds @ -3db and 9.4GHz	75 $\pm$ 20%
Line Width (ΔH) in oersteds @ -15db and 9.4 GHz	360 $\pm$ 20%
Dielectric Constant ($\acute{\varepsilon}$) @ 9.4 GHz	15.2 $\pm$ 5%
Dielectric Loss Tangent ($\tan\delta$) @ 9.4 GHz	< .0002
Curie Temperature in °C	280
Spin Wave Line Width (ΔH_k) in oersteds @ 9.4 GHz	4.30
Switching Coefficient* (S_w) in oersted · μsec	1.02
Switching Intercept* (H_0) in orsteds	0.89
Initial Permeability (μ_0) @ 1 KHz	72
*10% output voltage measurement	

TABLE 2

EXPERIMENTAL RESULT

Resonance frequency vs. transverse (y-direction) applied biasing magnetic field of microstrip transmission line

G-1001 1" x 1" dimension
D = .635 mm W = 0.508 mm
E_r = 15.2 $4\pi M_s$ = 1200.0 gauss

Frequency F_r in GHz	Applied Magnetic Field H_a, in Gauss
1.1	1450
1.31	1500
1.383	1520
1.456	1550
1.536	1570
1.54	1570
1.943	1650
2.083	1705
2.211	1735
2.215	1745
2.275	1755
2.414	1770
2.49	1800
2.734	1855
3.02	1960
3.313	2055
3.616	2150
3.731	2200
3.863	2250
3.956	2280
4.087	2345
4.412	2450
4.671	2535
5.099	2700
6.042	3050
6.418	3195
6.541	3230
6.662	3280
6.791	3320
6.915	3370
8.196	3800
8.507	3910
9.499	4240
10.257	4480
10.633	4750
10.77	4800
10.809	4700
10.995	4750
11.012	4860

TABLE 2 (Continued)

THEORETICAL RESULT

$$F_r = \gamma(H_A - 4\pi M_s)$$

Frequency F_r in GHz	Applied Magnetic Field H_a, in Gauss
1.393	1700
2.5	2100
3.343	2400
4.06	2660
4.4576	2800
5.572	3200
0.0	1200

TABLE 3

EXPERIMENTAL RESULTS

Microstrip transmission line on ferrite substrate G1001, 1"x1" , in the absence of any external magnetic field

Thickness of Dielectric D = 0.635 mm, W/D = .8

FREQUENCY IN GHZ	PHASE SHIFT IN DEG/INCH.
3.0	0
3.2	15
3.6	82
3.8	132
4.0	186
4.4	225
4.8	264
5.2	303.9
5.6	393.9
6.0	434.9
6.4	455.9
6.8	487.9
7.2	536.9
7.6	608.9
8.0	653.9
8.44	680.9
8.88	711.9
9.1	734.9
9.32	779.9
9.54	824.9
9.76	847.9
9.98	869.9
10.20	887.9
10.64	920
11.08	977.9
11.52	1049.9
11.96	1085.9
12.40	1157.9

TABLE 4

Microstrip on ferrite substrate G1001, 1" x 1"

Thickness of dielectric D = 0.635 mm., W/D = .8

Permittivity = 15.2

Saturation Magnetization = 1200 + 5% Gauss

Magnetic Biasing Field = 1730.0 Orstead

Line width = 75.0 Orstead, LANDE -G Factor = 1.99

Z^{+} Directions

FREQUENCY GHZ	PHASE SHIFT DEG./INCH
2.0	360.0
2.1	382.0
2.2	416.0
2.3	472.0
2.4	577.0
2.5	707.0
2.6	877.0
2.7	1092.0
2.75	1192.0
3.3	360.0
3.4	378.0
3.5	388.0
3.6	424.0
3.7	455.0
3.8	470.0
3.9	486.0
4.0	516.0

TABLE 5

Microstrip on ferrite substrate G1001, 1" x 1"

Thickness of dielectric D = 0.635 mm, W/D = 0.8

Permittivity = 15.2

Saturation Magnetization = 1200 ± 5% Gauss

Magnetic Biasing Field = 1730.0 Orstead

Line width = 75.0 Orstead LANDE -G Factor = 1.99

Z^- Direction of Propagation

FREQUENCY GHZ	PHASE SHIFT DEG/INCH
2.0	360.0
2.2	415.0
2.3	486.0
2.4	589.0
2.5	742.0
2.6	900.0
2.7	1125.0
2.8	1444.0
2.85	1597.0
3.3	360.0
3.4	374.0
3.5	390.0
3.6	426.0
3.7	448.0
3.8	462.0
3.9	480.0
4.0	503.0

TABLE 6

Microstrip on ferrite substrate G1001, 1" x 1"

Thickness of dielectric D = 0.635 mm, W/D = 0.8

Permittivity = 15.2

Saturation Magnetization = 1200 $\pm$ 5% Gauss

Magnetic Biasing Field = 2670.0 Orsted

Line width = 75.0 Orstead LANDE-G Factor = 1.99

FREQUENCY GHZ	PHASE SHIFT DEG/INCH
4.0	360.0
4.2	405.0
4.4	517.0
4.6	652.0
4.8	832.0
5.0	1125.0
5.1	1260.0
5.7	360.0
5.8	369.0
6.0	414.0
6.2	531.0
6.4	576.0
6.6	630.0
6.8	684.0
7.0	738.0
7.2	760.0
7.6	796.0
7.8	804.0
8.0	849.0

TABLE 7

Microstrip on ferrite substrate G1001, 1" x 1"

Thickness of dielectric D = .635 mm, W/D = .8

Permittivity = 15.2

Saturation Magnetization = 1200 $\pm$ 5% Gauss

Magnetic Biasing Field = 3100.0 Orsted

Line width = 75.0 Orstead LANDE-G Factor = 1.99

FREQUENCY GHZ	β-PHASE SHIFT DEG/INCH
4.0	360.0
4.2	418.0
4.3	441.0
4.4	459.0
4.6	486.0
4.8	513.0
4.9	531.0
5.0	561.0
5.1	607.0
5.2	648.0
5.4	711.0
5.5	779.0
5.6	846.0
5.8	954.0
6.0	1143.0
6.2	1404.0
6.3	1593.0
7.1	360.0
7.2	391.5
7.4	494.0
7.6	585.0
7.8	662.5
8.0	707.0

TABLE 8

THEORETICAL PHASE SHIFT OF TRANSVERSELY MAGNETIZED MICROSTRIP TRANSMISSION LINE

H_a = 3100.0 oersted

G1001 material

FREQUENCY IN GHz	$\mu_{eff} = \frac{\mu^2 - \kappa^2}{\mu}$	PHASE SHIFT IN DEG/INC
1	1.6457	152.55
2	1.6921	309.37
3	1.7864	464.05
4	1.9716	667.0
5	2.3937	919.9
6	3.97	1421.6
6.5	4.3937	9236
6.8	-54.2	
6.9	-14.25	
7	-3.375	
8	- .5793	
8.5	- .08824	
8.6	- .02235	
8.7	.0376	200.6
8.8	.0898	366.36
9.0	.1667	436.9

TABLE 9

Microstrip on ferrite substrate G1001, 1" x 1"

Thickness of dielectric D = 0.635 mm, W/D = .8

Permittivity = 15.2

Saturation Magnetization = 1200 ± 5% Gauss

Magnetic Biasing Field = 3100.0 Orsted

Line width = 75.0 Orstead LANDE-G Factor = 1.99

FREQUENCY GHZ	PHASE SHIFT DEG/INCH
8.0	
8.44	
8.66	
8.88	615.0
9.10	702.0
9.32	810.0
9.54	1035.0
9.63	1112.0
12.16	360.0
12.18	383.0
12.29	477.0
12.4	594.0

TABLE 10

Microstrip on ferrite substrate G1001, 2" x 2"

Thickness of dielectric D = 0.635 mm, W/D = 0.8

Permittivity = 15.2

Saturation Magnetization = 1200 ± 5% Gauss

Magnetic Biasing Field = 2650.0 Orsted

Line width = 75.0 Orstead LANDE - G Factor = 1.99

Z^+ Direction of Propagation

FREQUENCY GHZ	PHASE SHIFT DEG/INCH
4.0	360.0
4.2	490.0
4.4	630.0
4.6	850.0
4.8	1080.0
5.0	1440.0
5.2	1890.0
6.3	360.0
6.4	450.0
6.5	540.0
6.6	630.0
6.8	720.0
6.9	810.0
7.0	845.0
7.2	890.0
7.4	990.0
7.6	1035.0
7.8	1080.0
8.0	1170.0

TABLE 11

Microstrip on ferrite substrate G1001, 2" x 2"

Thickness of dielectric D = 0.635 mm, W/D = 0.8

Permittivity = 15.2

Saturation Magnetization = 1200 ± 5% Gauss

Magnetic Biasing Field = 2650.0 Orsted

Line width = 75.0 Orstead LANDE-G Factor = 1.99

$\bar{Z}$ Direction of Propagation

FREQUENCY GHZ	PHASE SHIFT DEG/INCH
4.0	360
4.2	466
4.4	574
4.6	745
4.8	925
5.0	1210
5.2	1600
5.3	1830
6.4	360.0
6.6	495.0
6.8	630.0
7.0	780.0
7.1	810.0
7.2	900.0
7.4	945.0
7.6	999.0
7.8	1099.0
8.0	1149.0

TABLE 12

COMPUTER OUTPUT OF PHASE SHIFT AND ATTENUATION FOR BOTH DIRECTIONS OF PROPAGATION (Z^+, Z^-) AS A FUNCTION OF FREQUENCY OF MICROSTRIP TRANSMISSION LINE

Microstrip on Ferrite Substrate G1001, 1" x 1"
Thickness of Dielectric D = 0.635 mm, W/D = 0.8
Permittivity = 15.2
Saturation Magnetization = gauss
Magnetic Biasing Field Ha = 1730.0 orsteds
Line Width = 75.0 orsteds LANDE-G Factor = 1.99
Resonance Frequency F_r = 2.8 GHz

Frequency GHz	Phase Shift Deg./Inch Z^+ Direction	Phase Shift Deg./Inch Z^- Direction	Attenuation db./Inch Z^+ Direction	Attenuation db./Inch Z^- Direction
0.600	-8.952243	-2.925009	0.008835	0.002887
0.700	-10.709913	-3.538090	0.010927	0.003610
0.800	-12.591203	-4.203658	0.013351	0.004457
0.900	-14.620826	-4.930667	0.016196	0.005462
1.000	-16.827478	-5.730009	0.019579	0.006667
1.100	-19.245786	-6.615079	0.023650	0.008129
1.200	-21.920686	-7.602491	0.028615	0.009924
1.300	-24.907612	-8.713256	0.034747	0.012155
1.400	-28.275878	-9.974376	0.042426	0.014966
1.500	-32.118007	-11.421030	0.052190	0.018559
1.600	-36.556169	-13.100088	0.064822	0.023229
1.700	-41.753228	-15.075516	0.081479	0.029419
1.800	-47.945117	-17.436494	0.103964	0.037809
1.900	-55.464211	-20.312023	0.135155	0.049496
2.000	-64.811408	-23.895342	0.179896	0.066326
2.100	-76.768901	-28.489998	0.246816	0.091597
2.200	-92.649983	-34.600836	0.352520	0.131651
2.300	-114.800320	-43.135511	0.532110	0.199937
2.400	-147.907725	-55.903593	0.870541	0.329032
2.500	-202.834501	-77.104740	1.617932	0.615035
2.600	-311.775387	-119.174207	3.793495	1.450040
2.700	-627.842264	-241.277787	15.541324	5.972482
2.800	-11.817790	-4.565293	603.387815	233.092813
2.900	659.931622	256.220280	16.945996	6.579330
3.000	345.026561	134.614532	4.510439	1.759780
3.100	236.327530	92.642597	2.097890	0.822393
3.200	181.507626	71.479577	1.231148	0.484839

TABLE 12 (Continued)

Frequency GHz	Phase Shift Deg./Inch Z^+ Direction	Phase Shift Deg./Inch Z^- Direction	Attenuation db./Inch Z^+ Direction	Attenuation db./Inch Z^- Direction
3.300	148.477047	58.733277	0.820946	0.324743
3.400	126.395961	50.214886	0.593474	0.235777
3.500	110.585464	44.118573	0.453570	0.180954
3.600	98.701923	39.538318	0.361010	0.144615
3.700	89.439721	35.969834	0.296358	0.119186
3.800	82.013467	33.110202	0.249259	0.100630
3.900	75.923737	30.766434	0.213783	0.086631
4.000	70.839011	28.809695	0.186329	0.075779
4.100	66.525020	27.150989	0.164588	0.067174
4.200	62.820085	25.726411	0.147048	0.060220
4.300	59.600853	24.489338	0.132660	0.054509
4.400	56.777314	23.404652	0.120692	0.049751
4.500	54.280009	22.445521	0.110613	0.045740
4.600	52.054291	21.591108	0.102032	0.042321
4.700	50.058699	20.824858	0.094658	0.039378
4.800	48.257891	20.133648	0.088264	0.036825
4.900	46.624790	19.506765	0.082680	0.034591
5.000	45.135717	18.935528	0.077766	0.032625
5.100	43.773539	18.412621	0.073417	0.030882
5.200	42.521628	17.932085	0.069545	0.029328
5.300	41.366906	17.488857	0.066079	0.027937
5.400	40.298299	17.078657	0.062962	0.026684
5.500	39.306368	16.697833	0.060147	0.025551

TABLE 13

COMPUTER OUTPUT OF PHASE SHIFT AND ATTENUATION FOR BOTH DIRECTIONS OF PROPAGATION (Z^+, Z^-) AS A FUNCTION OF FREQUENCY OF MICROSTRIP TRANSMISSION LINE

Microstrip on Ferrite Substrate G1001, 1" x 1"
Thickness of Dielectric D = 0.635 mm, W/D = 0.8
Permittivity = 15.2
Saturation Magnetization =   gauss
Magnetic Biasing Field Ha = 2670.0 orsteds
Line Width = 75.0 orsteds   LANDE-G Factor = 1.99
Resonance Frequency F_r = 5.192GHz

Frequency GHz	Phase Shift Deg./Inch Z^+ Direction	Phase Shift Deg./Inch Z^- Direction	Attenuation db./Inch Z^+ Direction	Attenuation db./Inch Z^- Direction
2.692	-36.980804	-14.205681	0.031157	0.011969
2.792	-39.751393	-15.349932	0.035002	0.013516
2.892	-42.755436	-16.593209	0.039433	0.015304
2.992	-46.023054	-17.949070	0.044564	0.017380
3.092	-49.593527	-19.433499	0.050542	0.019805
3.192	-53.511461	-21.065796	0.057553	0.022657
3.292	-57.833539	-22.869198	0.065833	0.026032
3.392	-62.627621	-24.872167	0.075689	0.030059
3.492	-67.975046	-27.109990	0.087521	0.034905
3.592	-73.981707	-29.626561	0.101867	0.040793
3.692	-80.780881	-32.477515	0.119452	0.048025
3.792	-88.540797	-35.734534	0.141274	0.057018
3.892	-97.483546	-39.491233	0.168744	0.068359
3.992	-107.905173	-43.872415	0.203893	0.082899
4.092	-120.212094	-49.048068	0.249747	0.101900
4.192	-134.963808	-55.256609	0.310931	0.127301
4.292	-152.980172	-62.841625	0.394849	0.162197
4.392	-175.482490	-72.318638	0.513876	0.211775
4.492	-204.388284	-84.497135	0.689963	0.285241
4.592	-242.897992	-100.724267	0.965087	0.400199
4.692	-296.748939	-123.421383	1.427595	0.593753
4.792	-377.394139	-157.416140	2.290201	0.955273
4.892	-511.395765	-213.910584	4.076192	1.746850
4.992	-777.413854	-326.070578	9.612059	4.031584
5.092	-1549.462994	-651.619595	38.675397	16.264762
5.192	-15.584564	-6.570995	1475.455534	622.103446
5.292	1599.993165	676.305772	40.734867	17.218339
5.392	829.630511	351.535534	10.663098	4.518226

TABLE 13(Continued)

Frequency GHz	Phase Shift Deg./Inch Z^+ Direction	Phase Shift Deg./Inch Z^- Direction	Attenuation db./Inch Z^+ Direction	Attenuation db./Inch Z^- Direction
5.492	563.938170	239.522946	4.879675	2.072557
5.592	430.053603	183.080208	2.818606	1.199923
5.692	349.469599	149.109016	1.850685	0.789636
5.792	295.660006	126.424211	1.317895	0.563532
5.892	257.180665	110.204183	0.992540	0.425312
5.992	228.298708	98.030032	0.778767	0.334398
6.092	205.818740	88.555640	0.630432	0.271250
6.192	187.827196	80.971943	0.523081	0.225499
6.292	173.097935	74.764113	0.442726	0.191221
6.392	160.818103	69.588391	0.380911	0.164826
6.492	150.422321	65.206834	0.332260	0.144032
6.592	141.507332	61.449373	0.293227	0.127334
6.692	133.778045	58.191211	0.261393	0.113702
6.792	127.011077	55.338863	0.235055	0.102414
6.892	121.037463	52.820699	0.212993	0.092950
6.992	115.725168	50.581043	0.194309	0.084929
7.092	110.969351	48.575970	0.178332	0.078063
7.192	106.687804	46.770226	0.164550	0.072136
7.292	102.811835	45.135414	0.152569	0.066979
7.392	99.286246	43.648229	0.142079	0.062461
7.492	96.066442	42.289349	0.132838	0.058476

TABLE 14

COMPUTER OUTPUT OF PHASE SHIFT AND ATTENUATION FOR BOTH DIRECTIONS OF PROPAGATION (Z^+, Z^-) AS A FUNCTION OF FREQUENCY OF MICROSTRIP TRANSMISSION LINE

Microstrip on Ferrite Substrate G1001, 1" x 1"
Thickness of Dielectric D = 0.635 mm, W/D = 0.8
Permittivity = 15.2
Saturation Magnetization =   gauss
Magnetic Biasing Field Ha = 3100.0 orsteds
Line Width = 75.0 orsteds   LANDE-G Factor = 1.99
Resonance Frequency F_r = 6.364 GHz

Frequency GHz	Phase Shift Deg./Inch Z^+ Direction	Phase Shift Deg./Inch Z^- Direction	Attenuation db./Inch Z^+ Direction	Attenuation db./Inch Z^- Direction
3.364	-40.689227	-16.140354	0.028616	0.011351
3.464	-43.218489	-17.216413	0.031533	0.012561
3.564	-45.924498	-18.369680	0.034814	0.013926
3.664	-48.826542	-19.608707	0.038518	0.015469
3.764	-51.947441	-20.943334	0.042717	0.017222
3.864	-55.314321	-22.384941	0.047496	0.019221
3.964	-58.957478	-23.946879	0.052960	0.021511
4.064	-62.913903	-25.644745	0.059240	0.024147
4.164	-67.225781	-27.497058	0.066495	0.027198
4.264	-71.943269	-29.525866	0.074924	0.030749
4.364	-77.129181	-31.757488	0.084783	0.034909
4.464	-82.856793	-34.223932	0.096396	0.039816
4.564	-89.215586	-36.964324	0.110179	0.045650
4.664	-96.318229	-40.026876	0.126684	0.052646
4.764	-104.304421	-43.471912	0.146640	0.061116
4.864	-113.349798	-47.375910	0.171033	0.071485
4.964	-123.682873	-51.837035	0.201225	0.084336
5.064	-135.599435	-56.983807	0.239129	0.100491
5.164	-149.495383	-62.987470	0.287504	0.121135
5.264	-165.912304	-70.081365	0.350447	0.148029
5.364	-185.604131	-78.592315	0.434229	0.183870
5.464	-209.661634	-88.992073	0.548851	0.232963
5.564	-239.722711	-101.987708	0.711041	0.302505
5.664	-278.350068	-118.690023	0.950412	0.405261
5.764	-329.824174	-140.947358	1.323539	0.565602
5.864	-401.818894	-172.081897	1.949363	0.834829
5.964	-509.652403	-218.717227	3.113941	1.336347
6.064	-688.858348	-296.221821	5.654597	2.431581

TABLE 14 (Continued)

Frequency GHz	Phase Shift Deg./Inch Z^+ Direction	Phase Shift Deg./Inch Z^- Direction	Attenuation db./Inch Z^+ Direction	Attenuation db./Inch Z^- Direction
6.164	-1044.637713	-450.096404	12.961378	5.584586
6.264	-2077.178462	-896.699044	51.941140	22.422518
6.364	-17.007902	-7.355834	1973.681038	853.607375
6.464	2135.835994	925.407437	54.277239	23.517049
6.564	1105.194628	479.699295	14.153419	6.143158
6.664	749.785387	325.993374	6.452459	2.805415
6.764	570.714841	248.547290	3.713252	1.617128
6.864	462.944589	201.938529	2.429194	1.059625
6.964	390.985068	170.817819	1.723610	0.753029
7.064	339.540182	148.567714	1.293501	0.565978
7.164	300.931565	131.869488	1.011368	0.443186
7.264	270.888139	118.875720	0.815925	0.358058
7.364	246.846697	108.476413	0.674703	0.296497
7.464	227.170030	99.964921	0.569162	0.250457
7.564	210.768122	92.869712	0.488093	0.215066
7.664	196.885997	86.864193	0.424383	0.187234
7.764	184.985164	81.714933	0.373345	0.164920
7.864	174.669740	77.250762	0.331777	0.146734
7.964	165.640170	73.343458	0.297433	0.131700
8.064	157.672967	69.894556	0.268706	0.119114

TABLE 15

Co-planar Waveguide on Ferrite Substrate G-1001, 2" x 2" in the Absence of Any External Magnetic Field

Thickness of Dielectric D = 0.635 mm, W/D = 1.260, S/D = 3.15

a. Experimental Results

Frequency in GHz	Phase Shift in Deg/2 Inch
4.0	630.0 (arbitrary reference)
4.4	697.0
4.8	761.0
5.4	855.0
6.0	940.0

b. Computer Analysis Results (CoPlan)

Frequency in GHz	Phase Shift in Deg/2 Inch
6.0	843.153
7.0	990.30
8.0	1140.24
9.0	1292.133
10.0	1446.6

TABLE 16

Co-planar Waveguide on Ferrite Substrate, G1001, 2" x 2"

Thickness of dielectric D = 0.635 mm, W/D = 1.260, S/D = 3.15

Magnetic Biasing Field (Transverse x direction) = 2950.0 orsteads

FREQUENCY GHz	Z^+ DIRECTION PHASE SHIFT DEG/INCH	Z^- DIRECTION PHASE SHIFT DEG/INCH
8.0	360.0	360.0
8.44	405.0	412.0
8.66	-----	445.0
8.88	450.0	472.0
9.10	-----	508.0
9.32	498.0	558.0
9.42	503.0	-----
9.54	-----	597.0
10.2	360.0	-----
10.3	369.0	-----
10.42	387.0	-----
10.53	401.0	-----
10.64	423.0	-----
10.74	-----	360.0
10.75	445.0	-----
10.86	463.0	383.0
11.08	499.0	442.0
11.30	535.0	501.0
11.52	567.0	532.0
11.74	591.0	561.0
11.96	614.0	586.0
12.18	637.0	-----
12.40	664.0	645.0

TABLE 17

EXPERIMENTAL RESULTS

Co-planar Waveguide on Ferrite Substrate, G-1001, 2" x 2"

Thickness of dielectric D = 0.635 mm, W/D = 1.260, S/D = 3.15

Magnetic Biasing Field (Transverse, x direction) = 3215.0 orstead

FREQUENCY GHz	Z^+ DIRECTION PHASE SHIFT DEG/INCH	Z^- DIRECTION PHASE SHIFT DEG/INCH
8.0	360.0	360.0
8.44	396.0	400.0
8.88	445.0	458.0
9.32	492.0	517.0
9.76	542.0	589.0
9.98	587.0	634.0
10.09	621.0	-----
10.20	649.0	-----
11.08	360.0	-----
11.30	415.0	-----
11.33	-----	360.0
11.52	438.0	394.0
11.74	-----	462.0
11.96	517.0	502.0
12.18	550.0	540.0
12.4	584.0	576.0

TABLE 18

COPLANAR WAVEGUIDE ON FERRITE SUBSTRATE

THICKNESS OF DIELECTRIC = 0.064 CM   W/D = 1.260   S/D = 3.150
PERMITTIVITY = 15.2
SATURATION MAGNETIZATION = 1200.00 GAUSS
MAGNETIC BIASING FIELD = 2940.00 OERSTED
LINEWIDTH = 75.00 OERSTED   LANDE-G = 2.0

GENERAL DATA FOR DIELECTRIC SUBSTRATE				FERRITE SUBSTRATE WAVE TRAVELING FORWARD		REVERSE	
FREQ GHz	D / LAMBDA	LAMBDAP / LAMBDA	ZO	ALPHA DB/CM	BETA-FE / BETA-DI	ALPHA DB/CM	BETA-FE / BETA-DI
9.120	0.0193	0.4243	57.0	5.170	200.047	7.488	294.856
9.170	0.0194	0.4240	57.0	6.167	218.391	8.926	321.258
9.220	0.0195	0.4239	57.1	7.469	240.011	10.791	352.006
9.270	0.0196	0.4238	57.1	9.205	265.775	13.277	388.626
9.320	0.0197	0.4236	57.2	11.587	296.875	16.684	432.803
9.370	0.0198	0.4234	57.2	14.963	334.877	21.530	487.264
9.420	0.0199	0.4233	57.3	19.943	381.918	28.647	554.072
9.470	0.0200	0.4231	57.3	27.637	440.311	39.630	636.935
9.520	0.0202	0.4229	57.3	40.171	511.175	57.569	738.163
9.570	0.0203	0.4227	57.4	61.709	588.027	88.286	846.943
9.620	0.0204	0.4226	57.4	99.379	630.487	141.940	906.241
9.670	0.0205	0.4225	57.5	156.069	494.844	222.535	711.392
9.720	0.0206	0.4222	57.5	192.923	1.590	274.932	8.128
9.770	0.0207	0.4221	57.6	157.894	-496.278	224.640	-700.141
9.820	0.0208	0.4220	57.6	102.005	-640.940	144.887	-904.387
9.870	0.0209	0.4217	57.6	64.342	-605.621	91.343	-853.719
9.920	0.0210	0.4216	57.7	42.564	-533.364	60.328	-749.839

TABLE 18

(CONTINUED)

GENERAL DATA FOR DIELECTRIC SUBSTRATE				FERRITE SUBSTRATE WAVE TRAVELING FORWARD		REVERSE	
FREQ GHz	D / LAMBDA	LAMBDAP / LAMBDA	ZO	ALPHA DB/CM	BETA-FE / BETA-DI	ALPHA DB/CM	BETA-FE / BETA-DI
9.970	0.0211	0.4215	57.7	29.754	-465.292	42.103	-652.222
10.020	0.0212	0.4212	57.8	21.812	-408.653	30.852	-571.740
10.070	0.0213	0.4211	57.8	16.628	-362.823	23.481	-506.028
10.120	0.0214	0.4210	57.8	13.081	-325.627	18.442	-452.703
10.170	0.0215	0.4207	57.9	10.555	-295.084	14.875	-409.398
10.220	0.0216	0.4206	57.9	8.699	-269.767	12.240	-373.053
10.270	0.0217	0.4205	58.0	7.297	-248.486	10.252	-342.492
10.320	0.0218	0.4202	58.0	6.212	-230.351	8.723	-316.825
10.370	0.0219	0.4201	58.0	5.356	-214.798	7.510	-294.447
10.420	0.0221	0.4200	58.1	4.669	-201.301	6.537	-275.018
10.470	0.0222	0.4197	58.1	4.109	-189.457	5.750	-258.278
10.520	0.0223	0.4196	58.2	3.647	-179.039	5.095	-243.247
10.570	0.0224	0.4195	58.2	3.260	-169.786	4.549	-229.887
10.620	0.0225	0.4192	58.2	2.934	-161.488	4.092	-218.173
10.670	0.0226	0.4191	58.3	2.656	-154.056	3.699	-207.414
10.720	0.0227	0.4190	58.3	2.418	-147.340	3.362	-197.684
10.770	0.0228	0.4187	58.4	2.211	-141.218	3.074	-189.051
10.820	0.0229	0.4186	58.4	2.031	-135.662	2.819	-180.976

TABLE 19

COPLANAR WAVEGUIDE ON FERRITE SUBSTRATE

THICKNESS OF DIELECTRIC = 0.064 CM   W/D = 1.260   S/D = 3.150
PERMITTIVITY = 15.2
SATURATION MAGNETIZATION = 1200.00 GAUSS
MAGNETIC BIASING FIELD = 3215.00 OERSTED
LINEWIDTH = 75.00 OERSTED   LANDE-G FACTOR = 2.0

GENERAL DATA FOR DIELECTRIC SUBSTRATE				FERRITE SUBSTRATE WAVE TRAVELING FORWARD		REVERSE	
FREQ GHz	D / LAMBDA	LAMBDAP / LAMBDA	ZO	ALPHA DB/CM	BETA-FE	ALPHA DB/CM	BETA-FE
9.800	0.0207	0.4220	57.6	4.343	195.355	6.206	284.687
9.850	0.0208	0.4219	57.6	5.061	210.986	7.220	306.567
9.900	0.0210	0.4217	57.7	5.964	229.028	8.493	331.807
99.950	0.0211	0.4215	57.7	7.117	250.031	10.129	361.557
10.000	0.0212	0.4214	57.7	8.624	274.808	12.253	396.219
10.050	0.0213	0.4212	57.8	10.638	304.358	15.088	437.535
10.100	0.0214	0.4210	57.8	13.404	340.017	19.000	487.895
10.150	0.0215	0.4209	57.9	17.335	383.704	24.532	548.978
10.200	0.0216	0.4207	57.9	23.148	437.763	32.704	624.514
10.250	0.0217	0.4205	57.9	32.153	504.772	45.402	718.859
10.300	0.0218	0.4204	58.0	46.885	585.904	66.095	832.125
10.350	0.0219	0.4202	58.0	72.262	672.359	101.702	952.512
10.400	0.0220	0.4200	58.1	116.510	713.360	163.895	1009.771
10.450	0.0221	0.4199	58.1	181.447	535.481	254.828	758.395
10.500	0.0222	0.4197	58.2	218.420	-45.902	306.255	-57.937
10.550	0.0223	0.4195	58.2	174.244	-585.670	244.201	-814.330
10.600	0.0224	0.4194	58.2	111.765	-726.707	156.387	-1010.290
10.650	0.0225	0.4192	58.3	70.624	-680.299	98.662	-943.767

TABLE 19

(CONTINUED)

GENERAL DATA FOR DIELECTRIC SUBSTRATE				FERRITE SUBSTRATE WAVE TRAVELING FORWARD		REVERSE	
FREQ GHz	D / LAMBDA	LAMBDAP / LAMBDA	ZO	ALPHA DB/CM	BETA-FE	ALPHA DB/CM	BETA-FE
10.700	0.0226	0.4190	58.3	46.870	-597.738	65.450	-828.010
10.750	0.0228	0.4189	58.4	32.864	-521.333	45.819	-720.099
10.800	0.0229	0.4187	58.4	24.155	-458.070	33.625	-630.823
10.850	0.0230	0.4185	58.4	18.446	-406.785	25.666	-559.150
10.900	0.0231	0.4184	58.5	14.531	-365.20;	20.188	-500.427
10.950	0.0232	0.4182	58.5	11.739	-331.079	16.284	-452.239
11.000	0.0233	0.4180	58.5	9.682	-302.678	13.426	-412.629
11.050	0.0234	0.4179	58.6	8.126	-278.829	11.251	-378.896
11.100	0.0235	0.4177	58.6	6.922	-258.532	9.569	-350.177
11.150	0.0236	0.4175	58.7	5.969	-241.034	8.249	-325.816
11.200	0.0237	0.4174	58.7	5.205	-225.877	7.182	-304.328
11.250	0.0238	0.4171	58.7	4.580	-212.566	6.319	-285.810
11.300	0.0239	0.4170	58.8	4.065	-200.855	5.600	-269.168
11.350	0.0240	0.4169	58.8	3.635	-190.447	4.999	-254.371
11.400	0.0241	0.4166	58.9	3.271	-181.108	4.497	-241.396
11.450	0.0242	0.4165	58.9	2.961	-172.741	4.065	-229.470
11.500	0.0243	0.4165	58.9	2.695	-165.179	3.694	-218.682

LIST OF REFERENCES

1. A. M. Tufekcioglu, Hybrid Mode Analysis of Microstrip on Dielectric and Ferrite Substrate, E.E. Thesis, Naval Postgraduate School, Monterey, Ca., September 1974.

2. Klaus-Dieter Kuchler, Hybrid Mode Analysis of Coplanar Transmission Lines, Ph.D. Thesis, Naval Postgraduate School, Monterey, Ca., June 1975.

3. T. Helszain, Principles of Microwave Engineering, Wiley, 1969.

4. J. B. Knorr, "Analysis of Single and Couple Microstrip," unpublished class notes, Naval Postgraduate School Monterey, Ca.

5. J. B. Knorr, "Perturbation of Wave Guide Material," unpublished class notes, Naval Postgraduate School, Monterey, Ca.

6. Microwave Engineering Handbook, Vol. 1 , p.137, Artech House, Inc., 1971.

7. Fred Y. Rosenbaum, "Integrated Ferrimagnetic Devices," Advances in Microwave, Academic Press, 1974, Vol. 8, pp. 203-262.

8. D. H. Harris, F. T. Rosenbaum, & C. G. Aumiller, "Ferrite/ Dielectric Composite Integrated Microwave Circuits Development," Technical Report AFAL-TR-71-313, Defense Documentation Center, Alexandria, Va., November 1971.

9. Ernst Schlomann, "Microwave Behavior of Partially Magnetized Ferrites," Journal of Applied Physics, Vol. 41, No. 1, January 1970.

INITIAL DISTRIBUTION LIST

		No. Copies
1.	Defense Documentation Center Cameron Station Alexandria, Virginia 22314	2
2.	Library, Code 0212 Naval Postgraduate School Monterey, CA 93940	2
3.	Professor Richard W. Adler, Code 62Ab Department of Electrical Engineering Naval Postgraduate School Monterey, CA 93940	1
4.	Professor Jeffery B. Knorr, Code 62Ko Department of Electrical Engineering Naval Postgraduate School Monterey, CA 93940	2
5.	CDR Hooshang Aminelahi Iranian Navy c/o Training Officer, Navy Section, ARMISH-MAAG, Box 2500 APO, New York, New York 09205	2
6.	Department of Electrical Engineering University of Tehran Tehran, Iran	1
7.	Professor Donald E. Kirk Department of Electrical Engineering Naval Postgraduate School Monterey, CA 93940	1